How myelin-specific CD8 T cells contribute to CNS autoimmunity.

Catriona A. Wagner

A dissertation
submitted in partial fulfillment of the
requirements for the degree of

Doctor of Philosophy

University of Washington
2019

Reading Committee:
Joan Goverman, Chair
Daniel Campbell
Estelle Bettelli

Program Authorized to Offer Degree:
Immunology

University of Washington

Abstract

How myelin-specific CD8 T cells contribute to CNS autoimmunity.

Catriona A. Wagner

Chair of the Supervisory Committee:

Joan Goverman

Department of Immunology

Multiple sclerosis (MS) is an inflammatory, demyelinating disease of the central nervous system (CNS). CD4 T cells are implicated in MS pathogenesis and have been the main focus of MS research using the animal model experimental autoimmune encephalomyelitis (EAE). However, the extensive clinical and pathological heterogeneity seen in MS suggests that multiple pathways may be involved. Substantial evidence from patients with MS point to a role for CD8 T cells in disease pathogenesis. The ability of myelin-specific CD8 T cells to induce CNS autoimmunity and to exacerbate EAE initiated by CD4 T cells demonstrates a pathogenic role; however, the mechanisms by which CD8 T cells exert either activity have not been defined. Here

we show that myelin basic protein (MBP)-specific CD8 T cells employ distinct mechanisms to induce CNS autoimmunity versus exacerbate EAE initiated by CD4 T cells. MBP-specific CD8 T cells activated by peripheral viral infection require both IFNγ and perforin to initiate EAE. In contrast, naïve MBP-specific CD8 T cells recruited to the CNS during CD4 T cell initiated-EAE exacerbate disease via a Fas ligand-dependent mechanism that is independent of IFNγ and perforin expression. Interestingly, MBP-specific CD8 T cells exacerbated brain but not spinal cord inflammation. Reactive oxygen species production by monocyte-derived cells was elevated in the brain but not spinal cord only if MBP-specific CD8 T cells expressed Fas ligand. These results demonstrate that the ability of myelin-specific CD8 T cells to exert distinct effector functions with diverse pathologic outcomes may contribute to the heterogeneity seen in MS.

Acknowledgements

I would like to thank the many people who have provided support and guidance to me throughout my graduate school career. I would first like to thank my mentor, Joan Goverman, for challenging me to become a better scientist and for always believing in me. Her positive outlook, enthusiasm, and encouragement have been crucial to my success as a graduate student. I would also like to thank my dissertation committee members, Daniel Campbell, Estelle Bettelli, and Jonathan Weinstein for providing many helpful suggestions and asking questions that contributed to the success of my project. Current and former members of the Goverman lab have provided invaluable support, mentorship, and friendship throughout the years. Emily Pierson and Sarah Simmons provided guidance and training during my rotation and beyond. Mark Johnson not only initiated the CD8-initiated EAE project but also provided constant positivity and laughter. Neal Mausolf provided invaluable technical help. Pam Roque was another source of optimism and encouragement throughout the years and with Trevor Mileur helped to tie up the CD8-initiated EAE project. I would also like to thank my classmates, Lauren Aarreberg and Nicole Arroyo for their support and friendship.

I am also lucky to have had the constant support of my family. A special thanks to my parents, Donald and Susan Cramb, for their unconditional love and support. They have provided me with so many opportunities that have made my success as a scientist possible. Most importantly, I would like to thank my husband Jamie who has been by my side since college. I could not have asked for a more supportive and patient partner in life. His belief in me kept me going even when I felt like giving up. And of course, a thank you to our beautiful son, Connor, who never fails to make me smile and put my life into perspective.

Table of Contents

List of Abbreviations ..... **iv**

List of Figures and Tables ..... **vi**

Chapter 1: Introduction **1**

Multiple Sclerosis **1**

Overview of Multiple Sclerosis 1

Heterogeneity in MS 1

Experimental Autoimmune Encephalomyelitis **4**

Overview of EAE 4

CD4 T cell subsets in EAE 5

CD8 T cells in MS and EAE **6**

Overview of CD8 T cells 7

CD8 T cells in MS 8

Regulatory CD8 T cells in MS and EAE 8

Pathogenic CD8 T cells in MS and EAE 9

Chapter 2: MBP-specific CD8 T cells induce CNS autoimmunity via IFNγ- and perforin-dependent mechanisms. **12**

Introduction **12**

Results **13**

Virally-activated 8.8 CD8 T cells initiate CNS autoimmunity. 13

Mice with CD8-initiated EAE exhibit distinct pathology compared to mice with CD4-initiated EAE. 14

Virally-activated 8.8 CD8 T cells require IFNγ and perforin expression to initiate EAE..... 15

Chapter 3: MBP-specific CD8 T cells preferentially enhance brain inflammation during CD4-initiated EAE. 22

Introduction 22

Results 24

8.8 CD8 T cells are recruited to and activated within the CNS during CD4-initiated EAE. 24

8.8 CD8 T cells exacerbate atypical EAE in an intact TCR transgenic model. 24

Development of a less severe EAE model. 25

8.8 CD8 T cells exacerbate atypical but not classic CD4-initiated EAE in a polyclonal model. 27

8.8 CD8 T cells accumulate and acquire an activated effector phenotype in the brain but not spinal cord. 29

Recruitment from the periphery is important for the maintenance of 8.8 CD8 T cell numbers in the brain and spinal cord. 32

8.8 CD8 T cells proliferate to a similar extent in the brain and spinal cord. 33

A higher frequency of 8.8 CD8 T cells die in the spinal cord compared to the brain. 34

Chapter 4: MBP-specific CD8 T cells enhance brain inflammation during CD4-initiated EAE via a FasL-dependent mechanism. 56

Introduction **56**

Results **56**

Recruitment of 8.8 CD8 T cells enhances chemokine and cytokine expression in the brain. 56

8.8 CD8 T cells increase the recruitment and pathogenicity of CD4 T cells, monocytes, and monocyte-derived cells. 57

8.8 CD8 T cells do not exacerbate atypical EAE due to a lack of regulatory CD8 T cells... 60

IFNγ, perforin, and TNFα are not required for 8.8 CD8 T cell exacerbation of atypical EAE. 60

Cells from 8.8 mice deficient in GM-CSF ameliorate atypical EAE. 61

FasL-mediated signaling is required for MBP-specific CD8 T cells to exacerbate atypical EAE. 62

A higher frequency of monocytes and monocyte-derived cells present MBP-K^k in the brain compared to the spinal cord. 63

Chapter 5: Concluding remarks and outstanding questions **78**

Chapter 6: Materials and Methods. **84**

References **92**

List of Abbreviations

8.6	K^k/MBP79-87-specific TCR transgenic mouse (Vα8, Vβ8)
8.8	K^k/MBP79-87-specific TCR Transgenic mouse (Vα8, Vβ6)
12H4	Antibody recognizing MBP/K^k
APC	Antigen presenting cell
BBB	Blood brain barrier
BrdU	Bromodeoxyuridine
C3H	C3Heb/Fej mice
CD	Cluster of differentiation
CFA	Complete Freund's adjuvant
CNS	Central nervous system
CSF	Cerebral spinal fluid
DC	Dendritic cell
EAE	Experimental autoimmune encephalomyelitis
FTY720	Spingosine-1-phosphate receptor modulator
GA	Glatiramer acetate
GFAP	glial fibrillary acidic protein
GM-CSF	Granulocyte-macrophage colony-stimulating factor
i.p.	Intraperitoneal
IFN	Interferon
IL	Interleukin
iNOS	inducible nitric oxide synthase

MBP	Myelin basic protein
MHC	Major histocompatibility complex
MOG	Myelin oligodendrocyte glycoprotein
MS	Multiple sclerosis
PBS	Phosphate-buffered saline
RT-PCR	Reverse transcriptase-polymerase chain reaction
PLP	Proteolipid protein
PPMS	Primary progressive MS
ROS	Reactive oxygen species
RRMS	Relapsing-remitting MS
SC	Spinal cord
SPMS	Secondary progressive MS
T_{CM}	Central memory T cells
TCR	T cell receptor
T_{EFF}	Effector T cells
T_{EM}	Effector memory T cells
Th	T helper cell
TNF	Tumor necrosis factor
T_{RM}	Resident memory T cells
Vac	Vaccinia virus
WT	Wild-type

List of Figures and Tables

Figure Number		
1.1	Model of CD4-initiated EAE.	11
2.1	Virally-activated 8.8 CD8 T cells induce CNS autoimmunity.	17
2.2	Classic and atypical EAE incidence and clinical scores of virally-infected mice.	18
2.3	8.8 CD8 T cells induce CNS pathology distinct from CD4-initiated EAE.	19
2.4	8.8 CD8 T cells induce CNS autoimmunity via IFNγ- and perforin-dependent mechanisms.	21
2.5	TNFα and FasL are not required for virally-activated 8.8 CD8 T cells to induce CNS autoimmunity.	22
3.1	8.8 CD8 T cells are recruited to the CNS during CD4-initiated EAE.	37
3.2	8.8 CD8 T cells acquire an activated, effector phenotype in the CNS and not spleen in mice with CD4-initiated EAE.	38
3.3	8.8 CD8 T cells enhance incidence and severity of atypical but not classic EAE induced by CD4 T cells in an intact TCR transgenic model.	39
3.4	Development of a less severe CD4-initiated EAE model.	40
3.5	Splenocytes have a lower IL-17:IFNγ ratio and induce more severe disease compared to LN cells.	41

3.6	Th1-skewed donor CD4 T cells induce more severe disease compared to Th17-skewed donor CD4 T cells.	43
3.7	8.8 CD8 T cells enhance incidence and severity of atypical but not classic EAE induced by CD4 T cells in a polyclonal model.	44
3.8	8.8 CD8 T cells enhance incidence and severity of atypical but not classic EAE induced by CD4 T cells in a polyclonal model when 8.8 CD8 T cells are transferred one day post-CD4 T cell transfer.	45
3.9	8.8 CD8 T cells enhance tissue injury in the brain during CD4-initiated EAE.	46
3.10	8.8 CD8 T cells increase the frequency of parenchymal vessel-associated lesions in the brain during CD4-initiated EAE.	47
3.11	8.8 CD8 T cells accumulate in the brain and not spinal cord in mice with CD4-initiated EAE	49
3.12	$CD45^{hi}$ infiltrating immune cells and donor CD4 T cells accumulate in both the brain and spinal cord during CD4-initiated EAE.	50
3.13	8.8 CD8 T cells acquire an activated effector memory phenotype in the brain and spinal cord during CD4-initiated EAE.	51
3.14	A higher frequency of 8.8 CD8 T cells produce IFNγ and TNFα in the brain compared to the spinal cord in CD4-initiated EAE.	52
3.15	A higher frequency of 8.8 CD8 T cells express cytotoxic molecules in the	53

brain compared to the spinal cord in CD4-initiated EAE.

3.16 WT CD8 T cells accumulate and acquire an activated phenotype in both the brain and spinal cord in mice with CD4-initiated EAE. 54

3.17 Recruitment from the periphery contributes to 8.8 CD8 T cell numbers in the brain and spinal cord. 55

3.18 8.8 CD8 T cells proliferate to a similar extent in the brain and spinal cord. 56

3.19 A higher frequency of 8.8 CD8 T cells undergo cell death in the spinal cord compared to the brain. 57

4.1 Recruitment of 8.8 CD8 T cells enhances chemokine gene expression in the brain but not spinal cord. 66

4.2 Recruitment of 8.8 CD8 T cells enhances cytokine gene expression in the brain but not spinal cord. 67

4.3 Gating strategy to identify immune cell subsets in the CNS of mice with EAE. 68

4.4 Numbers of infiltrating immune cells in the brain inversely correlate with the day of euthanasia. 69

4.5 Brain-infiltrating 8.8 CD8 T cells enhance the recruitment of donor CD4 T cells. 70

4.6 8.8 CD8 T cells enhance the frequencies of cytokine producing donor CD4 T cells in the brain. 71

4.7	8.8 CD8 T cells promote the recruitment and differentiation of monocytes in the brain.	72
4.8	8.8 CD8 T cells do not promote myeloid cell production of IL-1b or TNFα in the brain or spinal cord.	73
4.9	8.8 CD8 T cells increase the production of ROS by monocytes and MdCs in the brain.	74
4.10	CD4-initiated/$CD8_{8.8}$ EAE mice do not exhibit enhanced incidence and severity of atypical because of a lack of regulatory CD8 T cells.	75
4.11	8.8 CD8 T cells do not exacerbate atypical EAE via IFNγ-, perforin-, or TNFα-dependent mechanisms.	76
4.12	Cells from GM-CSF-/- 8.8 mice ameliorate atypical EAE.	77
4.13	Fas-FasL signaling is required for 8.8 CD8 T cells to increase monocyte and MdC ROS production.	78
4.14	A higher frequency of MdCs and monocytes present MBP/K^k in the brain compared to the spinal cord.	79
6.1	Similar frequencies of CD8 T cells in enriched populations from WT or 8.8 mice.	93

Table Number

6.1	Primers used for qRT-PCR.	92

Chapter 1: Introduction

Multiple Sclerosis

Overview of Multiple Sclerosis

Multiple sclerosis (MS) is the most common cause of non-traumatic neurological disability affecting over one million people world-wide and presents significant public health and socioeconomic problems[1]. MS is an autoimmune disease of the central nervous system (CNS) characterized by inflammatory multifocal lesions, plaques of demyelination, and loss of neurons, axons, and oligodendrocytes, the cells that synthesize myelin[2]. Current MS therapies are broadly anti-inflammatory and are often associated with side effects and do not prevent disease progression[3]. Therefore, there is a need to identify more specific therapeutic targets, which requires an in-depth understanding of the pathogenesis of the disease.

Myelin-specific CD4 T cells have been the main focus of MS research based in part on the strong association of MS susceptibility with MHC class II alleles[4]. Furthermore, adoptive transfer of myelin-specific CD4 T cells into naïve animals is sufficient to induce experimental autoimmune encephalomyelitis (EAE), a widely used animal model of MS[5]. However, global depletion of all CD4 T cells was not an effective therapy in MS[6], highlighting the importance of other cell types in MS pathogenesis. A more complete understanding of the multiple effector cells involved in MS pathogenesis may reveal additional therapeutic targets.

Heterogeneity in MS

While the etiology of MS is still unknown, it is hypothesized to involve a complex interplay between genetic and environmental risk factors, triggering the activation of myelin-specific T cells in the periphery that normally circulate in a naïve state[7]. GWAS studies have identified >200 genetic risk variants for MS with small individual effects[8]. The majority of the genes identified are associated with immune cell function, including those involved in T cell activation and proliferation, with polymorphisms in HLA class II genes contributing to the highest risk[9]. However, genetic factors only account for approximately 30% of the overall disease risk[2]. Other factors influencing MS susceptibility include mononucleosis from Epstein-Barr virus, smoking, obesity, and low vitamin D levels[9]. The multifactorial nature of MS and the possibility of different gene-environment interactions in individual patients likely results in extensive heterogeneity in the clinical presentation, regional distribution of lesions, and pathology (described below).

For the majority of patients with MS, disease course begins with a relapsing-remitting phase (RRMS) with intermittent, discrete periods of neurological symptoms followed by periods of remission. Relapses coincide with the appearance of inflammatory lesions detected by gadolinium-enhancing lesions seen on MRI. Over time, most patients with RRMS convert to a progressive stage called secondary progressive MS (SPMS) characterized by a decrease in the frequency, or complete cessation, of relapses and the gradual accumulation of disability associated with brain and spinal cord atrophy. A small subset of patients with MS initially present with a progressive disease course that is not preceded by a course of relapsing and remitting clinical exacerbations, called primary progressive MS (PPMS)[1, 10]. A reduction in gadolinium-enhancing MRI lesions[11] and the lack of efficacy of anti-inflammatory therapies in patients with SPMS and PPMS suggest that neurodegeneration proceeds independently of

inflammation in these stages[12, 13]. However, further analyses of normal appearing white matter and meninges tissue sections revealed that inflammation was still present, albeit in a different form[13]. Staining using a marker that selectively stains for leaky endothelial cells indicated that inflammation is compartmentalized behind a less permeable BBB and likely involves continual activation of innate immune cells within the CNS with little contribution from the periphery[2, 14]. This suggests that different disease mechanisms and effector cell responses may be at play in different stages of MS.

Patients with MS also present with highly variable disease symptoms that reflect differences in the location of lesions within the CNS. The vast majority of patients with RRMS exhibit lesions predominantly in the brain, specifically the brainstem, cerebellum, cerebral hemispheres and optic nerves, with some involvement of the spinal cord[9]. However, a small subset (2-10%) of patients with clinical definite MS exhibit lesions predominantly in the spinal cord with relatively sparse brain involvement[15, 16]. These differences in lesion localization suggest that the brain and spinal cord are distinct microenvironments.

Significant heterogeneity is also observed in the structure of lesions and types of tissue injury seen in patients with MS. Lesions have been grouped into four different patterns based on the presence or absence of antibody deposition and complement activation, differential loss of certain myelin proteins, whether lesions occur at perivenous sites and whether oligodendrocytes are spared or die by apoptosis or necrotic cell death[17, 18]. The observation that individual patients with MS exhibit only one pattern of lesions led to the proposal that different patterns may arise from distinct pathogenic pathways.

Together, the extensive heterogeneity seen in patients with MS suggest that multiple pathways contribute to disease development. Understanding the specific pathways relevant to

individual patients is important to understand which patients will respond well to current therapies and to identify new therapeutic targets tailored for individual patients. However, mechanistic studies in MS patients are difficult due to limited access to CNS tissue. Therefore, animal models are critical for defining mechanisms of CNS autoimmunity.

Experimental Autoimmune Encephalomyelitis

Overview of EAE

MS has been extensively studied using the EAE model, which is induced by the activation or adoptive transfer of myelin-specific CD4 T cells[5]. Collectively, EAE research indicates that the following events lead to EAE (Fig. 1.1). Myelin-specific CD4 T cells are activated in the periphery which induces the expression of adhesion molecules and integrins that facilitate their extravasation across the blood brain barrier (BBB). Following entry into the CNS, myelin-specific CD4 T cells are reactivated by the small number of antigen-presenting cells (APCs) in the healthy CNS that constitutively present myelin antigens in the meninges and perivascular spaces. This reactivation triggers the T cells to produce soluble, inflammatory mediators that activate CNS-resident cells including astrocytes which form a layer of the BBB. Astrocytes secrete chemokines and cytokines that promote permeabilization of the BBB and the recruitment of additional leukocytes from the periphery. These leukocytes include monocytes that can differentiate into dendritic cells (DCs) and macrophages (collectively referred to as monocyte-derived cells or MdCs) in the tissue[19]. MdCs can cause direct demyelination and axonal damage through the secretion of neurotoxic factors such as TNFα and reactive oxygen species (ROS) generated by inducible nitric oxide synthase (iNOS)[20-23]. MdCs can also

propagate inflammation via antigen presentation of additional myelin antigens[24], referred to as epitope spreading. Naïve CD4 and CD8 T cells with distinct specificities from the initial CD4 T cell population are also recruited to the inflamed CNS and can be activated via epitope spreading[24]. While CD8 T cells could potentially contribute to tissue damage indirectly through the secretion of cytokines, such as IFNγ and TNFα, or directly through cytotoxic functions via granzyme-perforin- or Fas-FasL-mediated mechanisms, the role of CD8 T cells in EAE pathogenesis is still unknown.

CD4 T cell subsets in EAE

EAE research has focused primarily on the role of CD4 T cells as the adoptive transfer of myelin-specific CD4 T cells alone is sufficient to trigger EAE, highlighting their role in disease induction. Studies of effector CD4 T cells in EAE implicated both IFNγ-producing Th1 and IL-17-producing Th17 cells as pathogenic mediators[25]. Originally, Th1 cells were considered the main effector cells as adoptive transfer of Th1 cells could induce EAE[26, 27]. This finding was consistent with an earlier observation that MS was exacerbated by the administration of IFNγ[28]. However, mice deficient in cytokines associated with the differentiation and function of Th1 cells developed severe EAE[29]. In contrast, deficiency in IL-23, which is important for Th17 cell stabilization, conferred resistance to EAE, suggesting that Th17 cells may be the true effector cells[30]. An increase in IL-17 transcripts was also reported in chronic MS lesions[31]. However, IL-17A$^{-/-}$, and IL-17F$^{-/-}$ mice treated with anti-IL-17A blocking antibody, are still susceptible to EAE[32]. Subsequently, GM-CSF was reported to be essential for EAE pathogenesis[33-35], and recent studies have suggested that T cells producing GM-CSF may represent a distinct T cell subset[36, 37].

The majority of EAE models develop inflammation predominantly in the spinal cord, which is distinct from patients with MS where lesions are predominantly located in the brain. However, brain inflammation does occur in a few EAE models using certain mouse strains and myelin antigen combinations[38]. Our laboratory utilizes C3Heb/Fej (C3H) mice in which immunization with MOG results in extensive inflammation in both the brain and spinal cord[39]. Using the C3H EAE model, we have demonstrated that the relative amounts of the cytokines IL-17, IFNγ, and GM-CSF produced by CD4 T cells infiltrating the CNS influence lesion distribution between the brain and the spinal cord. IL-17, IFNγ, and GM-CSF all promote spinal cord inflammation resulting in "classic" EAE symptoms of ascending paralysis. IL-17 and GM-CSF also promote inflammation in the brain resulting in "atypical" EAE symptoms of ataxia, leaning, and axial rotation[39-41]. In contrast, IFNγ inhibits brain inflammation[42]. We identified neutrophils as the key players in the IL-17 and GM-CSF-mediated pathways of initiating brain inflammation[40, 41], and have found that neutrophils are required for parenchymal infiltration of immune cells and subsequent tissue damage in the brain[40]. Surprisingly, while IFNγ inhibits neutrophil recruitment to the brain, it promotes neutrophil recruitment to the spinal cord. Despite the enhanced IFNγ-mediated neutrophil recruitment to the spinal cord, neutrophils contributed less to spinal cord parenchymal tissue damage compared to their role in the brain[40]. This work highlights the distinct nature of the response within the brain versus spinal cord to infiltrating inflammatory cells and suggests that differences in the relative amounts of cytokines produced by CD4 T cells may account for some of the heterogeneity seen in MS pathology.

CD8 T cells in MS and EAE

Overview of CD8 T cells

Upon activation, CD8 T cells expand, differentiate into effector cells, and acquire several effector functions. These effector functions include the production of cytokines, such as IFNγ and TNFα. CD8 T cells can also lyse target cells by the release of perforin and granzyme-B or by the expression of FasL on their cell surface which signals through Fas to induce apoptosis. After the initial activation and expansion of CD8 T cells, the majority of effector CD8 T cells die by apoptosis during the contraction phase. The remaining CD8 T cells form the memory subset which persist long-term and protect against reinfection. There are at least three subtypes of memory: central memory (T_{CM}), effector memory (T_{EM}), and tissue resident memory (T_{RM}). While both T_{CM} and T_{EM} CD8 T cells circulate, T_{CM} have an increased proliferative response and produce more IL-2 while T_{EM} respond rapidly to reinfection[43]. In contrast, T_{RM} permanently reside in peripheral tissues.

Interestingly, CD8 T cell populations exhibit substantial phenotypic and functional diversity which is regulated by many factors including the strength of the activating stimulus and the cytokines present in the inflammatory environment[44]. For example, KLRG1, a marker of effector CD8 T cells (T_{EFF}) which express high amounts of cytotoxic molecules, is induced upon strong TCR and inflammatory signals[45, 46]. In particular, high expression of IL-12 is important for the generation of T_{EFF} through the induction of T-bet[45, 47, 48]. In less inflammatory environments with low levels of IL-12, effector CD8 T cells that do not express KLRG1 differentiate and are termed memory precursor T cells[45]. Memory precursor T cells express low levels of cytotoxic molecules but have a high potential to generate memory. In summary, the tissue microenvironment is important in determining the function of CD8 T cells.

CD8 T cells in MS

Substantial evidence indicates that CD8 T cells contribute to MS pathogenesis. CD8 T cells outnumber CD4 T cells in both the lesions and CSF of MS patients, and clonal expansion is more commonly observed among CD8 compared to CD4 T cells[49-54]. The clonal nature of CD8 T cells in MS suggests that they are antigen-experienced, however, the specific antigen recognized by CNS-infiltrating CD8 T cells is still unknown. Early work identified CD8 T cells specific for several myelin proteins including myelin basic protein (MBP) and myelin proteolipid protein (PLP) in the peripheral blood of patients with MS as well as healthy controls[55, 56]. Although it is controversial whether there is a higher frequency of myelin-specific CD8 T cells in the blood of MS patients compared to healthy controls, some groups have reported that these CD8 T cells exhibit a more activated, memory phenotype in MS patients[57]. Together, these data suggest that CD8 T cells participate in MS pathogenesis; however, their exact contributions are still unclear. One study investigating myelin-specific CD8 T cells in patients with MS detected expression of both pro- and anti-inflammatory immune mediators within this population, suggesting the presence of both pathogenic and regulatory CD8 T cells[58]. In support of the notion that there is functional heterogeneity among CNS antigen-specific CD8 T cells, different HLA-A alleles have been associated with both increased and decreased susceptibility to MS[59], a finding that has been reproduced in humanized mouse models[60].

Regulatory CD8 T cells in MS and EAE

Initial studies demonstrated that the suppressor function of CD8 T cells was defective in patients with MS compared to healthy controls, attributing a regulatory role to CD8 T cells in

MS[61]. This suppressor function was ultimately linked to CD4 T cells as CD8 T cells can kill myelin-specific CD4 T cells in a HLA-E dependent manner[62]. In support of this, CD8 T cells can suppress CD4 T cells via a Qa-1 dependent mechanism, which is the mouse equivalent to HLA-E[63, 64]. Furthermore, some of the disease-ameliorating effects of Glatiramer acetate (GA) are attributed to the induction of suppressive GA-specific CD8 T cells in MS patients[65], which are also required for the effects of GA in EAE[66].

Myelin-specific CD8 T cells isolated from patients with MS have also been shown to suppress the activity of myelin-specific CD4 T cells, and relapses have been correlated with a reduction in the suppressive function of myelin-specific CD8 T cells[67, 68]. In mice, myelin peptide immunization or infection with recombinant *Listeria monocytogenes* expressing myelin antigens can generate CD8 T cells that ameliorate EAE by modulating myelin-specific CD4 T cell and DC activity in an IFNγ and perforin-dependent manner[69-72]. However, the mechanisms by which CD4 T cells cross-present myelin antigens to regulatory CD8 T cells are still unknown.

Pathogenic CD8 T cells in MS and EAE

Evidence from MS patients also supports a pathogenic role for CD8 T cells. In MS brain tissues, CD8 T cells with polarized cytotoxic granules have been observed in close proximity to demyelinated axons[73] and the number of CD8 T cells correlates with the extent of axon damage[74]. *In vitro,* myelin-specific CD8 T cells isolated from the blood of MS patients can lyse oligodendrocytes[75] and produce IFNγ and TNFα in response to myelin antigens[55, 58, 76], suggesting that they can contribute to disease pathogenesis through both cytotoxic and proinflammatory mechanisms.

In mice, CD8 T cells specific for myelin antigens as well as glial fibrillary acidic protein (GFAP), a protein expressed in astrocytes, can induce disease following activation in the periphery via peptide immunization or viral infection[60, 77-82]. Importantly, our lab has shown that following activation, MBP-specific CD8 T cells induce severe CNS autoimmunity with some parallels to MS pathology[77]. Specifically, lesions are found throughout the brain and are primarily vascular with perivascular cuffing. Interestingly, lesions are associated with severe demyelination and cell death, suggesting cytotoxic functions[77]. Similar to some of the regulatory CD8 T cells that have been described[83], evidence suggests IFNγ may be important for CD8 T cells to initiate disease[77] and *in vitro* and *ex vivo* data support a role for cytotoxicity[84, 85]. However, the mechanisms by which CD8 T cells exert pathogenic activity in CNS autoimmunity have not been established *in vivo*.

Collectively, animal models have provided some insights into the contribution of CD8 T cells to CNS autoimmunity. Although CD8 T cells can induce disease on their own, GWAS studies provide strong support for a role of CD4 T cells in MS[5]. As myelin-specific CD8 T cells can not only induce CNS autoimmunity but can also exacerbate CD4 T cell mediated EAE[86], it is important to investigate the role of myelin-specific CD8 T cells in both scenarios. Understanding the multiple roles of CD8 T cells in CNS autoimmunity may shed light on the heterogeneity of the immune mechanisms involved in MS.

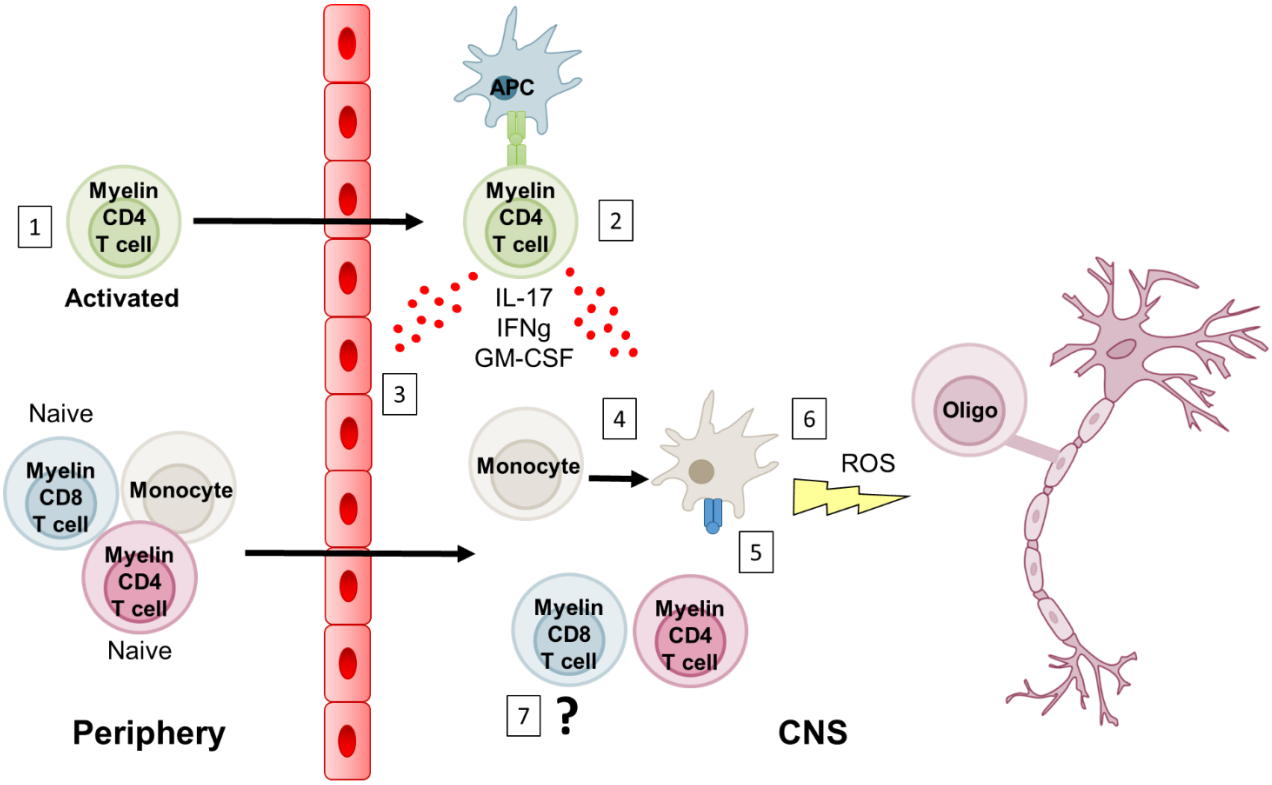

Figure 1.1. Model of CD4-initiated EAE. Collectively, EAE research has proposed several mechanisms for CD4-initiated EAE. (1) A combination of genetic and environmental factors promote the activation of myelin-specific CD4 T cells in the periphery. (2) Activated CD4 T cells cross the blood brain barrier (BBB) into the CNS and are reactivted by resident APCs, promoting the production of inflammatory mediators, such as cytokines. (3) These inflammatory mediators promote the production of chemokines by astrocytes that form the BBB, allowing the recruitment of other leukocytes including monocytes and naïve CD4 and CD8 T cells. (4) Monocytes differentiate into macrophages and dendritic cells (MdCs). (5) MdCs can present additional myelin antigens to activate CD4 and CD8 T cells of different myelin specificites. (6) MdCs can also cause direct demyelination via the production of ROS. (7) Although CD8 T cells are recruited to the CNS, their role in CNS autoimmunity pathogenesis is still unknown.

Chapter 2: MBP-specific CD8 T cells induce CNS autoimmunity via IFNγ- and perforin-dependent mechanisms.

Introduction

To investigate the role of myelin-specific CD8 T cells in CNS autoimmunity, our lab previously identified MBP-specific CD8 T cells by infecting WT or $MBP^{-/-}$ C3H mice with a recombinant virus expressing MBP[87]. All MBP-specific CD8 T cell clones isolated from $MBP^{-/-}$ C3H mice were specific for MBP_{79-87} restricted by the H-$2K^k$ MHC molecule[87]. In this study, MBP_{79-87}-specific CD8 T cells were not isolated from WT C3H mice following infection with virus expressing MBP, indicating these cells are regulated via immune tolerance[87]. However, MBP_{79-87} CD8 T cells can escape immune tolerance as MBP_{79-87} CD8 T cells were isolated from WT C3H mice following immunization with MBP_{79-87} peptide, although at a lower frequency compared to $MBP^{-/-}$ mice[77]. Adoptive transfer of activated MBP_{79-87}-specific CD8 T cell clones isolated from WT C3H mice resulted in CNS autoimmune disease characterized by lesions within the brain, atypical EAE symptoms, severe demyelination, and cytotoxic injury, similar to a type of lesion seen in some MS patients that is not recapitulated in classic murine EAE models. This work demonstrated that MBP-specific CD8 T cells can function as effector cells to induce CNS autoimmunity and that the CD8 T cells may have different effector mechanisms for CNS injury than CD4 T cells.

Our lab then developed a mouse model in which T cells express a transgenic TCR specific for the MBP_{79-87} epitope (termed "8.8" mice)[88]. 8.8 CD8 T cells are not subjected to immune tolerance mechanisms and naïve 8.8 T cells can be isolated from the lymphoid tissues of

these TCR transgenic 8.8 mice. 8.8 mice do not undergo spontaneous EAE, but infection of 8.8 mice with recombinant vaccinia virus expressing MBP induces CNS autoimmune disease[81], demonstrating the pathogenic potential of the 8.8 T cells once they are activated. However, the mechanisms by which myelin-specific CD8 T cells initiate CNS autoimmunity have not been established.

Results

Virally-activated 8.8 CD8 T cells initiate CNS autoimmunity.

We previously showed that infection of intact 8.8 mice with Vac-MBP induced clinically atypical and classic signs of EAE as well as weight loss[81]. To study the pathogenic activity of 8.8 CD8 T cells in mice with a polyclonal CD8 T cell repertoire, we developed a model in which either 8.8 or non-transgenic (WT) CD8 T cells were introduced into the periphery of WT mice prior to Vac-MBP infection. As observed in the intact 8.8 model, WT mice that received 8.8 CD8 T cells developed signs of classic and atypical EAE (Fig. 2.1). 55% of Vac-MBP infected mice that had received 8.8 CD8 T cells developed ascending paralysis including limp tail and weak hindlimbs, indicating spinal cord involvement (Fig. 2.1a,b). 30% of Vac-MBP infected mice developed mild atypical EAE (Fig. 2.1c,d). Interestingly, non-classical EAE symptoms in this model were primarily associated with cerebellar dysfunction including wide and dragging gate and reduced pelvic elevation[89]. These signs are distinct from the ataxia, body lean, and axial-rotatory atypical EAE signs that are typically observed in CD4-initiated EAE in C3Heb/Fej mice[40]. Control Vac-MBP-infected mice that received WT instead of 8.8 CD8 T cells, and mice that received 8.8 CD8 T cells and were infected with WT vaccinia virus lacking MBP (Vac-WT),

exhibited no clinical signs (Fig. 2.1), demonstrating that CNS autoimmunity does not result from vaccinia infection itself or from transfer of naïve 8.8 CD8 T cells alone.

Mice with CD8-initiated EAE exhibit distinct pathology compared to mice with CD4-initiated EAE.

To understand why atypical clinical signs seen in C3Heb/Fej mice with CD8-initiated versus CD4-initiated EAE were different, we compared the histological features and localization of lesions in these two models. We found that brain lesions in the CD8-initiated EAE model targeted the cerebellum with minimal involvement seen in the brainstem and pons (Fig. 2.2a-c), and no involvement of the olfactory bulb (data not shown). The inflammatory cells within the lesions in CD8-initiated EAE were primarily associated with parenchymal vessels (Fig. 2.2a-c), with some inflammation surrounding meningeal vessels as well (Fig. 2.2b,c). There was minimal extension of inflammatory cells beyond the perivascular space into the brain parenchyma or submeningeal regions (Fig. 2.2a-c). These lesions were predominantly composed of mononuclear cells and exhibited substantial nuclear fragmentation consistent with apoptosis (Fig. 2.2d). Lesions with similar characteristics were also observed in the spinal cord (data not shown). In contrast, lesions in the brains of mice with CD4-initiated EAE targeted the olfactory bulb (data not shown), midbrain and brainstem, with no cerebellar involvement (Fig. 2.2e-g). These mice frequently exhibited meningitis and submeningeal inflammation (Fig. 2.2f,g), with approximately half of the mice also exhibiting lesions associated with parenchymal vessels (Fig. 2.2f). Within the brain parenchyma, inflammatory cells were often observed not just within the perivascular space but also extending into tissue adjacent to perivascular cuffs (Fig. 2.2f). The CD4-initiated EAE lesions were associated with high levels of necrosis and were typically

neutrophil predominant (Fig. 2.2h). Necrotic instead of apoptotic cells were the predominant feature of CD4-initiated EAE lesions. Lesion characteristics were similar and often more severe in the spinal cord in mice with CD4-initiated EAE (data not shown). These differences in lesion characteristics, especially the pronounced apoptosis seen in CD8-initiated compared to CD4-initiated EAE, suggest that 8.8 CD8 T cells and CD4 T cells may use different effector mechanisms to cause tissue injury.

Virally-activated 8.8 CD8 T cells require IFNγ and perforin expression to initiate EAE.

Other studies of CD8 T cell-initiated CNS autoimmunity have suggested that IFNγ may be important for their pathogenic activity[77]. To determine if 8.8 CD8 T cells required IFNγ expression to initiate EAE, we transferred CD8 T cells isolated from 8.8 mice or from 8.8 mice on an IFNγ-deficient ($IFN\gamma^{-/-}$) background prior to infection with Vac-MBP. While mice that received 8.8 CD8 T cells developed clinical signs of classic and atypical EAE, mice that received $IFN\gamma^{-/-}$ 8.8 CD8 T cells exhibited no clinical signs of EAE (Fig. 2.3). Similarly, mice that received perforin-deficient ($Pfp^{-/-}$) 8.8 CD8 T cells remained healthy (Fig. 2.3). In contrast, mice that received TNFα-deficient ($TNF\alpha^{-/-}$) or FasL-deficient ($FasL^{gld}$) 8.8 CD8 T cells developed EAE with a similar incidence and severity of classic and atypical clinical signs as mice that received 8.8 CD8 T cells (Fig. 2.4). Interestingly, a higher frequency of mice that received $FasL^{gld}$ 8.8 CD8 T cells developed signs of classic EAE at day 6 and 7 compared to mice that received 8.8 CD8 T cells (Fig. 2.4a,b), suggesting that $FasL^{gld}$ 8.8 CD8 T cells induce disease faster than 8.8 CD8 T cells. CD8 T cells can control T cell expansion during immune responses via Fas-FasL-mediated apoptosis, which is important during the recovery from CD4-initiated EAE[90, 91]. CD8 T cells can express MHC class I molecules and can present antigens to other CD8

T cells, resulting in lysis of the MHC class I-expressing CD8 T cell via fratricide[92]. Although we do not yet know whether 8.8 CD8 T cells present MBP/K^k in this model, it is plausible that the vaccinia virus will infect 8.8 CD8 T cells, resulting in the presentation of MBP. Therefore, $FasL^{gld}$ 8.8 CD8 T cells may induce a faster disease course due to impaired elimination of pathogenic Fas-expressing 8.8 CD8 T cells. However, overall incidence was similar between all three groups. These genetic models demonstrated that both IFNγ and perforin, but not TNFα or FasL, are required for 8.8 CD8 T cells to induce EAE.

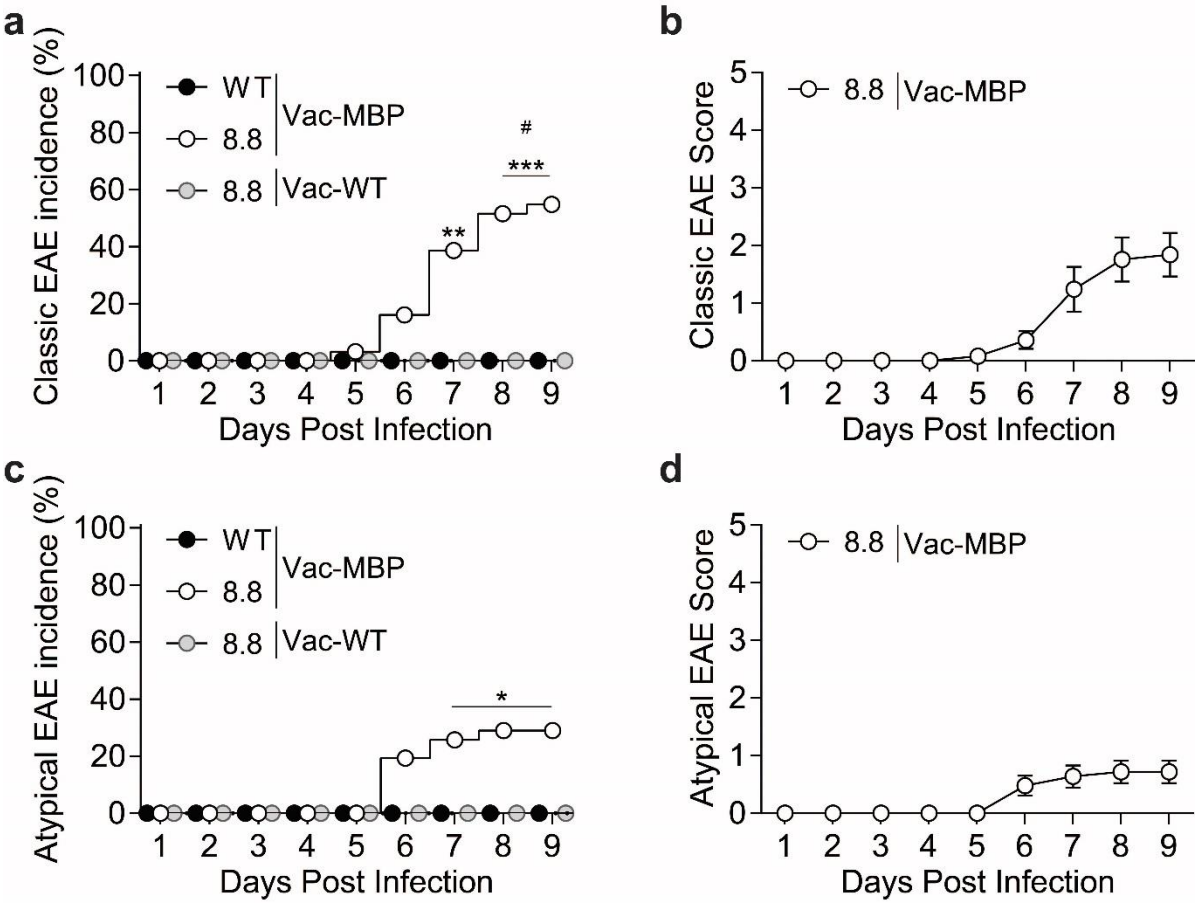

Figure 2.1. Virally-activated 8.8 CD8 T cells induce CNS autoimmunity. Clinical signs were monitored in the following groups: WT mice that received 8.8 CD8 T cells and were infected with either Vac-WT (n=5) or Vac-MBP (n=31); or WT mice that received WT CD8 T cells and were infected with Vac-MBP (n=15). **(a)** The percent of all mice induced for disease exhibiting classic EAE symptoms is shown for each indicated group. **(b)** Classic EAE scores (mean $\pm$ SEM) are shown for mice that developed EAE. **(c)** The percent of all mice induced for disease exhibiting atypical EAE symptoms is shown for each indicated group. **(d)** Atypical EAE scores (mean $\pm$ SEM) are shown for mice that developed EAE. Each graph is compiled from at least 3 independent experiments. Statistical significance in **a,c** was determined using Fisher's exact test. **(a,c)** * indicates significant difference relative to Vac-MBP-infected mice that received WT CD8 T cells; $^{\#}$ indicates significant difference relative to mice that received 8.8 CD8 T cells and Vac-WT infection. * or $^{\#}$ $p<0.05$, ** $p<0.01$, *** $p< 0.001$.

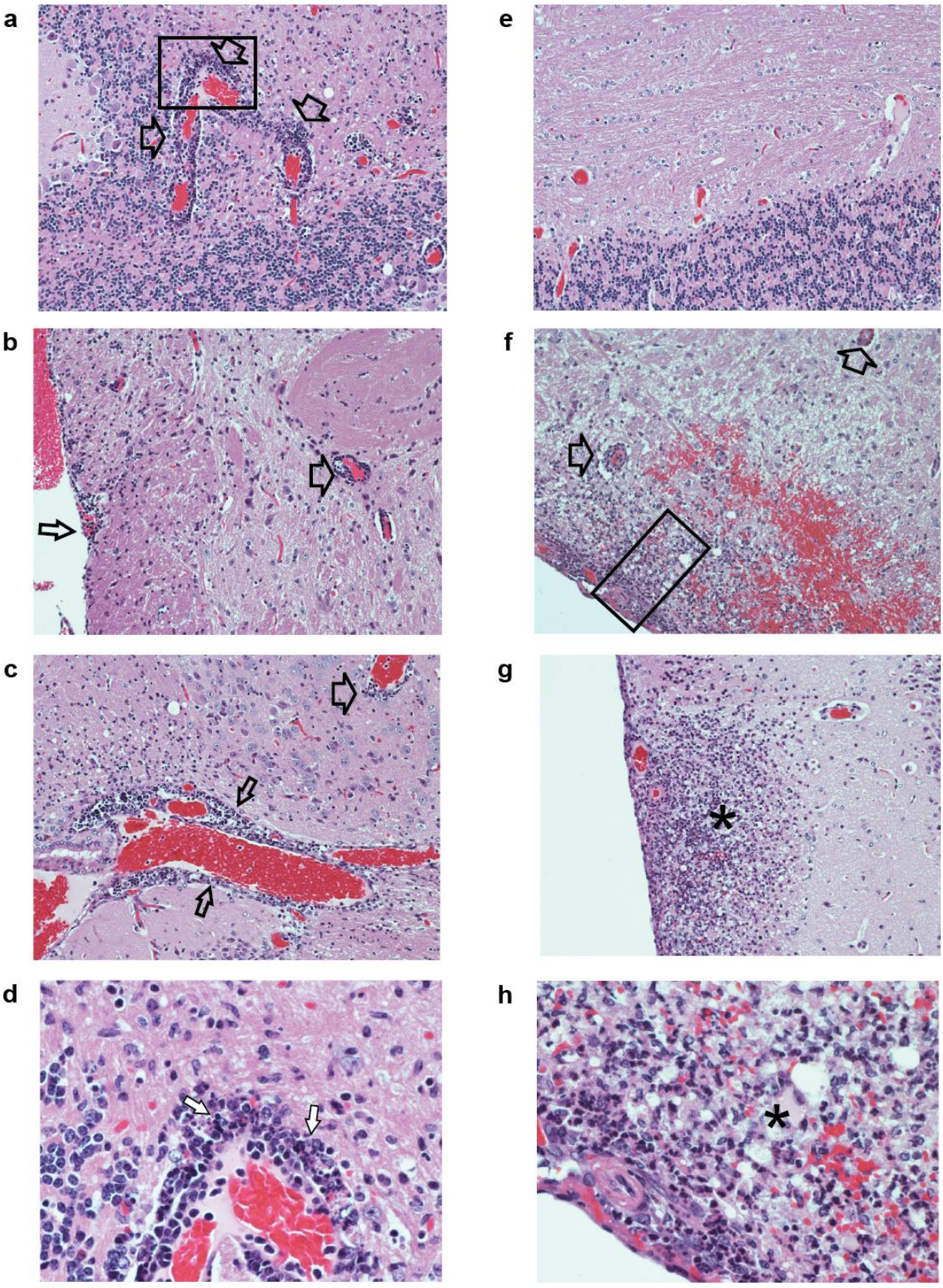
a
e
b
f
c
g
d
h

Figure 2.2. 8.8 CD8 T cells induce CNS pathology distinct from CD4-initiated EAE. (a-d) Histological sections from mice with CD8-initiated EAE. Disease was induced in WT mice that received 8.8 CD8 T cells followed by Vac-MBP infection. Tissues were harvested 7 days post-infection. **(a)** Histopathologic lesions in CD8-initiated EAE primarily target the white matter or gray-white junction of the cerebellum. Less commonly affected are widely scattered sites within the **(b)** brain stem **(c)** and midbrain. In all locations, lesions are perivascular (arrowheads) or involve the meninges (arrows) with generally minimal extension beyond these sites. **(d)** Higher power magnification of the boxed area in (a). Inflammatory cell populations are principally lymphocytic and are characterized by the presence of numerous condensed and fragmented nuclei consistent with apoptosis (white arrows). **(e-h)** Histological sections from mice with CD4-initiated EAE. Disease was induced in WT mice by transfer of polyclonal MOG-specific CD4 T cells skewed in vitro toward a Th17 phenotype prior to transfer. Tissues were harvested 8 days post-CD4 T cell transfer. **(e)** No lesions were observed in the cerebellum while **(f)** brainstem and **(g)** midbrain are common targets in this model. Affected regions have extensive meningeal involvement with marked submeningeal extension characterized by necrosis of large portions of the underlying brain parenchyma (asterisks) along with some perivascular cuffing (arrowheads). **(h)** Higher power magnification of the boxed area in (f) showing wide-spread parenchymal necrosis (asterisks) with focal hemorrhage. Necrotic cell debris is intermingled with numerous neutrophils and fewer mononuclear inflammatory cells. Original magnifications: **(a-c, e-g)** 20x; **(d,f)** 60x. Data are representative of 4 mice per group.

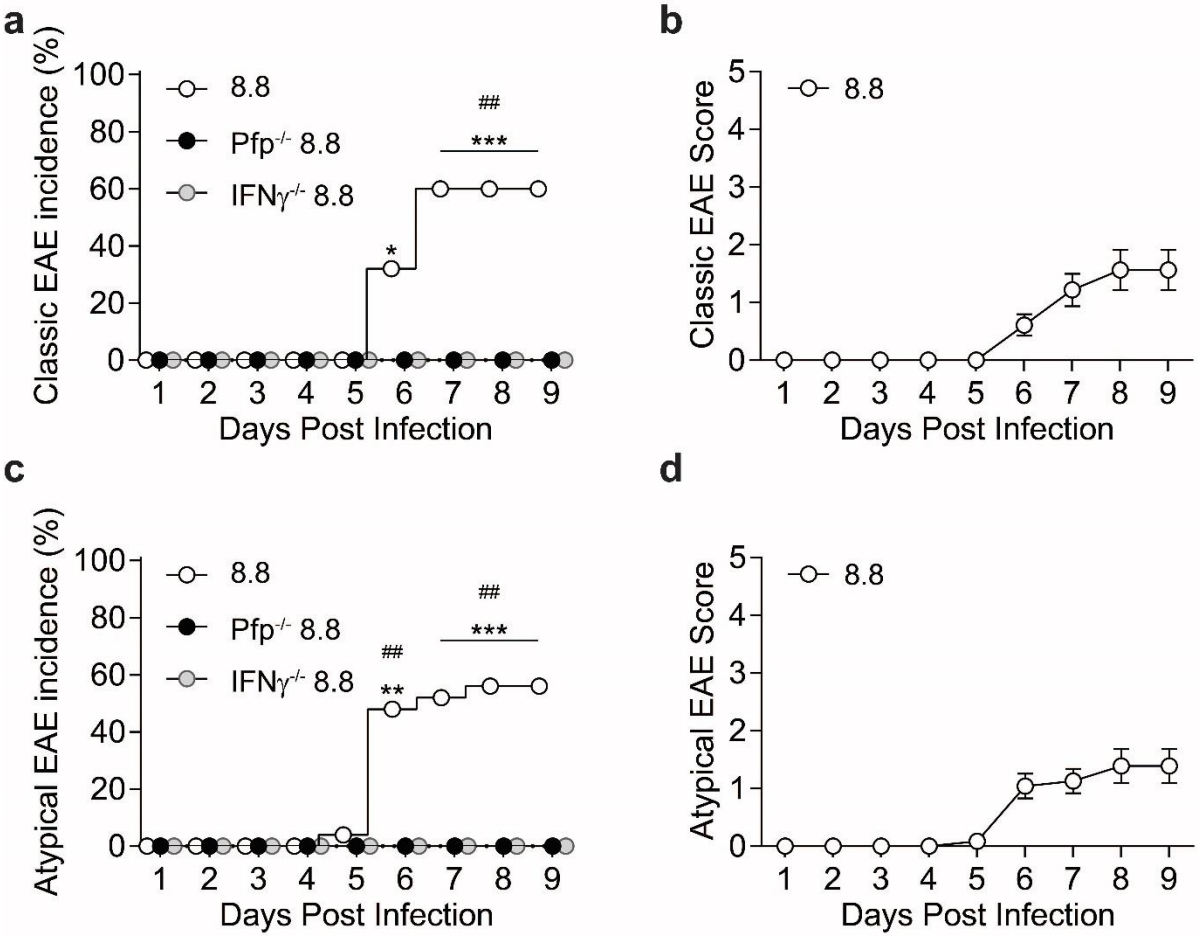

Figure 2.3. Virally-activated 8.8 CD8 T cells induce CNS autoimmunity via IFNγ- and perforin-dependent mechanisms. Clinical signs were monitored in WT mice that received 8.8 (n=25), IFNγ-deficient (IFNγ$^{-/-}$) 8.8 (n=15), or perforin-deficient (Pfp$^{-/-}$) 8.8 (n=7) CD8 T cells and were infected with Vac-MBP. **(a)** The percent of all mice induced for disease exhibiting classic EAE symptoms is shown for each indicated group. **(b)** Classic EAE scores (mean $\pm$ SEM) are shown for mice that developed EAE. **(c)** The percent of all mice induced for disease exhibiting atypical EAE symptoms is shown for each indicated group. **(d)** Atypical EAE scores (mean $\pm$ SEM) are shown for mice that developed EAE. Each graph is compiled from at least 3 independent experiments. Statistical significance in **a,c** was determined using Fisher's exact test. **(a,c)** * indicates significant difference relative to mice that received IFNγ$^{-/-}$ 8.8 CD8 T cells; $^{\#}$ indicates significant difference relative to mice that received Pfp$^{-/-}$ 8.8 CD8 T cells. ** or $^{\#\#}$ $p<0.01$, *** $p< 0.001$.

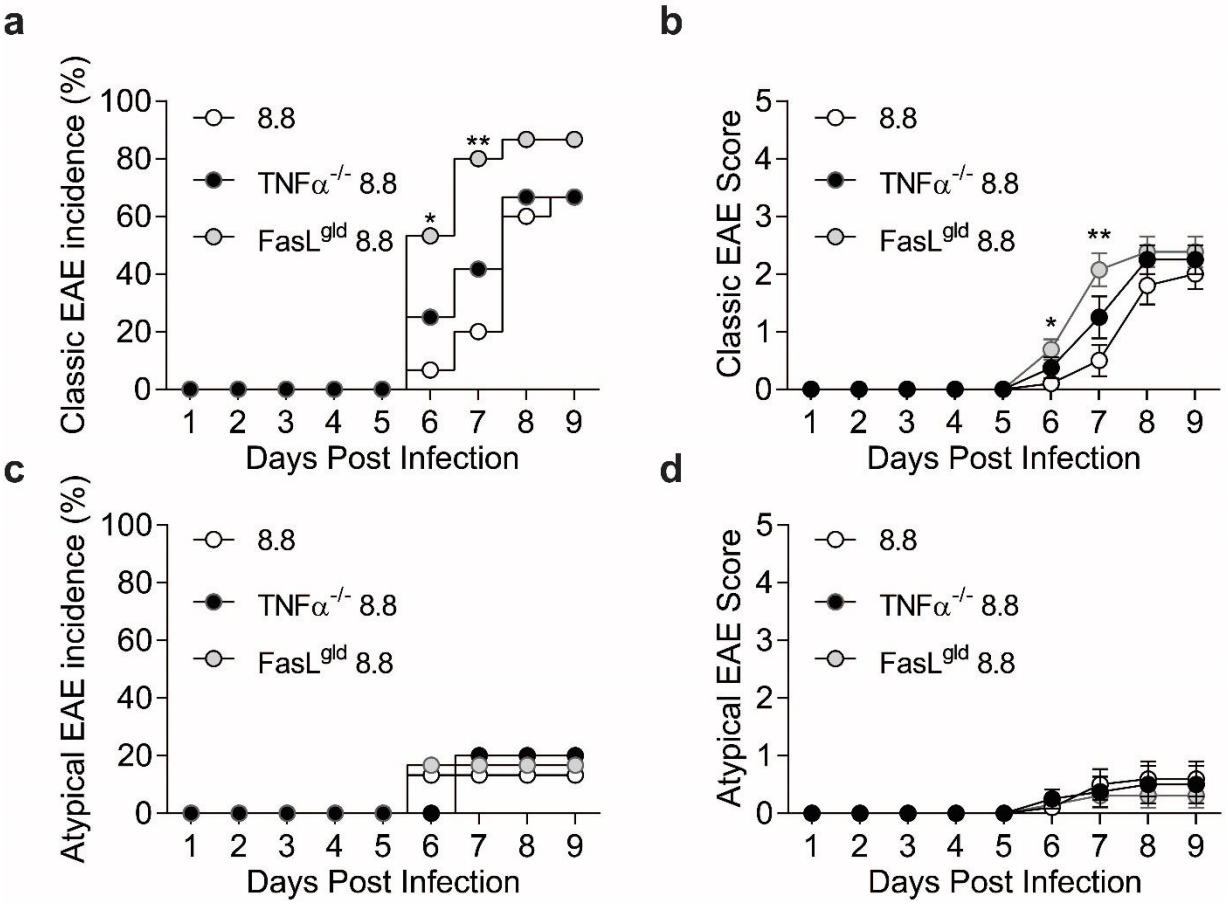

Figure 2.3. TNFα and FasL are not required for virally-activated 8.8 CD8 T cells to induce CNS autoimmunity. Clinical signs were monitored in WT mice that received 8.8 (n=15), TNFα-deficient ($TNF\alpha^{-/-}$) 8.8 (n=12), or FasL-deficient ($FasL^{gld}$) 8.8 (n=15) CD8 T cells and were infected with Vac-MBP. **(a)** The percent of all mice induced for disease exhibiting classic EAE symptoms is shown for each indicated group. **(b)** Classic EAE scores (mean $\pm$ SEM) are shown for mice that developed EAE. **(c)** The percent of all mice induced for disease exhibiting atypical EAE symptoms is shown for each indicated group. **(d)** Atypical EAE scores (mean $\pm$ SEM) are shown for mice that developed EAE. Each graph is compiled from 3 independent experiments. Statistical significance was determined using **(a,c)** Fisher's exact test or **(b,d)** Kruskal-Wallis with Dunn's post-test. * $p<0.05$, ** $p<0.01$.

Chapter 3: MBP-specific CD8 T cells preferentially enhance brain inflammation during CD4-initiated EAE.

Introduction

In the CD8-initiated EAE model, 8.8 CD8 T cells initiated CNS autoimmunity following activation in the periphery by viral infection. However, the strongest genetic susceptibility to MS is associated with MHC class II molecules that present antigen to CD4 T cells. Furthermore, CD4 T cells can initiate EAE on their own[5]. Together these observations suggest that CD4 T cells may be the primary inducers of disease in most MS patients. Nevertheless, CD8 T cells outnumber CD4 T cells in MS lesions, suggesting that CD8 T cells may play an important role in MS pathogenesis once they are recruited to the CNS following initiation of inflammation by CD4 T cells. Therefore, we investigated whether 8.8 CD8 T cells are recruited to the CNS during CD4-initiated EAE and whether their recruitment affects the manifestation of EAE.

Our lab previously generated a monoclonal antibody specific for MBP/K^k (designated 12H4), allowing detection of APCs in the CNS that present MBP to 8.8 CD8 T cells. In EAE initiated by MOG-specific CD4 T cells (referred to as CD4-initiated EAE), we identified a subset of monocyte-derived DCs generated in the CNS that present MBP/K^{k93}. Importantly, naïve 8.6 CD8 T cells, a TCR-transgenic line that recognizes the same MBP/K^k epitope as 8.8 CD8 T cells, proliferated when cultured with DCs sorted from mice with CD4-initiated EAE[93]. These results demonstrated that EAE initiated by MHC class II-restricted CD4 T cells specific for one myelin protein results in sufficient degradation of myelin that APCs generated within the

inflammatory environment can present MHC class I-restricted epitopes derived from a separate myelin protein.

We next investigated whether nonhematopoietic CNS-resident cells present MBP/K^k following the induction of CD4-inititiated EAE, suggesting they may be targets of 8.8 CD8 T cells. While astrocytes and cerebral endothelial cells did not present MBP/K^k, a low frequency of oligodendrocytes expressed MBP/K^k during CD4-initiated EAE[93]. Additionally, oligodendrocytes isolated from mice with CD4-initiated EAE induced the production of IFNγ by previously activated 8.6 CD8 T cells[93]. These data indicate that oligodendrocytes may be direct targets of MBP-specific CD8 T cells during CD4-initiated EAE. This finding is consistent with previous data demonstrating that human MBP-specific CD8 T cells can lyse oligodendrocytes in vitro[75]. Immunochemical staining of CNS tissues from MS patients also revealed co-localization of CD8 T cells with oligodendrocytes and polarized cytolytic granules within the CD8 T cells were observed in close proximity to axons[73]. Collectively, our published work analyzing presentation of MBP/K^k by APCs in the CNS during CD4-initiated EAE revealed two potential targets for MBP-specific CD8 T-cells in the inflamed CNS: DCs and oligodendrocytes.

The thesis for my predoctoral studies was based on these observations. I hypothesized that myelin-specific CD8 T cells recruited to the inflamed CNS during CD4-initiated EAE would be activated by DCs presenting their MBP/K^k ligand. The 8.8 CD8 T cells could be pathogenic if they are activated to produce inflammatory cytokines such as IFNγ and TNFα. In addition, 8.8 CD8 T cells might exert pathogenic activity by exhibiting lytic activity toward oligodendrocytes. Alternatively, 8.8 CD8 T cells activated within the CNS may be able to lyse DCs that present myelin antigen to them. Because 12H4+ DCs also expressed MHC class II and would be capable of presenting myelin antigens to both CD4 and CD8 T cells[93], this lytic activity could dampen

the overall inflammatory response via elimination of APCs needed to sustain both CD4 and CD8 T cell activation.

Results

8.8 CD8 T cells are recruited to and activated within the CNS during CD4-initiated EAE.

We previously demonstrated that 8.8 CD8 T cells could be isolated from the CNS during CD4-initiated EAE and that they exhibited an activated phenotype in the CNS compared to the spleen[93]. To confirm these findings, we induced EAE by adoptive transfer of $2x10^6$ congenically marked myelin oligodendrocyte glycoprotein (MOG_{97-114})-specific CD4 T cells (referred to as donor CD4 T cells) into intact TCR transgenic 8.8 mice. At peak disease, 8.8 CD8 T cells infiltrated the CNS compared to irradiated control mice that did not receive CD4 T cells (Fig. 3.1). A higher frequency of 8.8 CD8 T cells exhibited a $CD44^{hi}CD62^{low}$ activated phenotype and expressed IFNγ and granzyme-B in the CNS (pooled brain and spinal cord) compared to the spleen (Fig. 3.2), demonstrating that 8.8 CD8 T cells are activated *in situ*. These results are consistent with MBP/K^k being presented in the CNS during CD4-initiated EAE as shown previously[93] and suggest that CNS inflammation initiated by CD4 T cells specific for one myelin protein results in recruitment and activation of the 8.8 CD8 T cells specific for a different myelin protein

8.8 CD8 T cells exacerbate atypical EAE in an intact TCR transgenic model.

As 8.8 CD8 T cells were recruited to and activated within the CNS during CD4-initiated EAE, we next investigated the effect of 8.8 CD8 T cells on the manifestation of disease. Intact

TCR transgenic 8.8 and WT mice developed classic EAE with similar incidence and severity (Fig. 3.3a, b). However, both the incidence and severity of atypical EAE was significantly higher in intact TCR transgenic 8.8 mice compared to WT mice (Fig. 3.3c, d). These data suggest that recruitment of 8.8 CD8 T cells specifically enhances inflammation in the brain but not the spinal cord.

Development of a less severe EAE model.

We found that 8.8 CD8 T cells enhance brain but not spinal cord inflammation. However, the CD4-initiated EAE model used in these experiments were fairly acute as 80% of the WT mice developed EAE, the average EAE severity was 4.4 ± 0.2, and 63% of the mice with EAE reached a score of 5 and needed to be sacrificed. One hypothesis was that we did not see exacerbation of symptoms in the spinal cord because inflammation in the spinal cord is already severe. To highlight the effects of 8.8 CD8 T cells, we attempted to adapt our acute CD4-initiated EAE model to generate a less severe, chronic disease. We decreased the number of donor CD4 T cells transferred into each WT recipient to either $2x10^6$ or $1.5x10^6$, and found that mice developed classic EAE symptoms with similar kinetics, incidence, and severity (Fig. 3.4a,b). The onset of atypical symptoms was slightly delayed and occurred with a lower incidence and severity in mice that received $1.5x10^6$ CD4 T cells (Fig. 3.4c,d). Although transfer of $6x10^5$ donor CD4 T cells delayed the course of disease, the incidence and severity of both classic and atypical EAE was not changed compared to the transfer of $1.5x10^6$ CD4 T cells (data not shown). We therefore decided to transfer $1.5x10^6$ donor CD4 T cells for the following experiments, which equated to $2x10^5$ blasting CD4 T cells ($CD4^+FSC^{hi}/SSC^{hi}$).

Although donor CD4 T cells were incubated with IL-23 in vitro to skew their phenotype towards Th17 cells, the ratio of IL-17-producing to IFNγ-producing (IL-17:IFNγ) donor CD4 T cells prior to adoptive transfer varied between experiments. A low IL17:IFNγ ratio appeared to correlate with increased severity of EAE (data not shown). We found that donor CD4 T cells isolated from the spleens of immunized mice exhibited a lower IL-17:IFNγ ratio (typically ~1:1) after in vitro culture compared to donor CD4 T cells isolated from the draining lymph nodes (LN) (typically ~3:1) (Fig. 3.5a). To test the hypothesis that lower IL-17:IFNγ ratios induced more severe disease, we transferred donor CD4 T cells that had been isolated from the spleen or LN separately, or at a 1:1 mixture of cells from the spleen and LNs into WT recipients (resulting in a IL-17:IFNγ ratio of ~2:1). Although the incidence of both classic and atypical EAE as well as the severity of atypical EAE were similar between all three groups, donor CD4 T cells isolated from the spleen induced a more rapid disease with a higher severity of classic EAE (Fig. 3.5c-d). Consistent with these data, donor CD4 T cells that were Th1-skewed prior to adoptive transfer induced disease with faster kinetics compared to Th17-skewed cells (Fig. 3.6). Surprisingly, 100% of mice that received Th1-skewed cells developed atypical EAE (Fig. 3.6), which is contradictory to our previous data where we found Th1-skewed cells only develop classic EAE[39]. We hypothesize that this phenomenon results from the experiments being performed in different animal facilities. In our current facility, we have observed an increase in GM-CSF production by MOG-specific donor CD4 T cells, resulting in higher GM-CSF:IFNγ ratios which correlates with an increase in atypical EAE[41]. Therefore, the higher levels of GM-CSF results in a higher incidence of EAE with Th1-skewed cells. In summary, although we were unable to develop a consistently chronic model using Th17-skewed cells transferred into WT mice, these data

suggest that transfer of $2x10^5$ blasting donor CD4 T cells with an IL-17:IFNγ ratio greater than 1:1 induces a milder disease course.

8.8 CD8 T cells exacerbate atypical but not classic CD4-initiated EAE in a polyclonal model.

We next determined the effects of 8.8 CD8 T cells during CD4-initiated EAE in a more physiologically relevant model in which mice had a polyclonal CD8 T cell repertoire. Naïve 8.8 or WT (control) CD8 T cells were injected into WT mice prior to inducing EAE by adoptive transfer of Th17-skewed CD4 T cells specific for MOG_{97-114}. Mice that received naïve 8.8 CD8 T cells alone exhibited no clinical signs (Fig. 3.7a). Mice with CD4-initiated EAE that had received either naïve 8.8 CD8 T cells (referred to as CD4-initiated/$CD8_{8.8}$) or WT CD8 T cells (referred to as CD4-initiated/$CD8_{WT}$) developed classic EAE with comparable incidence and severity (Fig. 3.7a,b). However, both the incidence and severity of atypical EAE was significantly higher in mice with CD4-initiated/$CD8_{8.8}$ EAE compared to mice with CD4-initiated/$CD8_{WT}$ EAE (Fig. 3.7c,d). Similar results were observed when CD8 T cells were transferred one day following adoptive transfer of donor CD4 T cells (Fig. 3.8). However, disease course in these experiments were not consistent (data not shown). These data confirm that recruitment of 8.8 CD8 T cells specifically enhances inflammation in the brain but not the spinal cord.

Interestingly, in contrast to the distinct atypical signs observed in mice with CD8-initiated EAE, the most common clinical sign of atypical EAE in CD4-initiated/$CD8_{8.8}$ EAE mice was a body lean. This difference in clinical signs suggested that 8.8 CD8 T cells affect different CNS regions depending on the conditions under which they are activated. To

investigate this hypothesis, tissue injury was assessed histologically in mice with CD4-initiated/$CD8_{8.8}$ and CD4-initiated/$CD8_{WT}$ EAE by determining the extent of necrotic and apoptotic cell death associated with inflammatory cell accumulation. Consistent with the increased severity of atypical clinical signs in mice with CD4-initiated/$CD8_{8.8}$ EAE, more severe tissue injury was observed in the brains of these mice compared to mice with CD4-initiated/$CD8_{WT}$ EAE (Fig. 3.9). In addition to lesion severity, the lesions within each section were characterized as involving the meninges only, meninges with submeningeal tissue, or adjacent tissue surrounding parenchymal blood vessels. While all mice in both groups exhibited lesions involving the meningeal and submeningeal regions, more lesions associated with parenchymal blood vessels were observed in mice with CD4-initiated/$CD8_{8.8}$ EAE compared to those with CD4-initiated/$CD8_{WT}$ EAE (Fig. 3.10a-d). In contrast to CD8-initiated EAE, lesions were not seen in the cerebellum of mice in either group and necrosis rather than apoptosis was prominent in brain lesions in mice with CD4-initiated/$CD8_{8.8}$ and CD4-initiated/$CD8_{WT}$ EAE (Fig. 3.10e,f).

Surprisingly, 4 of the 12 mice with CD4-initiated/$CD8_{WT}$ EAE did not exhibit histological changes in the spinal cord, which lowered the histological score and frequency of parenchymal lesions for the spinal cords in this group compared to CD4-initiated/$CD8_{WT}$ EAE mice (Fig. 3.9 and Fig. 3.10d). However, these tissues were harvested at day 7 post-CD4 T cell transfer and the mice that did not exhibit lesions in the spinal cord had not yet developed clinical signs of EAE. Based on our previous experiments showing almost 100% incidence of classic EAE (Fig. 3.7a), we hypothesize that, if these mice had not been sacrificed for tissue harvest, they may have developed EAE and exhibited spinal cord lesions in subsequent days, which would increase the histology score and possibly parenchymal lesions. Together, these data

suggest that recruitment of 8.8 CD8 T cells during CD4-initiated EAE preferentially affects brain pathology by enhancing the inflammatory response initiated by CD4 T cells rather than mediating the distinct pathological features seen in virally-induced CD8-initiated EAE.

8.8 CD8 T cells accumulate and acquire an activated effector phenotype in the brain but not spinal cord.

As 8.8 CD8 T cells enhanced brain but not spinal cord inflammation, we hypothesized that their recruitment, activation, and activity would differ between these two regions. We analyzed the numbers of 8.8 CD8 T cells infiltrating the brain and spinal cord at days 4 and 5 (preclinical), day 6 (on or just prior to onset), and day 7 (a time point in which 80% of the mice develop EAE) post-CD4 T cell transfer by flow cytometry (Fig. 3.11a). Interestingly, although 8.8 CD8 T cells entered the spinal cord earlier compared to the brain (day 4 versus day 5), 8.8 CD8 T cells accumulated overtime only in the brain (Fig. 3.11b). This phenomenon was not a reflection of overall inflammation preferentially increasing in the brain versus the spinal cord as the number of $CD45^{hi}$ infiltrating inflammatory cells and the number of donor CD4 T cells accumulated over time in both the brain and spinal cord (Fig 3.12). The number of 8.8 CD8 T cells decreased in the spleen as disease progressed, consistent with recruitment of these T cells to the CNS (Fig. 3.11b).

We next analyzed the phenotype and function of 8.8 CD8 T cells in the brain and spinal cord. To increase the number of 8.8 CD8 T cells available for analyses by flow cytometry, we induced disease by transferring CD4 T cells directly into intact 8.8 TCR transgenic mice. Following activation, CD8 T cells differentiate into short-lived T_{EFF} and long-lived T_{CM}, T_{EM},

and T_{RM} CD8 T cells[43]. Although our disease is acute and true memory cells do not appear until after the contraction phase[94], CD8 T cells acquire markers of memory CD8 T cells early in the immune response[45]. In the spleen, 8.8 CD8 T cells exhibited a naïve or T_{CM} phenotype. In contrast, the majority of 8.8 CD8 T cells in the brain and spinal cord were $CD44^{+}CD62L^{-}CD103^{-}KLRG1^{-}$, representing a T_{EM} phenotype (Fig 3.13a), consistent with CD8 T cells isolated from the lesions of MS patients[95]. Interestingly, a significantly higher frequency of naïve 8.8 CD8 T cells were isolated from the spinal cord compared to the spleen and there was a trend towards a lower frequency of 8.8 CD8 T cells exhibiting a T_{EM} phenotype in the spinal cord (Fig. 3.13b). Although the frequency of 8.8 CD8 T cells exhibiting a T_{RM} phenotype ($CD44^{+}CD62L^{-}CD103^{+}CD69^{+}$) was minimal, there was a significantly lower frequency of these cells in the spinal cord compared to the brain (Fig. 3.13b). Together, these data suggest that 8.8 CD8 T cells differentiate into similar CD8 T cell subsets in the brain and spinal cord, but they appear more naïve in the spinal cord compared to the brain.

We next analyzed cytokine production and expression of cytotoxic molecules by 8.8 CD8 T cells in the brain and spinal cord during CD4-initiated EAE. At day 7 post-CD4 T cell transfer, 8.8 CD8 T cells isolated from the brain and spinal cord produced IFNγ and TNFα but not GM-CSF or IL-17 directly *ex-vivo* without peptide stimulation (Fig. 3.14a). The frequency of IFNγ- and TNFα-producing 8.8 CD8 T cells was significantly higher in the brain compared to the spinal cord (Fig. 3.14b). 8.8 CD8 T cells did not produce either cytokine in the spleen (Fig. 3.14a). 8.8 CD8 T cells also expressed the cytotoxic molecules FasL and granzyme-B in the brain and spinal cord but not the spleen (Fig. 3.15a). Importantly, the frequency of FasL-expressing 8.8 CD8 T cells was higher in the brain compared to the spinal cord (Fig. 3.15b). Although not statistically significant, there was a trend towards a higher frequency of granzyme-

B-expressing 8.8 CD8 T cells in the brain compared to the spinal cord (Fig. 3.15b). Together these data indicate that, while 8.8 CD8 T cells are recruited to both the brain and spinal cord, they accumulate and exhibit an activated phenotype preferentially in the brain.

Interestingly, the propensity for CD8 T cells to accumulate and exhibit markers of activation in the brain versus the spinal cord was only observed for 8.8 CD8 T cells and not for WT CD8 T cells. Consistent with overall inflammation increasing overtime in both the brain and spinal cord (as shown for mice that received 8.8 CD8 T cells in Fig. 3.12), transferred WT CD8 T cells accumulated in both the brain and spinal cord (Fig. 3.16a). This finding is consistent with previous reports demonstrating similar infiltration of naïve OVA-specific T cells and MBP-specific T cells to the inflamed CNS during EAE[96]. Although there were similar numbers of transferred WT and 8.8 CD8 T cells in the spleen at day 4 (WT CD8 T cells: $10.6x10^4$; 8.8 CD8 T cells: $9.4x10^4$), the numbers decreased overtime in the spleen of CD4-initiated/$CD8_{8.8}$ and not CD4-initiated/$CD8_{WT}$ EAE mice. This may suggest that 8.8 CD8 T cells are recruited from the periphery to the CNS at a higher extent compared to WT CD8 T cells. However, more WT CD8 T cells were isolated from the brain and spinal cord at days 5, 6, and 7 compared to 8.8 CD8 T cells. We hypothesize that the discrepancy in WT and 8.8 CD8 T cell numbers isolated from the brain and spinal cord arises from the difficulty in recovering activated T cells from tissues. The 8.8 CD8 T cells are activated within the CNS and common methods of isolation are inefficient for activated, antigen-specific CD8 T cells in non-lymphoid tissues[97]. Thus, it is likely that the numbers of 8.8 CD8 T cells within the CNS are actually higher than what we have observed after processing the tissue. Additionally, we do not know the location of these CD8 T cells within the CNS. Previous studies found that OVA-specific T cells entered the meninges similar to MBP-specific T cells, but unlike MBP-specific T cells did not enter the parenchyma[98]. Therefore,

although the WT CD8 T cells are present in the CNS, they may not be in an anatomic location poised to contribute to disease pathogenesis.

At day 7, WT CD8 T cells exhibited a similar phenotypic profile, including a predominance of T_{EM} cells in the brain and spinal cord, and the expression of IFNγ, TNFα, FasL, and granzyme-B (Fig. 3.16b-d). Interestingly, when comparing the expression of IFNγ, TNFα, FasL, and granzyme-B by WT versus 8.8 CD8 T cells, only the increase in IFNγ by 8.8 CD8 T cells in the brain was antigen-specific (Fig. 3.16c,d). Together these data indicate that, apart from the antigen-specific response of IFNγ production by 8.8 CD8 T cells in the brain, expression of other activation markers is caused by the inflammatory milieu initiated by CD4 T cells the CNS. However, these analyses revealed a striking difference between 8.8 and WT CD8 T cells in that only 8.8 CD8 T cells exhibited a higher frequency of cells expressing these activation markers in the brain versus the spinal cord (Fig. 3.16c,d).

Recruitment from the periphery is important for the maintenance of 8.8 CD8 T cell numbers in the brain and spinal cord.

The preferential accumulation of 8.8 CD8 T cells in the brain could result from differences in their recruitment from the periphery, proliferation, or survival in the brain versus the spinal cord. We compared 8.8 CD8 T cell recruitment by administering the spingosine-1-phosphate receptor modulator (FTY720), which sequesters lymphocytes in secondary lymphoid tissues[99], to mice with CD4-initiated/$CD8_{8.8}$ EAE on day 6 and analyzed the numbers of 8.8 CD8 T cells in the brain and spinal cord one day later. If there was greater recruitment of 8.8 CD8 T cells to the brain compared to the spinal cord, a larger fold-decrease in 8.8 CD8 T cell number in

the brain compared to the spinal cord should be observed in treated versus untreated mice. However, the similar fold-decrease in 8.8 CD8 T cell number observed in both CNS tissues following FTY720 administration is not consistent with differential recruitment of 8.8 CD8 T cells from the periphery to the brain versus the spinal cord (Fig. 3.17). These data suggest that recruitment is important to maintain 8.8 CD8 T cells in both the brain and spinal cord, and does not account for the preferential accumulation of 8.8 CD8 T cells in the brain. Either proliferation or increased survival may contribute to the increase in 8.8 CD8 T cell number overtime in the brain compared to the spinal cord.

8.8 CD8 T cells proliferate to a similar extent in the brain and spinal cord.

To analyze 8.8 CD8 T cell proliferation in the brain and spinal cord, we induced CD4-initiated EAE in intact TCR transgenic 8.8 mice and examined Ki67 expression in the brain, spinal cord, and spleen at day 7. Although a higher frequency of 8.8 CD8 T cells were proliferating in the brain and spinal compared to the spleen, there was no difference in proliferation between the brain and spinal cord (Fig. 3.18a,b). We also determined the levels of bromodeoxyuridine (BrdU) incorporation in 8.8 CD8 T cells from mice with CD4-initiated/$CD8_{8.8}$ EAE at days 6 and 7 post-CD4 T cell transfer. Consistent with the previous experiment, there was a similar extent of BrdU incorporation in the brain, spinal cord, and spleen at day 6 and 7 post-CD4 T cell transfer (Fig. 3.18c). In both experiments, there was a fairly low frequency of proliferating 8.8 CD8 T cells (Fig. 3.18). These data are consistent with reports demonstrating limited proliferation of T cells in the CNS during EAE, possibly due to nitric oxide mediated inhibition of proliferation[100-102]. Collectively, the similar extent of Ki67

expression and BrdU incorporation in 8.8 CD8 T cells in the brain and spinal cord suggests that proliferation does not account for the preferential accumulation of 8.8 CD8 T cells in the brain.

A higher frequency of 8.8 CD8 T cells die in the spinal cord compared to the brain.

Apoptosis is an important mechanism for the clearance of CNS infiltrating cells[100] and we hypothesized that 8.8 CD8 T cells may exhibit differential survival in the brain compared to the spinal cord. Using a cell-impermeable amine-reactive dye, we determined the percentage of dead 8.8 CD8 T cells in the brain, spinal cord, and spleen at day 7 post CD4-T cell transfer in WT and intact 8.8 TCR transgenic mice. 8.8 CD8 T cell death was observed in the brain and spinal cord with minimal cell death in the spleen (Fig. 3.19a). However, a significantly higher frequency of 8.8 CD8 T cells in the spinal cord stained positive for the amine-reactive dye, indicating a higher frequency of cell death in the spinal cord compared to the brain (Fig. 3.19b). In our CD4-initiated EAE model, the inflammation observed in the spinal cord is more severe than in the brain (data not shown). Therefore, increased cell death in the spinal cord may be a general effect resulting from higher overall inflammation in the tissue. To test this hypothesis, we also analyzed the frequency of cell death in the donor CD4 T cell population. Similar to the 8.8 CD8 T cells, the death of donor CD4 T cells was significantly higher in the spinal cord compared to the brain (Fig. 3.19c). This suggests that the 8.8 CD8 T cell death is not specific to 8.8 CD8 T cells and is a result of increased inflammation in the spinal cord. Similarly, there was a significantly higher frequency of dead WT CD8 T cells in the spinal cords compared to the brains of WT mice with CD4-initiated EAE (Fig. 3.19d). As donor CD4 T cell and WT CD8 T cell numbers increase in both the brain and spinal cord (Fig. 3.12 and 3.16a), it is unlikely that the difference in cell death accounts for the preferential increase in 8.8 CD8 T cells in the brain.

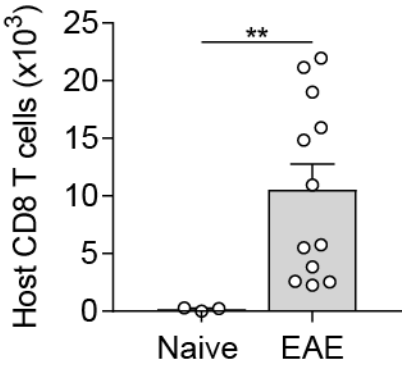

Figure 3.1. 8.8 CD8 T cells are recruited to the CNS during CD4-initiated EAE. EAE was induced by transfer of Thy1.1$^+$ MOG-specific CD4 T cells into Thy1.2$^+$ intact TCR transgenic 8.8 mice. The number of Thy1.2$^+$ 8.8 CD8 T cells (mean + SEM) was determined at peak disease (days 7-11) for mice with EAE (n=12) compared to irradiated control mice that did not receive donor CD4 T cells (n=3). Data are compiled from 2 independent experiments. Statistical significance was determined using a Mann-Whitney *U* test. **p<0.01.

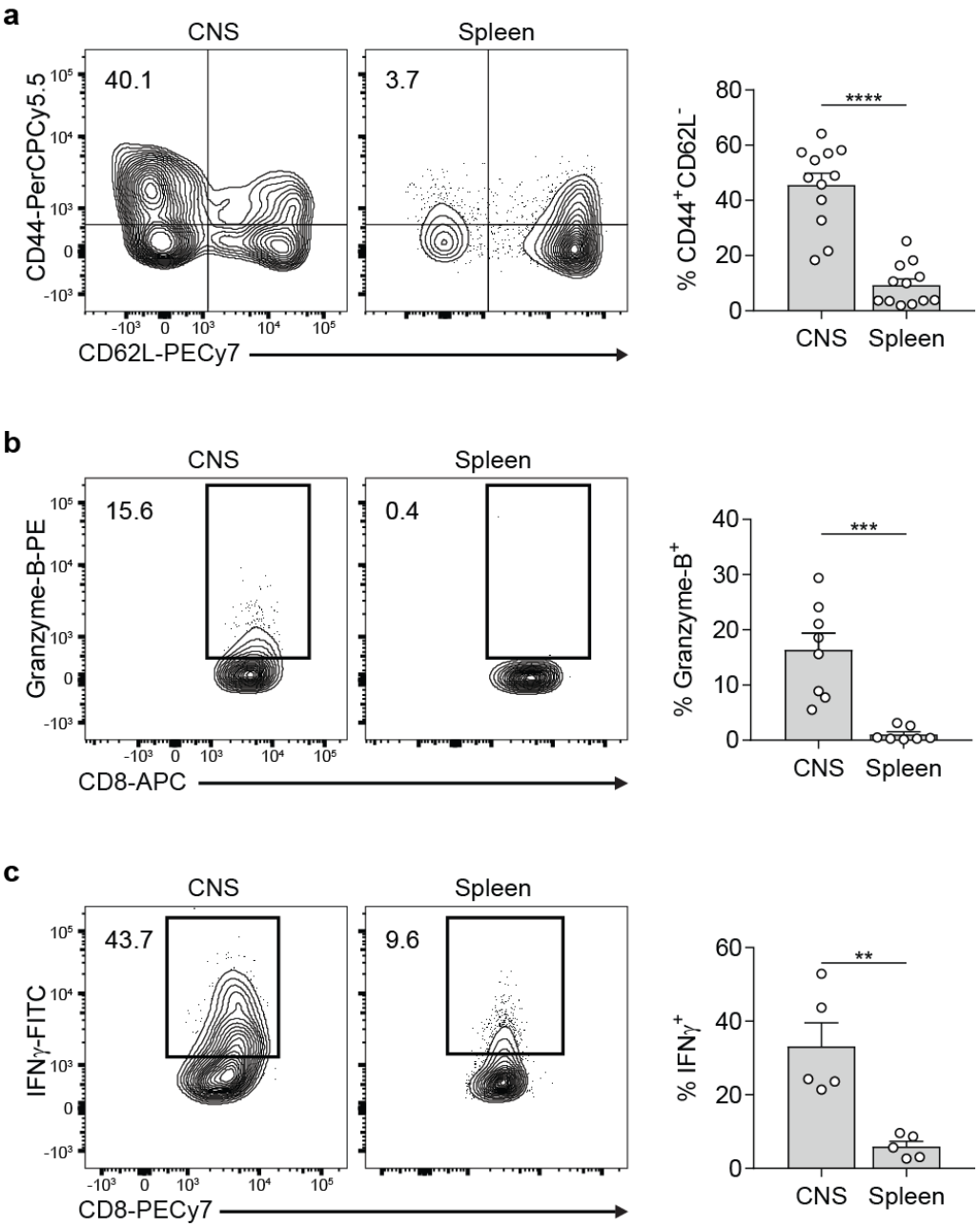

Figure 3.2. 8.8 CD8 T cells acquire an activated, effector phenotype in the CNS and not spleen in mice with CD4-initiated EAE. EAE was induced by transfer of Thy1.1$^+$ MOG-specific CD4 T cells into Thy1.2$^+$ intact TCR transgenic 8.8 mice and mononuclear cells were harvested from the CNS and spleen at peak disease. Frequency of **(a)** CD44$^+$CD62L$^-$ activated (n=12) and **(b)** granzyme-B-expressing (n=8) 8.8 CD8 T cells. **(c)** Mononuclear cells were stimulated with PMA and ionomycin prior to intracellular staining for IFNγ. Frequency of IFNγ-producing 8.8 CD8 T cells is shown (n=5). Graphs show mean + SEM (one symbol per mouse) and are compiled from **(a, b)** two and **(c)** one independent experiments. Statistical significance was determined using a Mann-Whitney *U* test. ** p<0.01, *** p<0.001, **** p<0.0001.

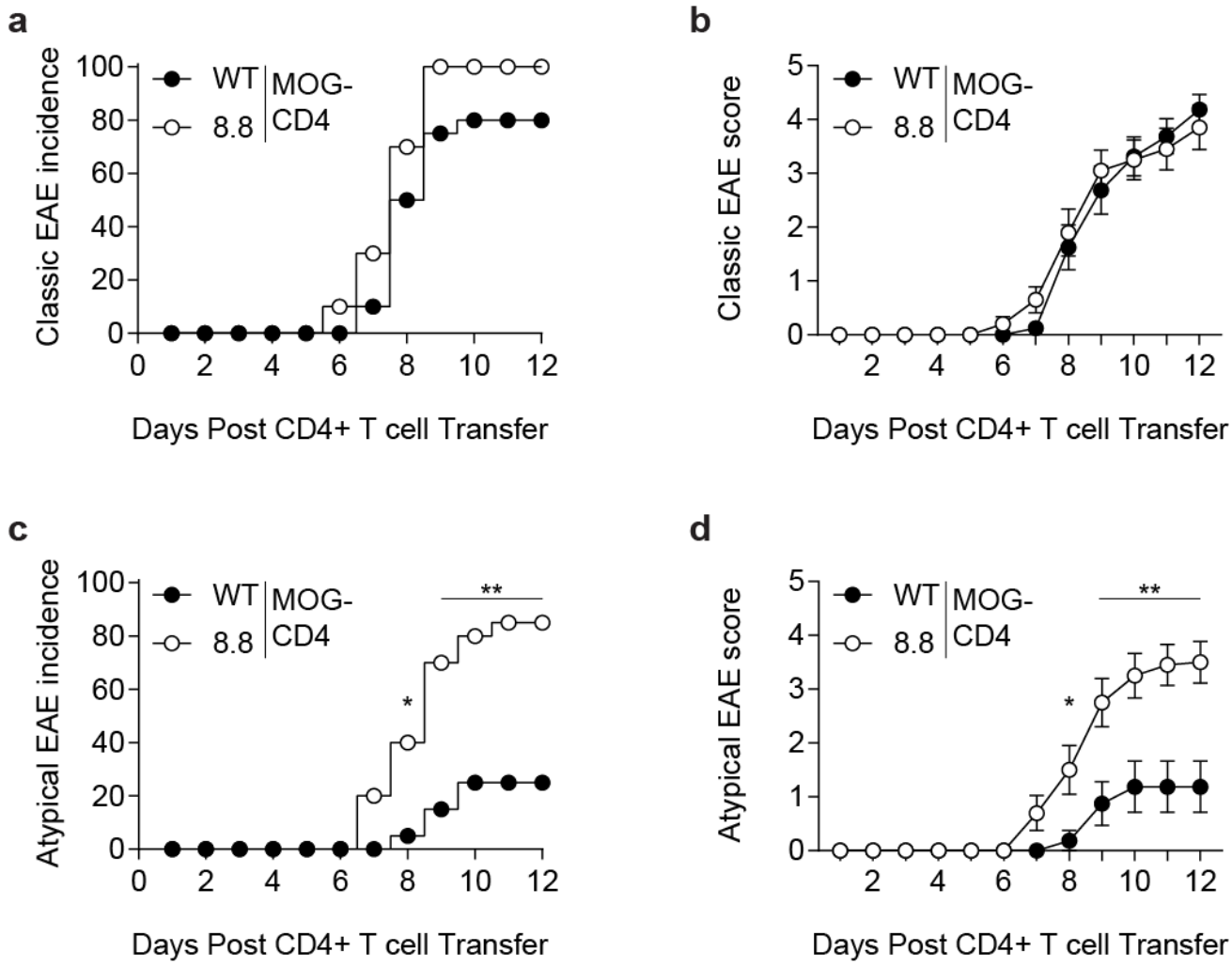

Figure 3.3. 8.8 CD8 T cells enhance incidence and severity of atypical but not classic EAE induced by CD4 T cells in an intact TCR transgenic model. EAE was induced by transfer of Thy1.1^{+} MOG-specific CD4 T cells into Thy1.2^{+} WT or intact TCR transgenic 8.8 mice and mice were monitored for clinical signs. **(a)** Incidence of classic EAE among all mice in each indicated group. **(b)** Clinical scores of classic EAE symptoms (mean $\pm$ SEM) for mice that developed EAE. **(c)** Incidence of atypical EAE among all mice in each indicated group. **(d)** Clinical scores of atypical EAE symptoms (mean $\pm$ SEM) for mice that developed EAE. Data are compiled from 3 independent experiments; n=20 for each group. Statistical significance was determined using **(a,c)** Fisher's Exact test or **(b,d)** Mann-Whitney *U* test. *$p<0.05$, ** $p<0.01$.

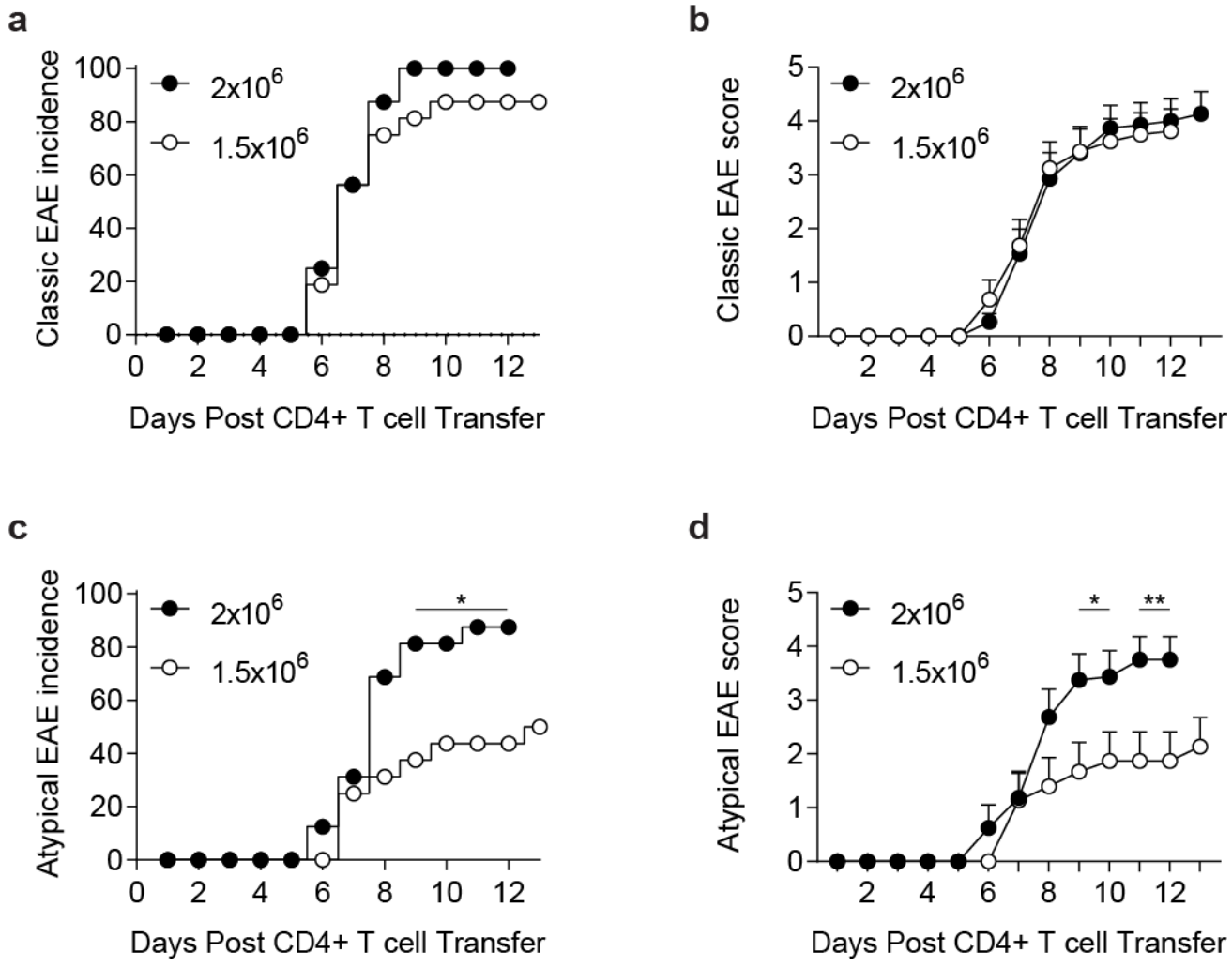

Figure 3.4. Development of a less severe CD4-initiated EAE model. EAE was induced by transfer of $2x10^6$ or $1.5x10^6$ MOG-specific CD4 T cells into WT mice and mice were monitored for clinical signs. **(a)** Incidence of classic EAE among all mice in each indicated group. **(b)** Clinical scores of classic EAE symptoms (mean $\pm$ SEM) for mice that developed EAE. **(c)** Incidence of atypical EAE among all mice in each indicated group. **(d)** Clinical scores of atypical EAE symptoms (mean $\pm$ SEM) for mice that developed EAE. Data are compiled from 3 independent experiments; n=16 for each group. Statistical significance was determined using **(a,c)** Fisher's Exact test or **(b,d)** Mann-Whitney *U* test. *$p<0.05$, ** $p<0.01$.

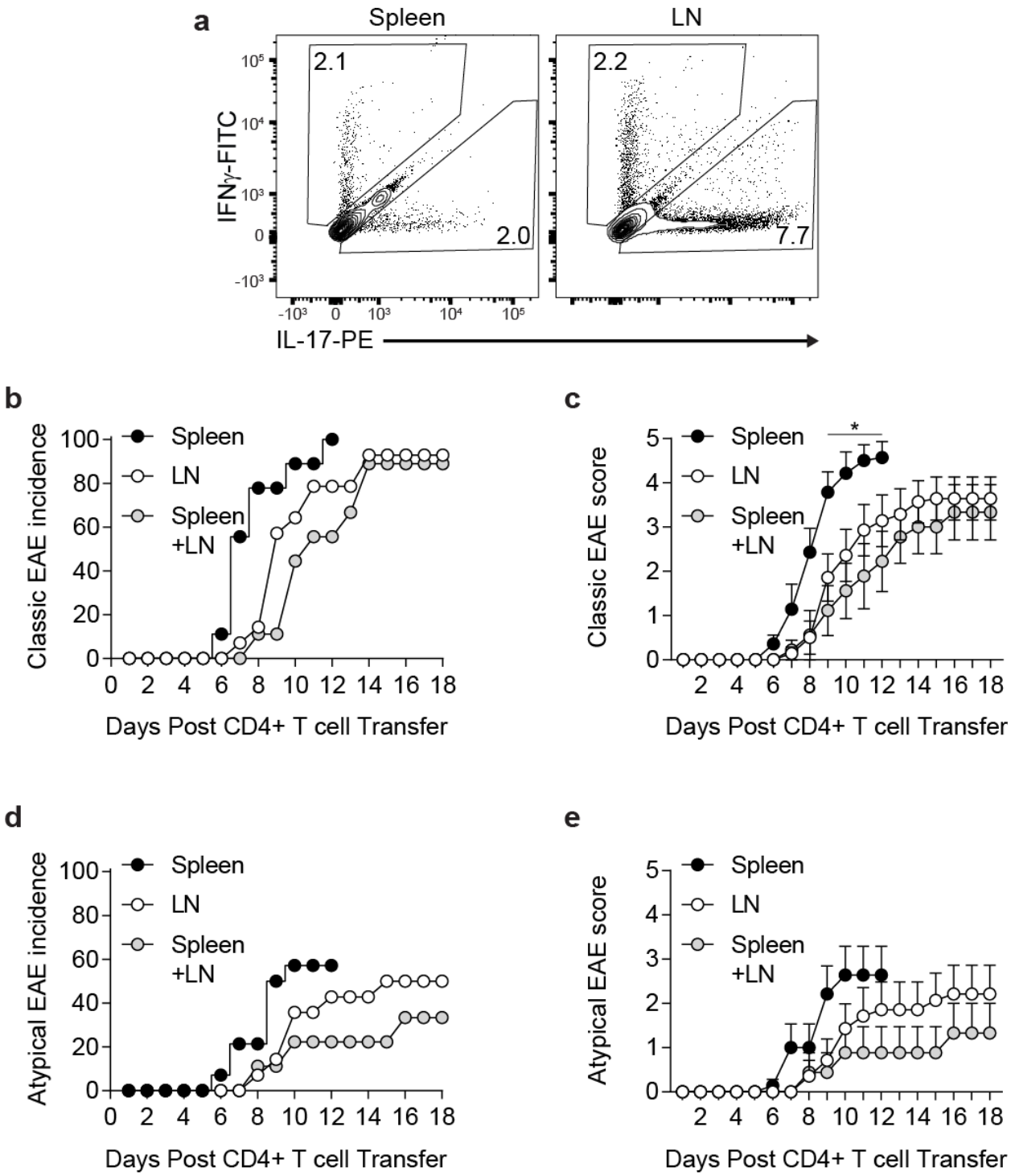

Figure 3.5. Splenocytes have a lower IL-17:IFNγ ratio and induce more severe disease compared to LN cells. (a) Donor CD4 T cells were isolated from the spleen and lymph nodes (LN) and cytokine production following restimulation with MOG_{97-114} peptide was analyzed prior to adoptive transfer. Representative flow cytometry of 3 independent experiments. **(c-e)** EAE was induced by transfer of $1.5x10^6$ MOG-specific CD4 T cells from the spleen (n=14), LN

(n=14) or a 1:1 mix of spleen and LN (n=9) into WT mice and mice were monitored for clinical signs. **(b)** Incidence of classic EAE among all mice in each indicated group. **(c)** Clinical scores of classic EAE symptoms (mean ± SEM) for mice that developed EAE. **(d)** Incidence of atypical EAE among all mice in each indicated group. **(e)** Clinical scores of atypical EAE symptoms (mean ± SEM) for mice that developed EAE. Data are compiled from 3 independent experiments. Statistical significance was determined using **(b,d)** Fisher's Exact test or **(c,e)** Kruskal-Wallis with Dunn's post-test. *$p<0.05$.

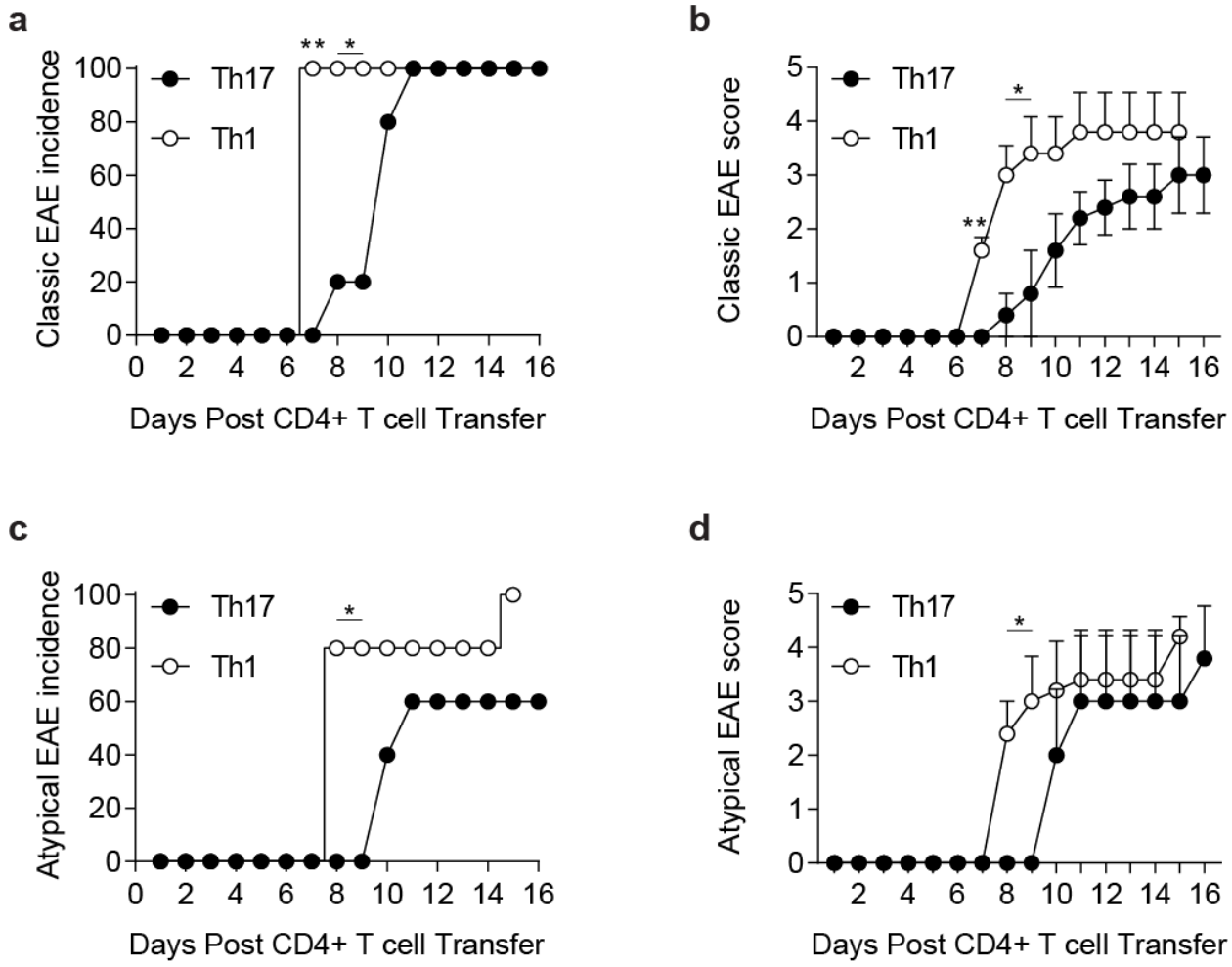

Figure 3.6. Th1-skewed donor CD4 T cells induce more severe disease compared to Th17-skewed donor CD4 T cells. EAE was induced by transfer of $1.5x10^6$ Th17- or Th1-skewed MOG-specific CD4 T cells into WT mice and mice were monitored for clinical signs. **(a)** Incidence of classic EAE among all mice in each indicated group. **(b)** Clinical scores of classic EAE symptoms (mean ± SEM) for mice that developed EAE. **(c)** Incidence of atypical EAE among all mice in each indicated group. **(d)** Clinical scores of atypical EAE symptoms (mean ± SEM) for mice that developed EAE. Data are compiled from one experiment; n=5 for each group. Statistical significance was determined using **(a,c)** Fisher's Exact test or **(b,d)** Mann-Whitney *U* test. *$p<0.05$, ** $p<0.01$.

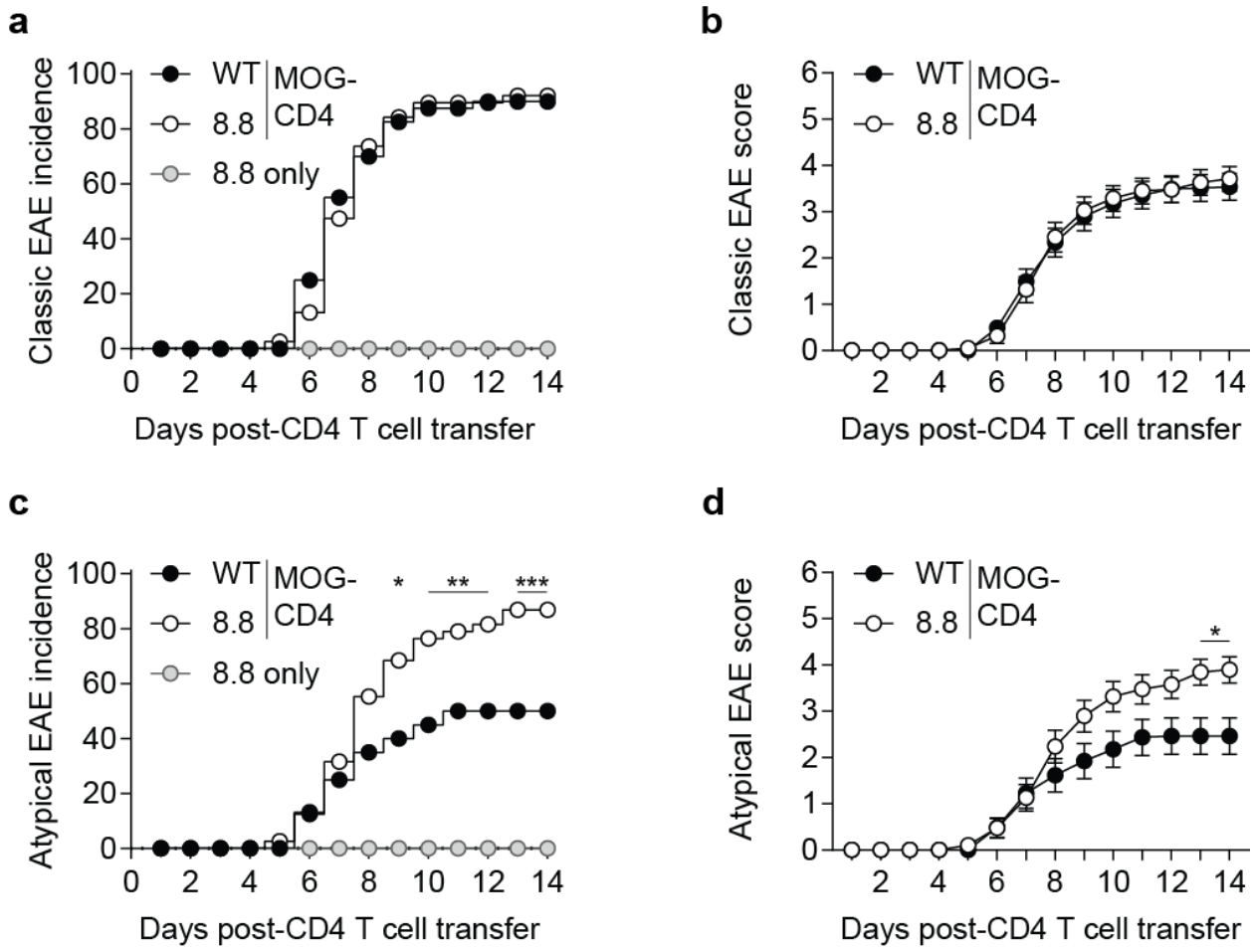

Figure 3.7. 8.8 CD8 T cells enhance incidence and severity of atypical but not classic EAE induced by CD4 T cells in a polyclonal model. EAE was induced by transfer of MOG-specific CD4 T cells into WT mice that received either WT or 8.8 CD8 T cells one day earlier. Control mice that received 8.8 CD8 T cells and no CD4 T cells are designated "8.8 only". **(a)** Incidence of classic EAE among all mice in each indicated group. **(b)** Clinical scores of classic EAE symptoms (mean $\pm$ SEM) for mice that developed EAE. **(c)** Incidence of atypical EAE among all mice in each indicated group. **(d)** Clinical scores of atypical EAE symptoms (mean $\pm$ SEM) for mice that developed EAE. Data are compiled from 8 independent experiments; n=40 for EAE-induced recipients of WT CD8 T cells; n=38 for EAE-induced recipients of 8.8 T cells; n=5 for mice that received only 8.8 T cells Statistical significance was determined using **(a,c)** Fisher's exact test or **(b,d)** Mann-Whitney *U* test. * $p<0.05$, ** $p<0.01$, *** $p< 0.001$.

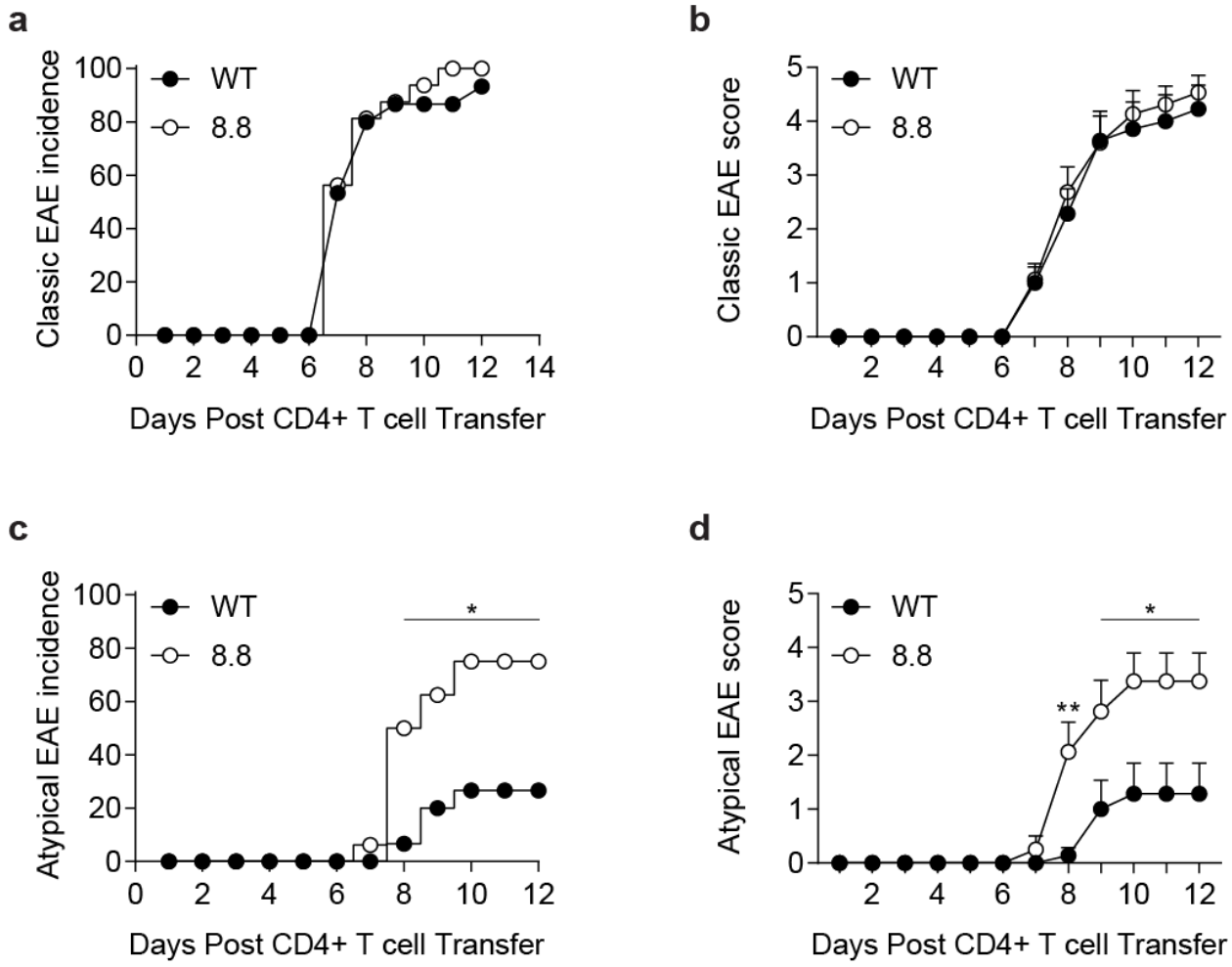

Figure 3.8. 8.8 CD8 T cells enhance incidence and severity of atypical but not classic EAE induced by CD4 T cells in a polyclonal model when 8.8 CD8 T cells are transferred one day post-CD4 T cell transfer. EAE was induced by transfer of MOG-specific CD4 T cells into WT mice and either WT or 8.8 CD8 T cells were transferred one day later. **(a)** Incidence of classic EAE among all mice in each indicated group. **(b)** Clinical scores of classic EAE symptoms (mean ± SEM) for mice that developed EAE. **(c)** Incidence of atypical EAE among all mice in each indicated group. **(d)** Clinical scores of atypical EAE symptoms (mean ± SEM) for mice that developed EAE. Data are compiled from 8 independent experiments; n=40 for EAE-induced recipients of WT CD8 T cells; n=38 for EAE-induced recipients of 8.8 T cells; n=5 for mice that received only 8.8 T cells Statistical significance was determined using **(a,c)** Fisher's exact test or **(b,d)** Mann-Whitney *U* test. * $p<0.05$, ** $p<0.01$.

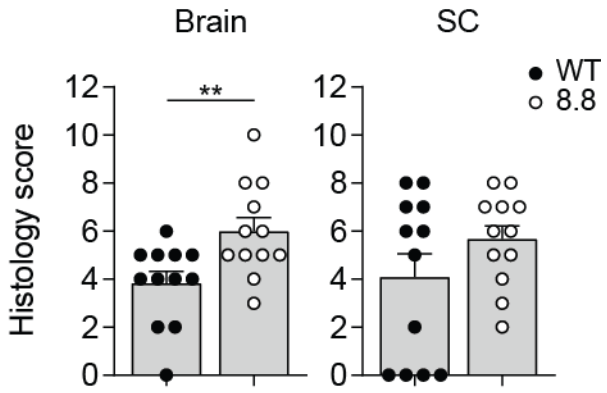

Figure 3.9. 8.8 CD8 T cells enhance tissue injury in the brain during CD4-initiated EAE. EAE was induced by transfer of MOG-specific CD4 T cells into WT mice that received either WT or 8.8 CD8 T cells one day earlier. Histology scores (assigned as described in Methods, mean + SEM) are shown for brain and spinal cord (SC) tissues harvested 7 days post-CD4 T cell transfer from mice that had received WT or 8.8 CD8 T cells. Data are compiled from 2 independent experiments, n=12 mice per group. Statistical significance was determined using Mann-Whitney *U* test. ** $p<0.01$.

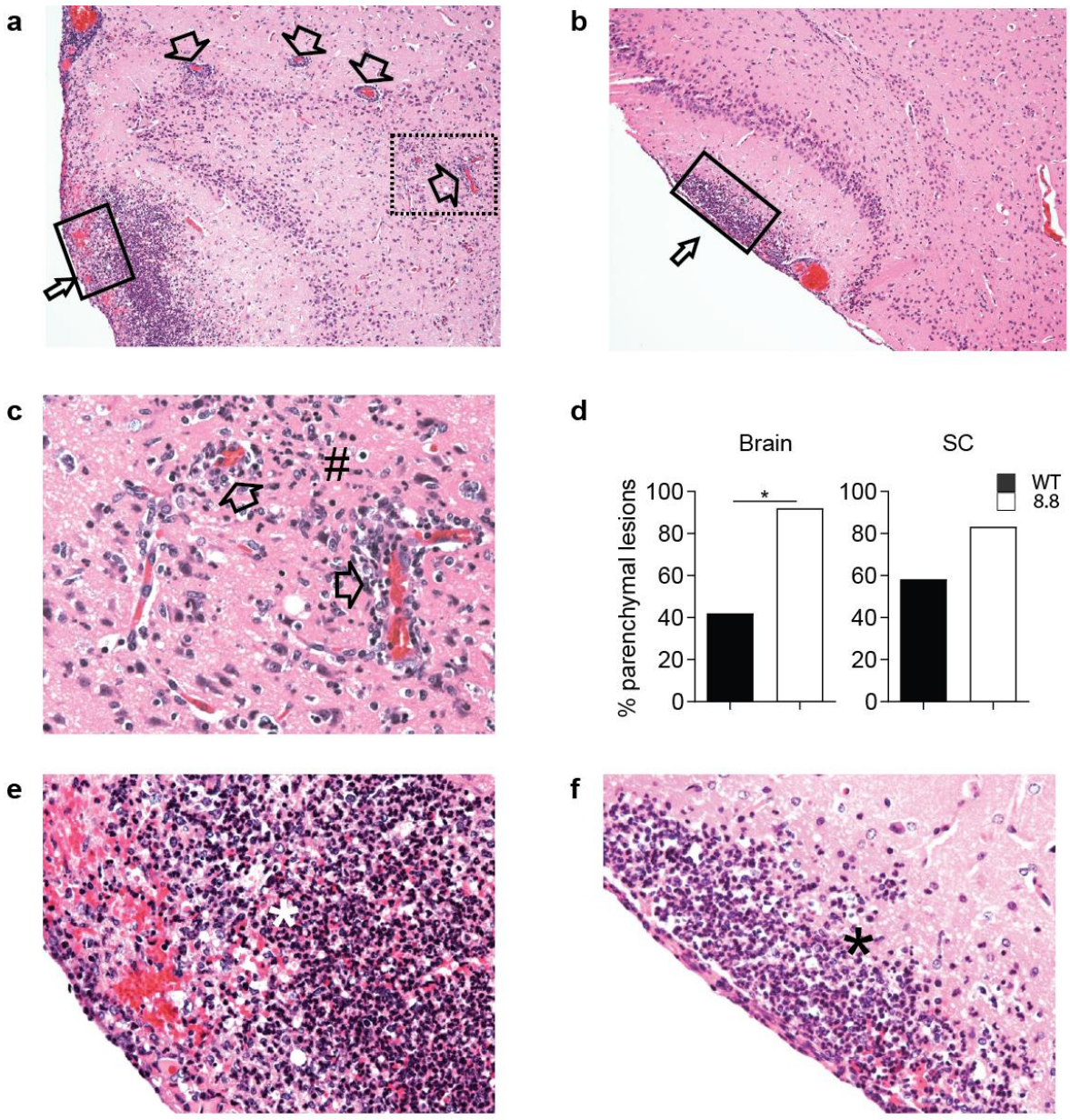

Figure 3.10. 8.8 CD8 T cells increase the frequency of parenchymal vessel-associated lesions in the brain during CD4-initiated EAE. EAE was induced by transfer of MOG-specific CD4 T cells into WT mice that received either WT or 8.8 CD8 T cells one day earlier. **(a,b)** Representative brain sections from the cortical region caudal to the olfactory bulb harvested from mice 7 days post-CD4 T cell transfer that had received **(a)** 8.8 or **(b)** WT CD8 T cells. Lesions in both groups demonstrate substantial necrotizing lesions involving the meninges and submeningeal regions (arrows). However, lesions in CD4-initiated/$CD8_{8.8}$ EAE mice (a) have additional complexity in that perivascular and closely associated parenchymal areas distal from the site of meningeal involvement (arrowheads) are more frequently observed, and have focal accumulations of neutrophilic and mononuclear inflammatory cells. **(c)** Higher power magnification of the dashed boxed area in (a) shows perivascular inflammatory cell cuffing

(arrowheads) along with parenchymal inflammatory cell accumulations (hash mark). **(d)** The percentage of mice that exhibited parenchymal blood vessel-associated lesions as well as meningeal lesions (data are compiled from two independent experiments; n=12 per group). **(e,f)** show higher power magnification of the solid boxed areas in (a) and (b) respectively. Markedly necrotic areas (asterisks) are observed in both groups that are heavily populated with predominantly neutrophils interspersed with necrotic cell debris. Original magnification **(a,b)** 10x **(c,e,f)** 40x. Data are representative of 12 mice per group from two independent experiments. **(d)** Statistical significance was determined using Fisher's exact test. * $p<0.05$.

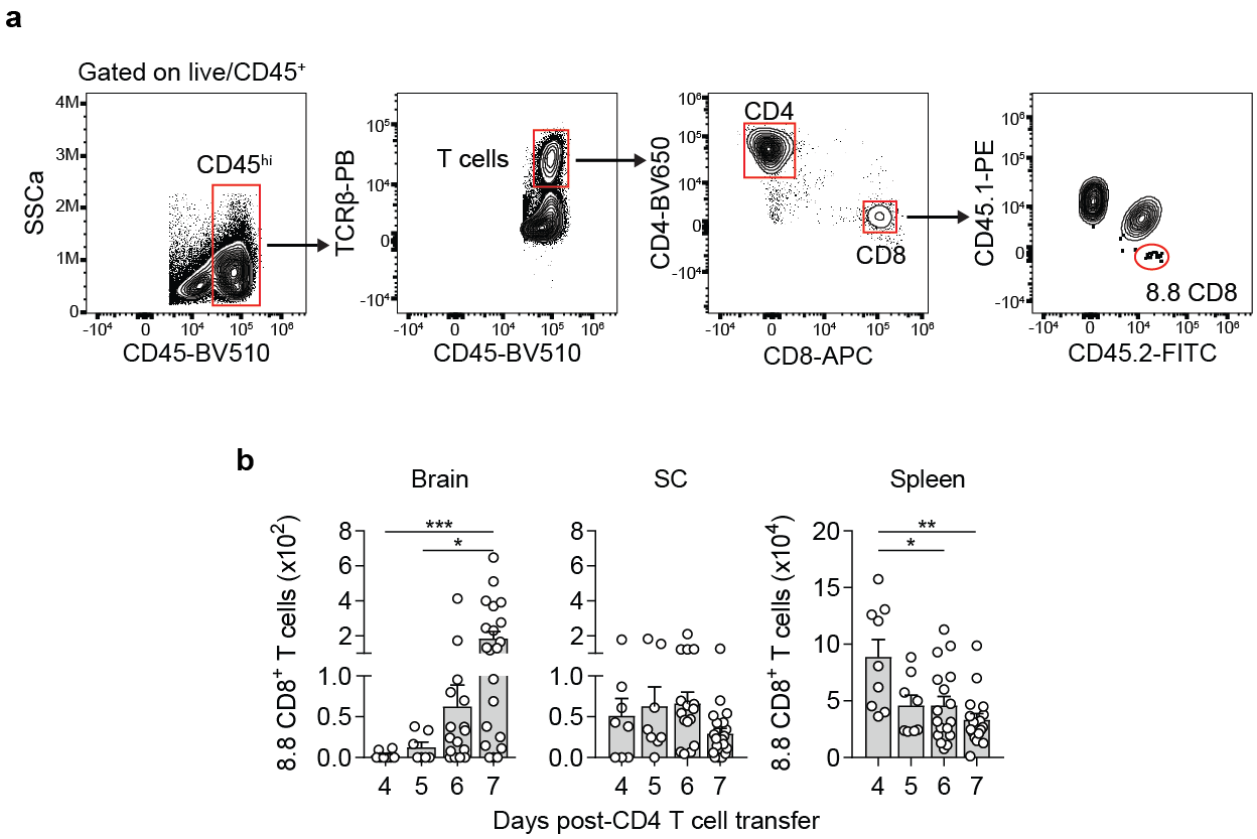

Figure 3.11. 8.8 CD8 T cells accumulate in the brain and not spinal cord in mice with CD4-initiated EAE. EAE was induced by the transfer of CD45.1.2$^+$ MOG-specific CD4 T cells into CD45.1.1$^+$ mice that had received CD45.2.2$^+$ 8.8 CD8 T cells one day prior to disease induction. **(a)** A representative flow cytometry analysis of mononuclear cells isolated from a brain harvest 7 days post-CD4 T cell transfer is shown to illustrate the gating strategy for 8.8 CD8 T cells. **(b)** The total number of 8.8 CD8 T cells was determined for brain, spinal cord (SC) and spleen by flow cytometry at the indicated days post-CD4 T cell transfer (n≥8 for each day). Graphs show mean + SEM (one symbol per mouse); data are compiled from at least two independent experiments. Statistical significance was determined using Kruskal-Wallis with Dunn's post-test. * p<0.05, ** p<0.01, *** p< 0.001.

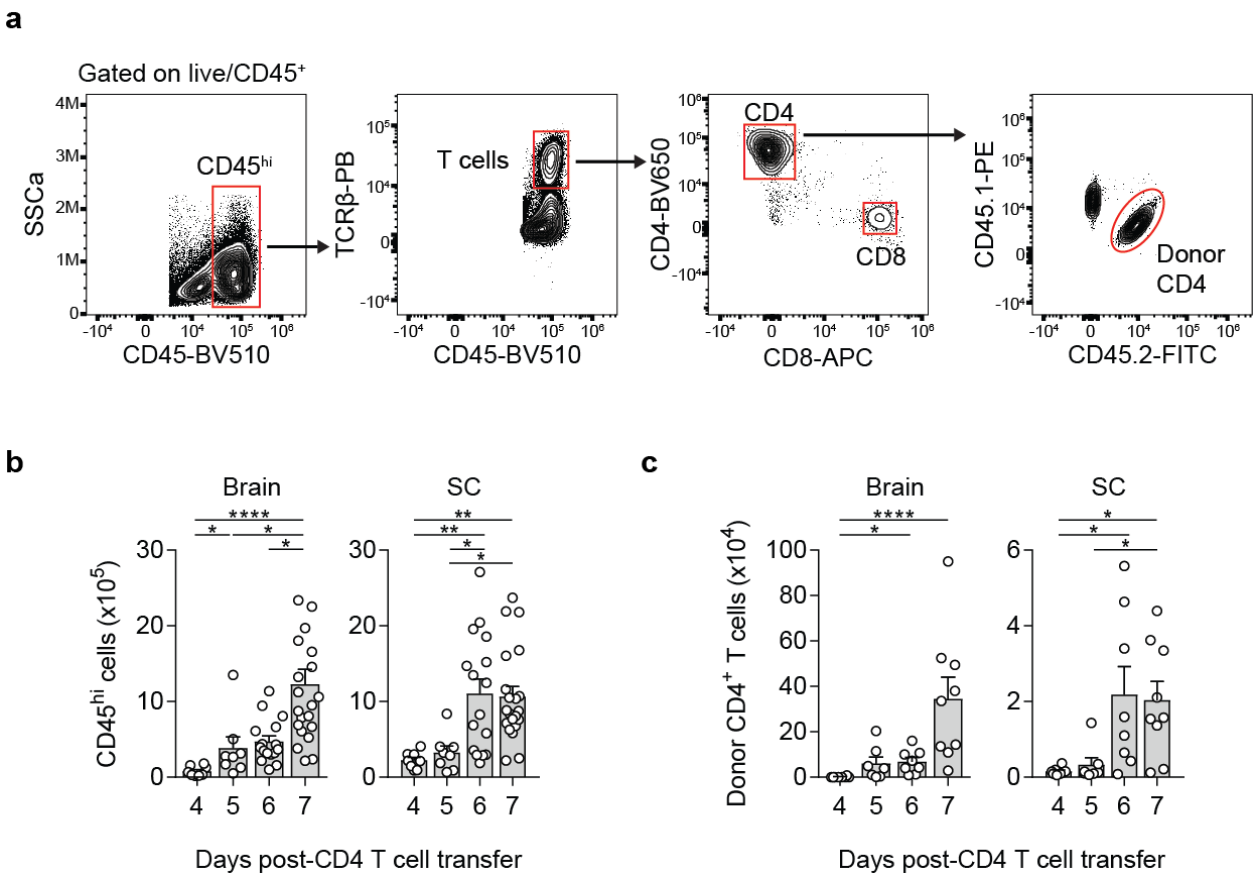

Figure 3.12. CD45^{hi} infiltrating immune cells and donor CD4 T cells accumulate in both the brain and spinal cord during CD4-initiated EAE. EAE was induced by transferring CD45.1.2^{+} MOG-specific CD4 T cells into CD45.1.1^{+} mice that received CD45.2.2^{+} 8.8 CD8 T cells one day prior to CD4 T cell transfer. **(a)** A representative flow cytometry analysis of mononuclear cells isolated from a brain harvested 7 days post-CD4 T cell transfer is shown to illustrate the gating strategy used to identify CD45^{hi} cells and donor CD4 T cells. The numbers of **(b)** CD45^{hi} inflammatory cells and **(c)** donor CD4 T cells in the brain and spinal cord (SC) were determined on the indicated days post-CD4 T cell transfer by flow cytometric analyses using this gating strategy. Graphs show mean + SEM (one symbol per mouse) and data are compiled from at least two independent experiments with at least n=8 mice per group. Statistical significance was determined using Kruskal-Wallis with Dunn's post test. * $p<0.05$, ** $p<0.01$, **** $p< 0.0001$.

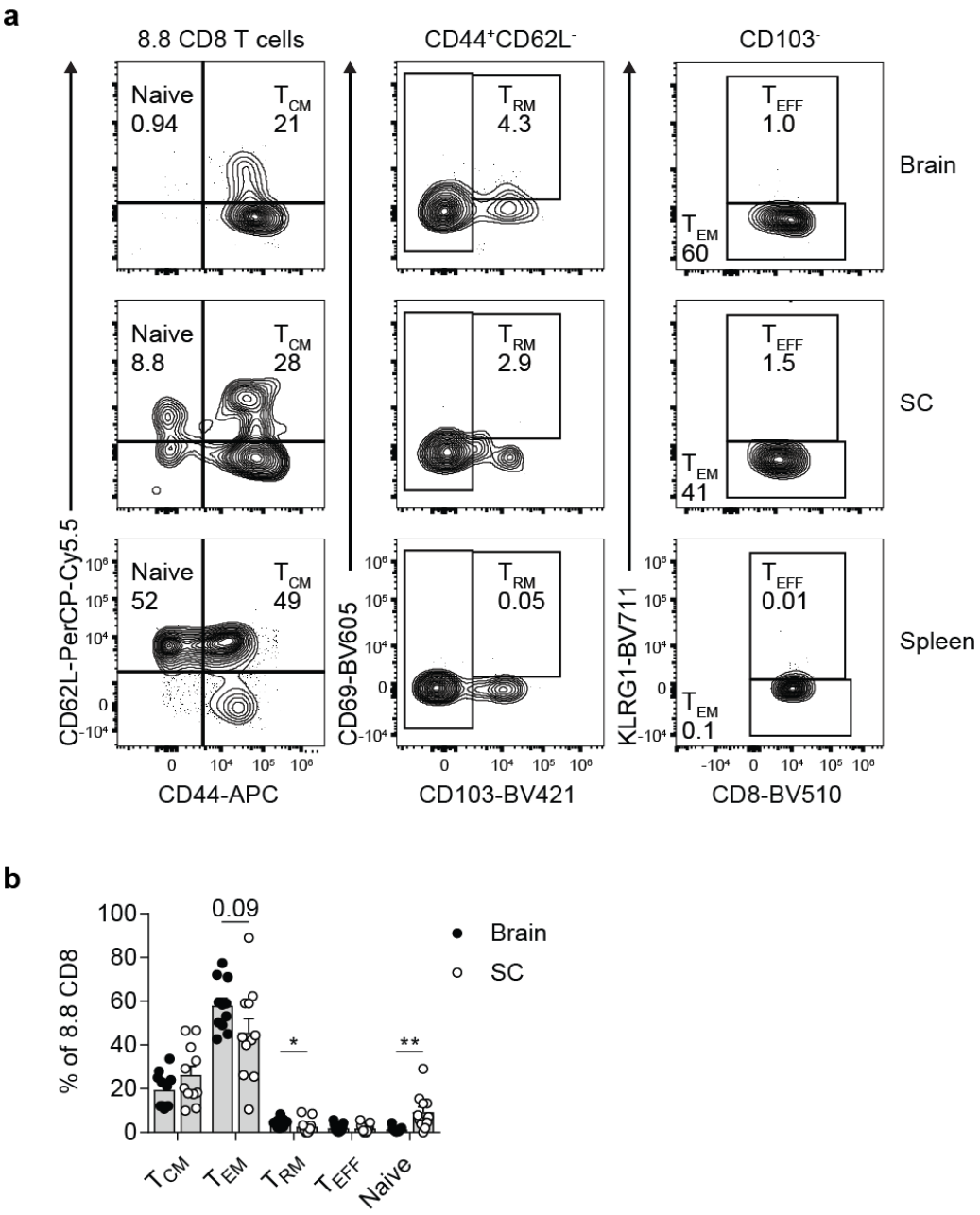

Figure 3.13. 8.8 CD8 T cells acquire an activated effector memory phenotype in the brain and spinal cord during CD4-initiated EAE. EAE was induced by the transfer of CD45.1.1$^+$ MOG-specific CD4 T cells into CD45.2.2$^+$ intact TCR transgenic 8.8 mice. Mononuclear cells from the brain, spinal cord (SC), and spleen were analyzed by flow cytometry at day 7. **(a)** Representative flow cytometry of the identification of 8.8 CD8 T cell subsets in the brain, SC and spleen. Numbers indicate frequencies of 8.8 CD8 T cells. **(b)** The percentage of 8.8 CD8 T cells exhibiting a naïve, central memory (T_{CM}), resident memory (T_{RM}), effector memory (T_{EM}), or effector (T_{EFF}) phenotype as defined in (a). Graphs show mean + SEM (one symbol per mouse) and are compiled from two independent experiments (n=12). Statistical significance was determined using Mann-Whitney *U* test. * $p<0.05$, ** $p<0.01$.

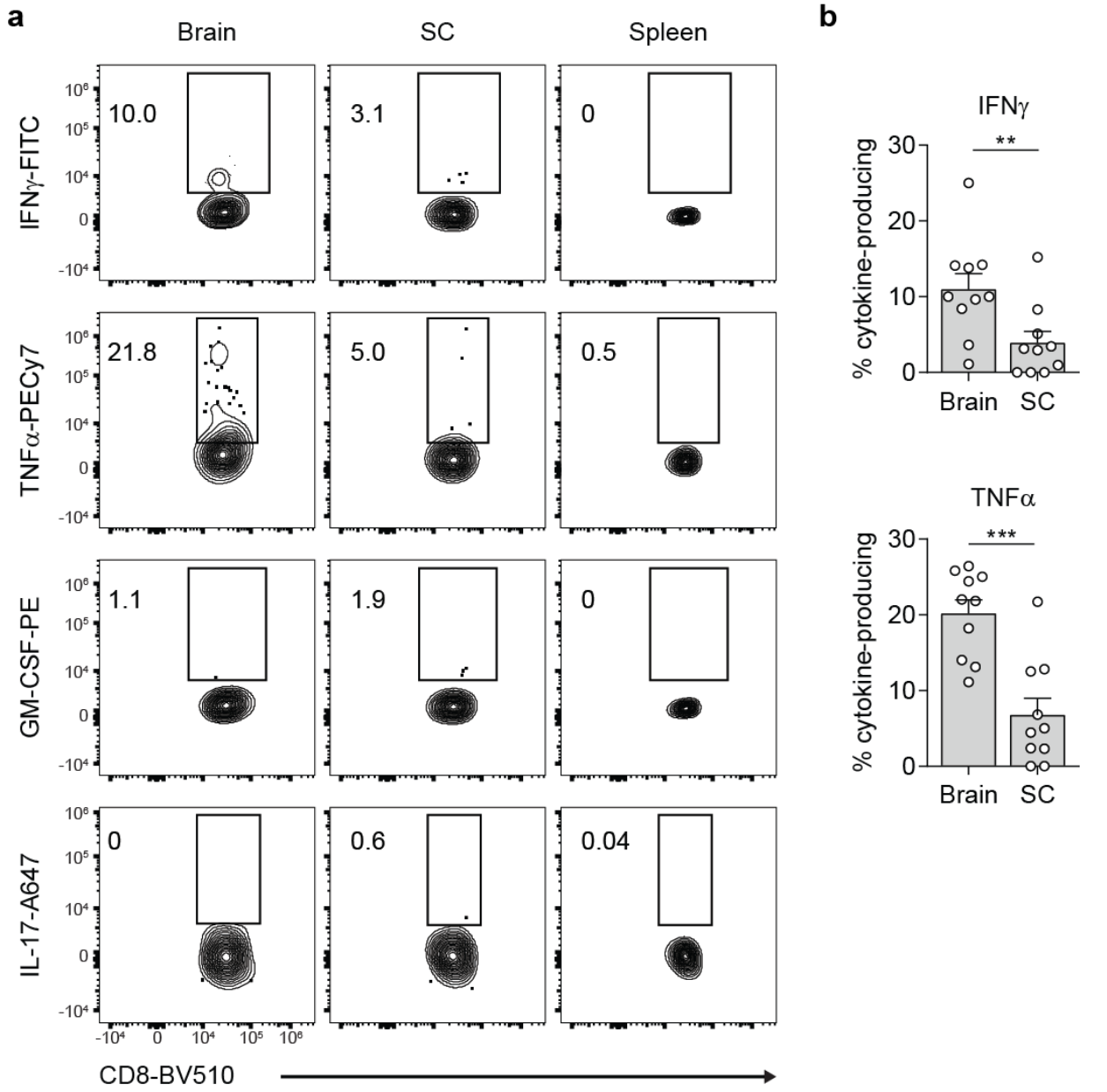

Figure 3.14. A higher frequency of 8.8 CD8 T cells produce IFNγ and TNFα in the brain compared to the spinal cord in CD4-initiated EAE. EAE was induced by transfer of Thy1.1$^+$ MOG-specific CD4 T cells into Thy1.2$^+$ intact TCR transgenic 8.8 mice. Mononuclear cells were isolated from brain, spinal cord (SC), and spleen 7 days post-CD4 T cell transfer and cultured with GolgiPlug without stimulation prior to intracellular staining for cytokines. **(a)** Representative flow cytometry showing IFNγ, TNFα, GM-CSF and IL-17 expression by 8.8 CD8 T cells (gated on CD45$^+$TCRb$^+$CD8$^+$Thy1.2$^+$ cells) in the brain and spinal cord. Data are representative of n=10 mice per group and are compiled from two independent experiments. **(b)** Frequency of cytokine-producing 8.8 T cells were quantified for mice described in (a). Graphs show mean + SEM (one symbol per mouse). Statistical significance was determined using Mann-Whitney *U* test ** $p<0.01$, *** $p< 0.001$.

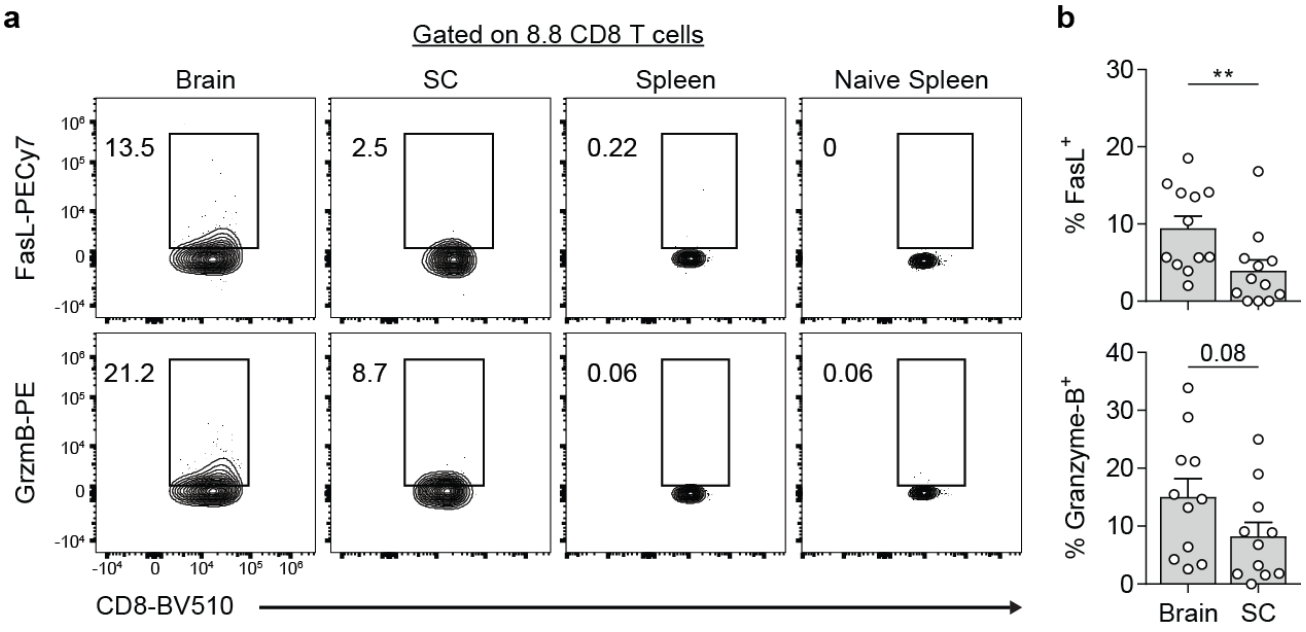

Figure 3.15. A higher frequency of 8.8 CD8 T cells express cytotoxic molecules in the brain compared to the spinal cord in CD4-initiated EAE. EAE was induced by transfer of CD45.1.1+ MOG-specific CD4 T cells into CD45.1.1+ intact TCR transgenic 8.8 mice. Mononuclear cells were isolated from brain and spinal cord (SC) 7 days post-CD4 T cell transfer and analyzed directly *ex vivo*. **(a)** Representative flow cytometry showing FasL and granzyme-B (GrzmB) expression by 8.8 CD8 T cells (gated on CD45+TCRb+CD8+CD45.2.2+ cells) in the brain, spinal cord, and spleen. Staining from a naïve spleen is shown as a negative control. Data are representative of n=12 mice per group and are compiled from two independent experiments. **(b)** Frequency of FasL and granzyme-B expressing 8.8 T cells were quantified for mice described in (a). Graphs show mean + SEM (one symbol per mouse. Statistical significance was determined using Mann-Whitney *U* test. ** $p<0.01$.

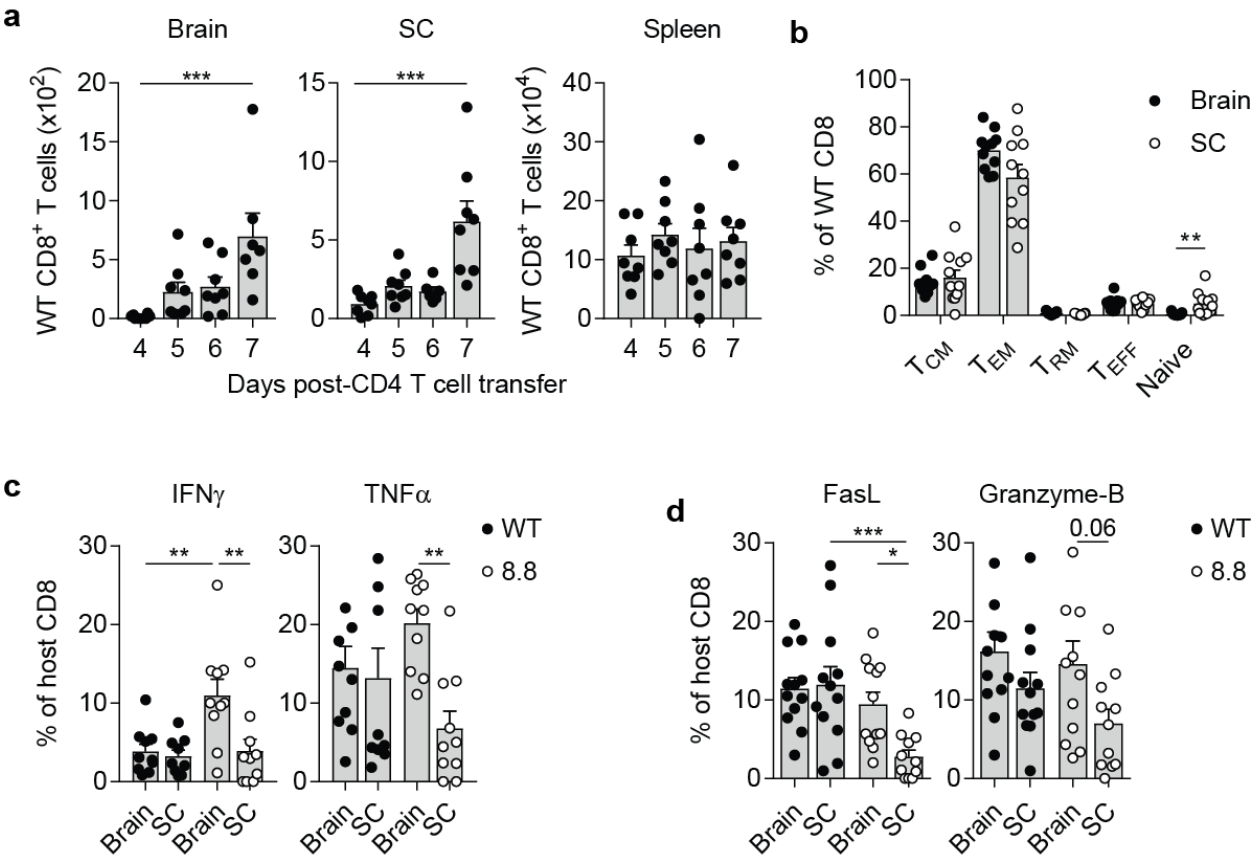

Figure 3.16. WT CD8 T cells accumulate and acquire an activated phenotype in both the brain and spinal cord in mice with CD4-initiated EAE. (a) EAE was induced by the transfer of CD45.1.2$^+$ MOG-specific CD4 T cells into CD45.1.1$^+$ mice that had received CD45.2.2$^+$ WT CD8 T cells one day prior to disease induction. **(a)** The total number of CD45.2.2$^+$ WT CD8 T cells was determined for brain, spinal cord (SC) and spleen by flow cytometry at the indicated days post-CD4 T cell transfer (n≥8 for each day). **(b-d)** EAE was induced by transfer of CD45.1.1$^+$ MOG-specific CD4 T cells into CD45.2.2$^+$ WT mice and **(c,d)** CD45.2.2$^+$ 8.8 mice. Mononuclear cells were isolated from brain and spinal cord 7 days post-CD4 T cell transfer. **(b)** Frequency of CD45.2.2+ WT CD8 T cells exhibiting CD8 T cell subsets as defined in Fig. 3.13 (n=12). **(c)** Frequency of cytokine-producing WT and 8.8 CD8 T cells following culture with GolgiPlug (n=10). **(d)** Frequency of FasL- and granzyme-B-expressing WT and 8.8 CD8 T cells. Graphs show mean + SEM (one symbol per mouse) and are compiled from at least two independent experiments. Statistical significance was determined using **(a)** Kruskal-Wallis with Dunn's post-test, **(b)** Mann-Whitney *U* test, **(c,d)** 2-way ANOVA with Sidaks post-test. * $p<0.05$, ** $p<0.01$, *** $p< 0.001$.

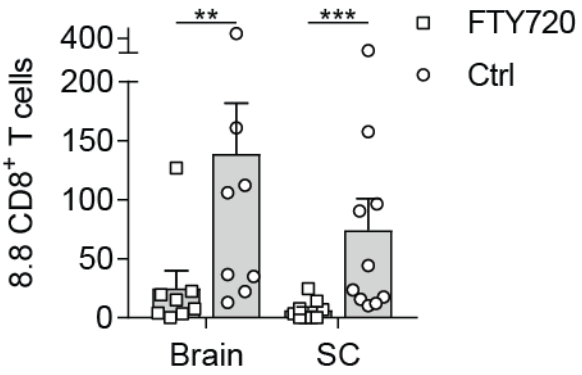

Figure 3.17. Recruitment from the periphery contributes to 8.8 CD8 T cell numbers in the brain and spinal cord. EAE was induced by the transfer of CD45.1.2$^+$ MOG-specific CD4 T cells into CD45.1.1$^+$ mice that had received CD45.2.2$^+$ WT CD8 T cells one day prior to disease induction (n=8). FTY720 or vehicle control were injected 6 days post-CD4 T cell transfer. Brains and spinal cords were harvest 7 days post-CD4 T cell transfer and 8.8 CD8 T cell numbers were determined by flow cytometry. Graphs show mean + SEM (one mouse per symbol) and data are compiled from two independent experiments. Statistical significance was determined using a Mann-Whitney *U* test. ** $p<0.01$.

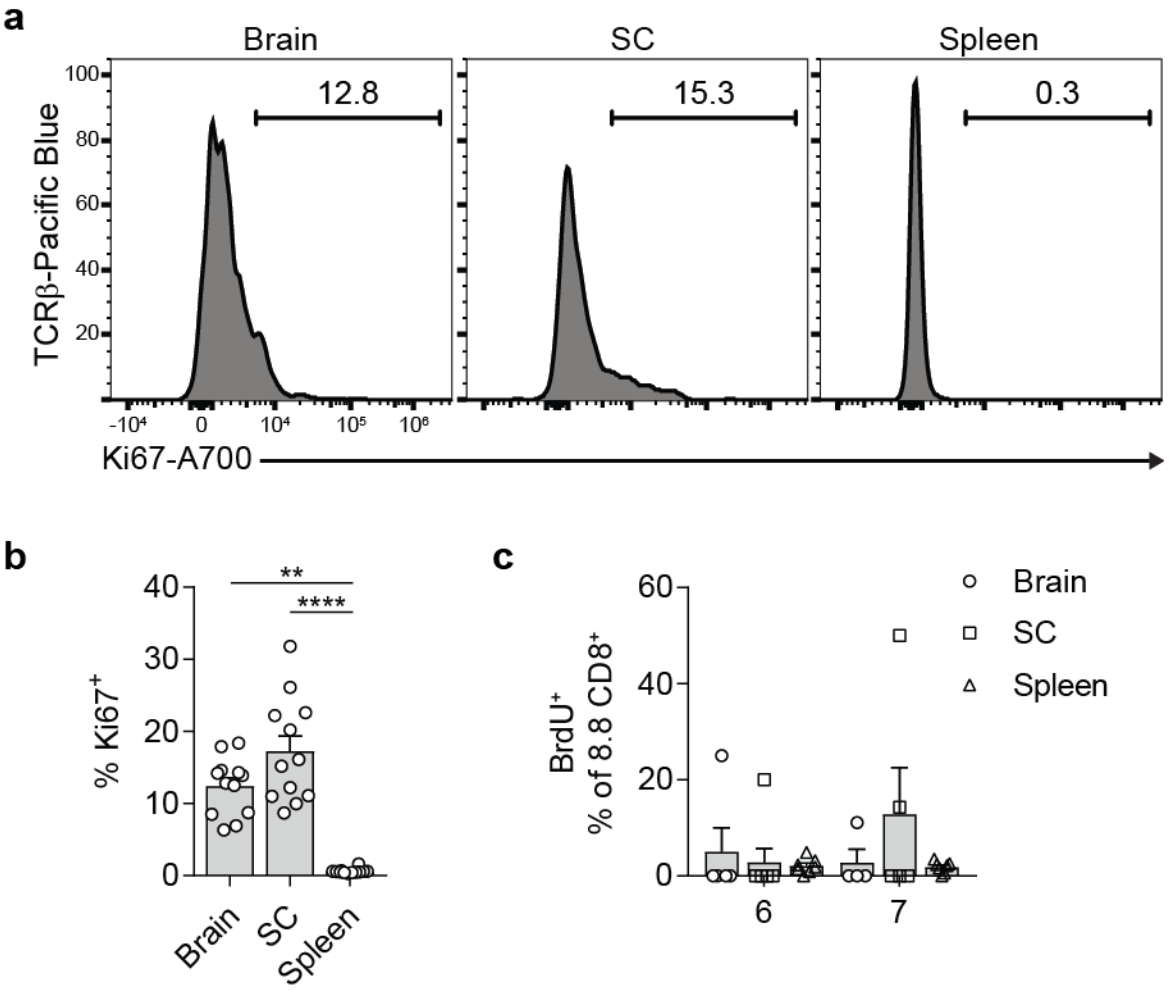

Figure 3.18. 8.8 CD8 T cells proliferate to a similar extent in the brain and spinal cord. **(a,b)** EAE was induced by transfer of CD45.1.1$^+$ MOG-specific CD4 T cells into CD45.2.2$^+$ intact TCR transgenic 8.8 mice. Mononuclear cells were isolated from brain and spinal cord (SC) 7 days post-CD4 T cell transfer and Ki67 expression was analyzed by flow cytometry. **(a)** Representative flow cytometry and **(b)** frequency of Ki67 expressing 8.8 CD8 T cells in (gated on CD45$^+$TCRb$^+$CD8$^+$CD45.2.2$^+$ cells) in the brain, spinal cord, and spleen. Data are representative of n=12 mice and are compiled from two independent experiments. **(c)** EAE was induced by the transfer of CD45.1.2$^+$ MOG-specific CD4 T cells into CD45.1.1$^+$ mice that had received CD45.2.2$^+$ WT CD8 T cells one day prior to disease induction. BrdU was injected into mice one day prior to euthanasia. The percentage of BrdU+ 8.8 CD8 T cells in the brain, spinal cord (SC), and spleen was determined by flow cytometry at day 7 for mice that had a detectable population of 8.8 CD8 T cells (n=7). Graphs show mean + SEM (one symbol per mouse) and data are compiled from two independent experiments. Statistical significance was determined using Kruskal-Wallis with Dunn's post-test. ** $p<0.01$, **** $p< 0.0001$.

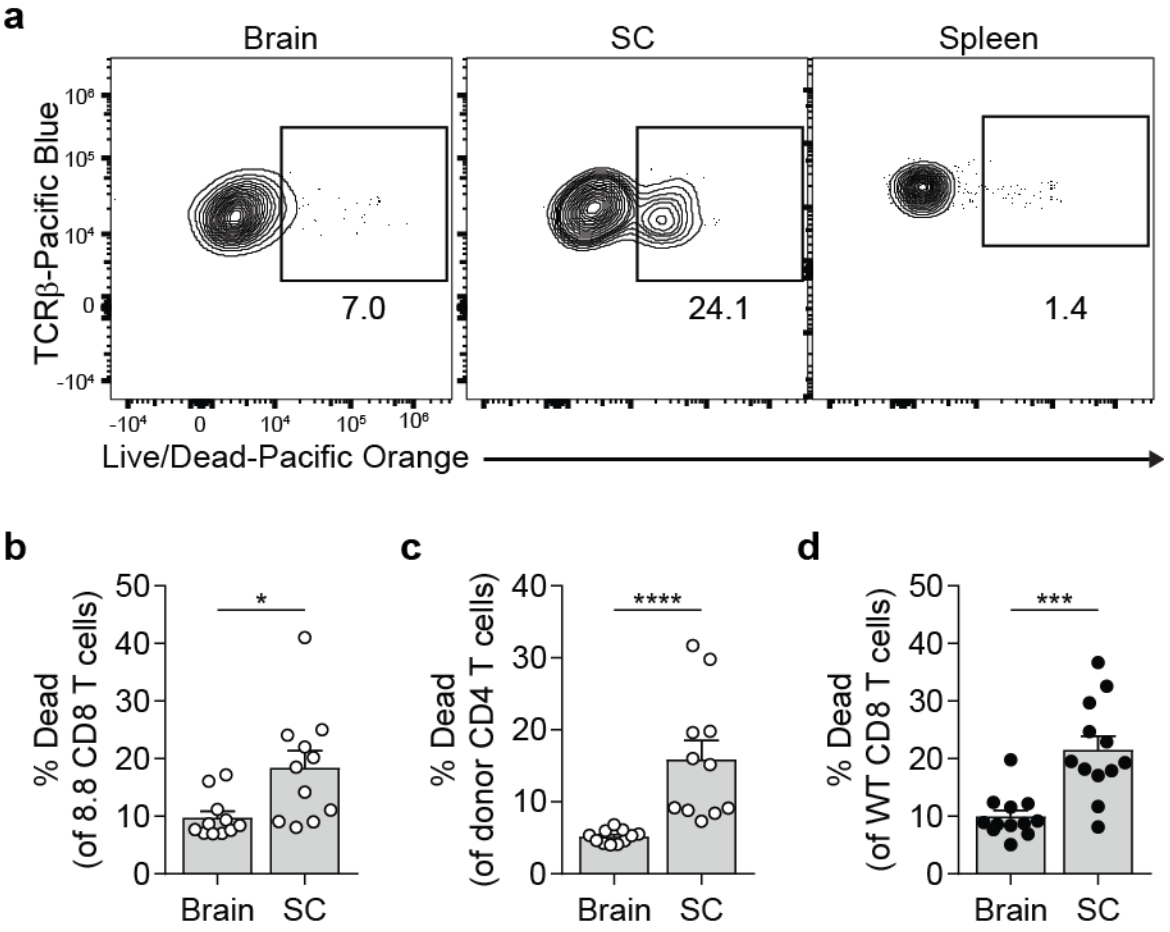

Figure 3.19. A higher frequency of 8.8 CD8 T cells undergo cell death in the spinal cord compared to the brain. EAE was induced by transfer of CD45.1.1$^+$ MOG-specific CD4 T cells into CD45.2.2$^+$ WT or intact TCR transgenic 8.8 mice. Mononuclear cells were isolated from brain and spinal cord (SC) 7 days post-CD4 T cell transfer and cell death was analyzed by flow cytometry using a cell-impermeable amine-reactive dye. **(a)** Representative flow cytometry showing Live/Dead staining for host CD8 T cells in 8.8 recipient mice (gated on CD45$^+$TCRb$^+$CD8$^+$Thy1.2$^+$ cells) in the brain, spinal cord, and spleen. Data are representative of n=12 mice and are compiled from two independent experiments. Frequency of **(b)** dead host 8.8 CD8 and **(c)** donor CD4 T cells were quantified for 8.8 mice with CD4-initiated EAE. **(d)** Frequency of dead host WT CD8 T cells were quantified for WT with CD4-initiated EAE. Graphs show mean + SEM (one symbol per mouse) and are compiled from two independent experiments (n=12). Statistical significance was determined using a two-way ANOVA with Tukey's post-test. * $p<0.05$, *** $p<0.001$, **** $p< 0.0001$.

Chapter 4: MBP-specific CD8 T cells enhance brain inflammation during CD4-initiated EAE via a FasL-dependent mechanism.

Introduction

In CD4-initiated EAE, we demonstrated that 8.8 CD8 T cells exacerbated brain inflammation. We next wanted to determine the mechanisms by which 8.8 CD8 T cells influenced CD4-initiated EAE. We previously found DCs, macrophages, and oligodendrocytes[93] presented MBP/K^k, suggesting 8.8 CD8 T cells could exert pathogenic activity through interactions with these cells. 8.8 CD8 T cells could be activated by DCs to produce inflammatory cytokines and 8.8 CD8 T cells could in turn activate DCs and macrophages to produce inflammatory mediators, such as cytokines and/or ROS. Additionally, 8.8 CD8 T cells could directly induce demyelination by lysing oligodendrocytes that present MBP/K^k through perforin/granzyme-B or Fas/FasL-mediated pathways. The following chapter investigates which 8.8 CD8 T cell effector functions are required for the exacerbation of atypical EAE.

Results

Recruitment of 8.8 CD8 T cells enhances chemokine and cytokine expression in the brain.

We hypothesized that expression of proinflammatory mediators would be induced to a greater extent in the brain but not spinal cord of mice with CD4-initiated/$CD8_{8.8}$ compared to CD4-initiated/$CD8_{WT}$ EAE, reflecting the exacerbation of atypical but not classic EAE that

occurs upon recruitment of 8.8 CD8 T cells. To test this hypothesis, we analyzed gene expression of inflammatory mediators in brain and spinal cord tissue harvested from mice 6 days post-donor CD4 T cell transfer in mice that had previously received either 8.8 or WT CD8 T cells. We compared the level of gene expression in these two groups of mice to the gene expression observed in tissues from irradiated healthy control mice that received no CD4 T cells. We observed a greater fold induction relative to control mice of multiple chemokines involved in myeloid and T cell recruitment in the brains but not the spinal cords of mice with CD4-initiated/$CD8_{8.8}$ versus CD4-initiated/$CD8_{WT}$ EAE (Fig. 4.1). Although there was a trend towards an increase in the expression of CCL2, CCL5, CCL6, CCL9, and CCL11 in the spinal cord, these data did not reach statistical significance and the differences were nto as large as seen for the brain (Fig 4.1). Pro-inflammatory cytokines implicated in EAE pathogenesis were also induced to a greater extent in the brains of CD4-initiated/$CD8_{8.8}$ compared to CD4-initiated/$CD8_{WT}$ EAE mice including IL-17, GM-CSF, TNFα, IL-6, and IL-1b (Fig. 4.2). IFNγ also demonstrated a trend towards increased expression in the brains of mice with CD4-initiated/$CD8_{8.8}$ EAE (Fig. 4.2). Significant differences in induction of these cytokines were not seen in the spinal cord. Both groups of mice exhibited similar fold changes in expression of CCL22, CCL24, IL-10, IL-12p35, IL-23p19, IFNβ, and TGFβ in the brain and spinal cord (Fig. 4.1 and 4.2). These data demonstrate that infiltration of 8.8 CD8 T cells in the brain, and to a lesser extent the spinal cord, is associated with enhanced production of soluble mediators that recruit inflammatory cells and enhance their pathogenic activity.

8.8 CD8 T cells increase the recruitment and pathogenicity of CD4 T cells, monocytes, and monocyte-derived cells.

We investigated whether the enhanced expression of chemokines and cytokines that occurs when 8.8 CD8 T cells infiltrate the brain causes an increase in recruitment of other inflammatory cell types by analyzing the inflammatory infiltrate in mice with CD4-initiated/$CD8_{WT}$ and CD4-initiated/$CD8_{8.8}$ EAE by flow cytometry (Fig. 4.3). Initial studies in which the infiltrate was analyzed at peak disease (days 7-10 post-CD4 T cell transfer) demonstrated that the numbers of infiltrating donor CD4 T cells, monocytes and neutrophils in the brain inversely correlated with the day of euthanasia (Fig. 4.4). Because 8.8 mice often reach peak disease at earlier time points compared to WT mice, we decided to analyze the inflammatory infiltrate in both groups of mice at day 5 and day 7 post-CD4 T cell transfer as the kinetics of the disease course do not significantly differ between CD4-initiated/$CD8_{8.8}$ and CD4-initiated/$CD8_{WT}$ EAE mice until day 8 (Fig. 3.7). While similar numbers of donor CD4 T cells were present in the brains of mice in both groups at day 5, a significantly higher number of donor CD4 T cells was found in the brains of CD4-initiated/$CD8_{8.8}$ compared to CD4-initiated/$CD8_{WT}$ EAE mice at day 7 (Fig. 4.5). No differences in donor CD4 T cell numbers were seen between groups at either time point in the spinal cord or spleen (Fig. 4.5). To assess the pathogenicity of the donor CD4 T cells, we analyzed their cytokine production at day 7 following re-stimulation with MOG_{97-114} in vitro. A significantly higher percentage of donor CD4 T cells produced TNFα and GM-CSF in the brain but not spinal cord of CD4-initiated/$CD8_{8.8}$ mice (Fig. 4.6). The frequencies of IL-17 and IFNγ-producing donor CD4 T cells trended higher in the brain and not spinal cord of CD4-initiated/CD88.8 mice but did not reach statistical significance. These results demonstrate that recruitment of 8.8 CD8 T cells increases the number and pathogenicity of donor MOG-specific CD4 T cells in the brain but not the spinal cord during CD4-initiated EAE.

The number of monocytes was also significantly higher in the brains of mice with CD4-initiated/$CD8_{8.8}$ compared to CD4-initiated/$CD8_{WT}$ EAE at both days 5 and 7 post-CD4 T cell transfer, and the number of MdCs was significantly higher at day 7 (Fig. 4.7a,b). The numbers did not differ for either cell type at either time point in the spinal cord. Microglia and neutrophil numbers were not significantly different in the brain or spinal cord at either time point (Fig. 4.7 c,d), although there was a trend towards higher neutrophil numbers of CD4-initiated/$CD8_{8.8}$ EAE mice in the brain at day 7 ($p=0.12$). We next investigated the pathogenic activity of the myeloid cells by analyzing their production of the cytokines IL-1b and TNFα. Similar frequencies of MdCs, monocytes, and microglia produced pro-IL-1b and TNFα in the brains and spinal cords of CD4-initiated/$CD8_{8.8}$ and CD4-initiated/$CD8_{WT}$ EAE mice (Fig. 4.8). However, as there are more MdCs and monocytes in the brain at day 7, the numbers of cytokine-producing MdCs and monocytes were higher in CD4-initiated/$CD8_{8.8}$ EAE mice (data not shown). Surprisingly, a lower frequency of neutrophils produced pro-IL-1b in CD4-intiated/$CD8_{8.8}$ EAE mice (Fig. 4.8). As we measured the production of the pro-form of IL-1b by intracellular cytokine staining, we do not know if there is truly less of the biologically active IL-1b produced by neutrophils or if it is secreted to a lesser extent.

We next analyzed the production of ROS, which are implicated in mediating demyelination, oligodendrocyte cell death, and axon degeneration in MS and EAE[23, 103-105]. At day 6, gene expression of iNOS was significantly higher in brain but not spinal cord tissue of mice with CD4-initiated/$CD8_{8.8}$ versus CD4-initiated/$CD8_{WT}$ EAE (Fig. 4.9a). We analyzed the production of ROS by flow cytometry at day 7 and found that monocytes and MdCs from the brain but not spinal cord produced higher amounts of ROS in mice with CD4-initiated/$CD8_{8.8}$ EAE compared to mice with CD4-initiated/$CD8_{WT}$ EAE (Fig. 4.9b,c). ROS production by

microglia and neutrophils was similar in the brains and spinal cords of mice in both groups (Fig. 4,9b,c). Together, these data suggest that 8.8 CD8 T cells enhance the recruitment and differentiation of monocytes followed by increased recruitment of donor CD4+ T cells specifically in the brain and not the spinal cord. Additionally, recruitment of 8.8 CD8 T cells enhanced the pathogenicity of these cells as demonstrated by increased cytokine production by donor CD4+ T cells and enhanced ROS production of myeloid cells.

8.8 CD8 T cells do not exacerbate atypical EAE due to a lack of regulatory CD8 T cells.

We hypothesized that 8.8 CD8 T cells acquire a pathogenic effector function in the brain that exacerbates atypical disease. However, 8.8 TCR transgenic mice may lack regulatory CD8 T cells, which could also result in more severe disease. To investigate this possibility, we induced CD4-initiated EAE in mice that received WT, 8.8, or no CD8 T cells (PBS only). The incidence and severity of classic EAE was similar in all three groups (Fig. 4.10a,b). As expected, the transfer of 8.8 CD8 T cells increased the incidence and severity of atypical EAE compared to WT CD8 T cells (Fig. 4.10c,d). The incidence of atypical EAE was significantly lower in mice that did not receive any CD8 T cells compared to those that received 8.8 CD8 T cells (Fig. 4.10c,d), suggesting that 8.8 CD8 T cell exacerbation of atypical EAE was not the result of a lack of regulatory CD8 T cells.

IFNγ, perforin, and TNFα are not required for 8.8 CD8 T cell exacerbation of atypical EAE.

To define the effector functions required for 8.8 CD8 T cells to exacerbate brain inflammation in CD4-initiated EAE, we introduced CD8 T cells from WT, 8.8, or 8.8 mice on an

IFNγ-, perforin, or TNFα- deficient background into WT mice prior to transfer of MOG-specific CD4 T cells. The incidence of classic EAE was similar between mice that received WT CD8 T cells and 8.8 CD8 T cells, regardless of the genotype of the 8.8 CD8 T cells (data not shown). As expected, the incidence of atypical EAE was significantly higher in mice that received 8.8 versus WT CD8 T cells (Fig. 4.11). Interestingly, the incidence of atypical EAE was the same for the groups of mice that received 8.8, IFNγ$^{-/-}$ 8.8 or Pfp$^{-/-}$ 8.8, and was significantly higher in these groups compared to mice that received WT CD8 T cells (Fig. 4.11a,b). Thus, in contrast to CD8-initiated EAE, neither IFNγ nor perforin were required for 8.8 T cells to exacerbate atypical EAE in CD4-initiated/CD8$_{8.8}$ EAE. TNFα was also not required for 8.8 T cells to exacerbate atypical EAE (Fig. 4.11c).

Cells from 8.8 mice deficient in GM-CSF ameliorate atypical EAE.

We next evaluated the 8.8 CD8 T cell requirement for GM-CSF expression to exacerbate atypical EAE using GM-CSF-deficient (GM-CSF$^{-/-}$) 8.8 CD8 T cells. Unexpectedly, mice that received GM-CSF$^{-/-}$ 8.8 CD8 T cells exhibited lower incidence and severity of atypical EAE compared to mice that received WT or 8.8 CD8 T cells (Fig. 4.12a,b). In these experiments, atypical disease in CD4-initiated/CD8$_{WT}$ EAE mice was unusually more severe, so we did not observe the normal exacerbation of atypical EAE in CD4-initiated/CD8$_{8.8}$ EAE mice compared to CD4-initiated/CD8$_{WT}$ EAE (Fig. 4.12a,b). As we see very little production of GM-CSF by 8.8 CD8 T cells in the CNS (Fig. 3.14a), we hypothesized that any effects of using enriched CD8 T cells obtained from 8.8 GM-CSF$^{-/-}$ mice could be due to the activity of another cell subset present in CD8 T cell-enriched population generated from GM-CSF$^{-/-}$ 8.8 but not WT or 8.8 mice. To investigate this, we analyzed the CD8 T cell enriched splenocytes from WT, 8.8, and

GM-CSF-/- 8.8 mice prior to transfer. Interestingly, GM-CSF-/- 8.8 mice had a higher frequency of $CD19^{+}CD45^{hi\text{-}int}$ cells that was more prominent in aged mice (Fig. 4.12c). As our enrichment protocol removes $B220^{+}$ cells, we speculate that these cells are $CD19^{+}B220^{lo/-}$, consistent with a B-1 B cell progenitor phenotype[106]. B-1 B cells have been shown to regulate EAE during disease initiation[107], possibly through the secretion of IL-10[108]. While more work is needed to determine the phenotype of these cells, we hypothesize that the unusual $CD19^{+}$ cell subset in the $GM\text{-}CSF^{-/-}$ 8.8 mice and not the CD8 T cells themselves are responsible for the amelioration of atypical EAE.

FasL-mediated signaling is required for MBP-specific CD8 T cells to exacerbate atypical EAE.

We next determined the role of FasL-mediated signaling by transferring WT, 8.8, or $FasL^{gld}$ 8.8 CD8 T cells into WT mice prior to transfer of MOG-specific CD4 T cells. $FasL^{gld}$ 8.8 CD8 T cells did not exacerbate atypical EAE as the incidence of atypical EAE in mice that received $FasL^{gld}$ 8.8 CD8 T cells was similar to that seen in mice that received WT CD8 T cells, and was significantly lower than the incidence of atypical EAE in 8.8 CD8 T cell recipients (Fig. 4.13a). We next investigated whether 8.8 CD8 T cell expression of FasL was required for the enhanced ROS production by MdCs and monocytes, as Fas-signaling has been shown to activate these innate immune cells[109 110 111 112]. MdCs present in mononuclear cells isolated from the brains of mice that received $FasL^{gld}$ 8.8 CD8 T cells did not upregulate ROS production as compared to mice that received 8.8 CD8 T cells (Fig. 4.13b,c). Monocytes in mice that received $FasL^{gld}$ 8.8 CD8 T cells also did not upregulate ROS production compared to mice that received 8.8 CD8 T cells, although the difference in normalized MFI for CellRox staining of monocytes in these two groups was not statistically significant (Fig. 4.13b,c). These data demonstrate that

FasL expression by 8.8 CD8 T cells is required for exacerbation of atypical EAE in CD4 T cell-initiated disease, and that Fas-FasL interactions are required for 8.8 CD8 T cells to trigger the enhanced ROS production observed in MdCs (and likely monocytes) that correlates with exacerbation of atypical EAE.

A higher frequency of monocytes and monocyte-derived cells present MBP-K^k in the brain compared to the spinal cord.

To investigate whether 8.8 CD8 T cells interact directly with monocytes and MdCs, we first analyzed the expression of MBP/K^k on mononuclear cells in the brain and spinal cord during CD4-initiated EAE using the 12H4 antibody[93]. MdCs and monocytes were the predominant myeloid cell presenting MBP/K^k in the brain and spinal cord (Fig 4.14a,b). As previously observed[93], a small percentage of microglia presented MBP/K^k (Fig 4.14a,b). However, our laboratory previously showed that microglia isolated from CD4 T cell-initiated EAE mice did not trigger 8.8 functional responses[93], consistent with our data here showing that recruitment of 8.8 CD8 T cells does not affect microglia ROS production. As expected, neutrophils did not present MBP/K^k in the brain or spinal cord (Fig 4.14a,b). These data support our hypothesis that 8.8 CD8 T cells interact directly with MdCs and monocytes, allowing 8.8 CD8 T cells to enhance ROS production via FasL-mediated signaling. Interestingly, the frequency of MBP/K^k-expressing MdCs and monocytes was higher in the brain compared to the spinal cord (4.14c), which may provide a mechanism for why the effects of 8.8 CD8 T cells are more prominent in the brain compared to the spinal cord.

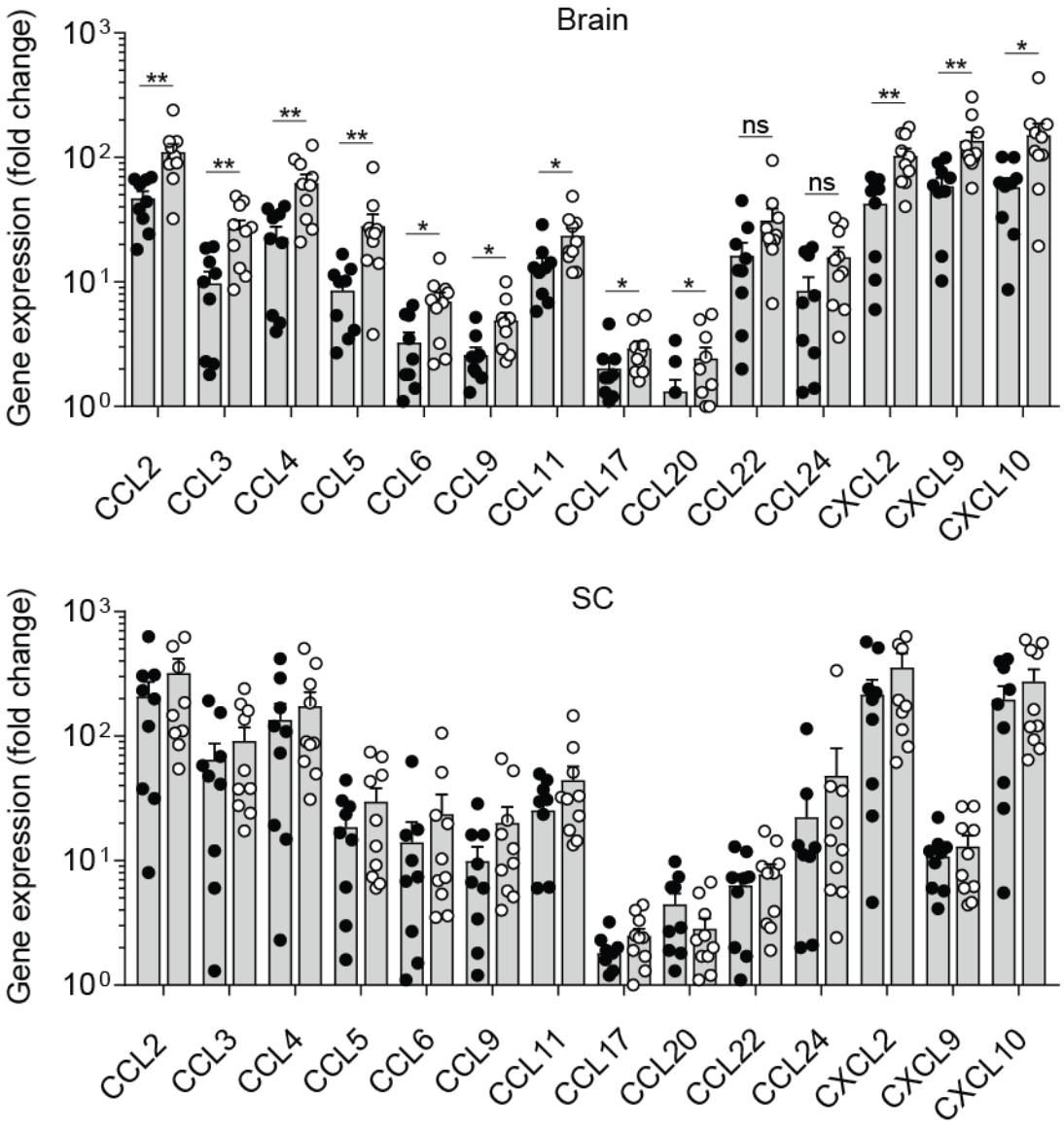

Figure 4.1. Recruitment of 8.8 CD8 T cells enhances chemokine gene expression in the brain but not spinal cord. EAE was induced by transfer of MOG-specific CD4 T cells into WT mice that received either WT (n=9) or 8.8 (n=10) CD8 T cells one day earlier. Brain and spinal cord (SC) tissues were harvested 6 days post-CD4 T cell transfer. Chemokine gene expression were analyzed directly ex-vivo by qPCR. All data were normalized to GAPDH. The fold change was calculated relative to gene expression values in irradiated healthy control mice (n=2). Graphs show mean + SEM (one mouse per symbol) and are compiled from two independent experiments. Statistical significance was determined using a Mann-Whitney *U* test. * $p<0.05$, ** $p<0.01$.

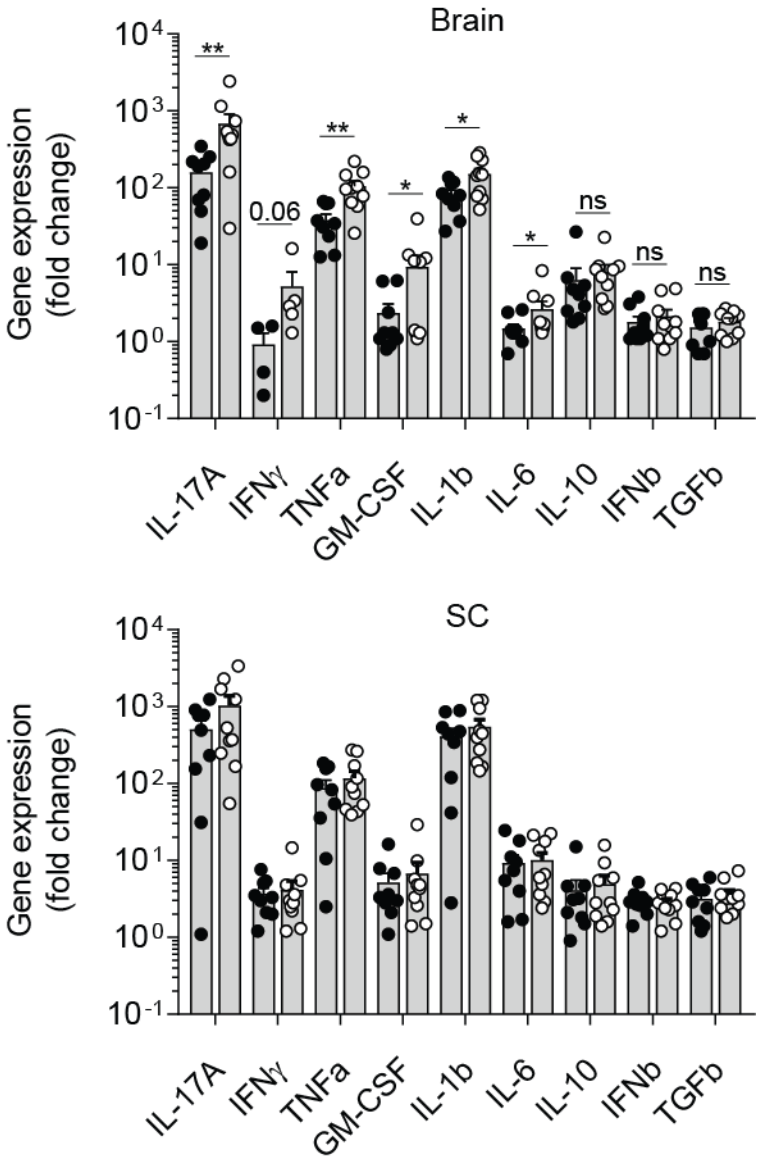

Figure 4.2. Recruitment of 8.8 CD8 T cells enhances cytokine gene expression in the brain but not spinal cord. EAE was induced by transfer of MOG-specific CD4 T cells into WT mice that received either WT (n=9) or 8.8 (n=10) CD8 T cells one day earlier. Brain and spinal cord (SC) tissues were harvested 6 days post-CD4 T cell transfer. Cytokine gene expression were analyzed directly ex-vivo by qPCR. All data were normalized to GAPDH. The fold change was calculated relative to gene expression values in irradiated healthy control mice (n=2). Graphs show mean + SEM (one mouse per symbol) and are compiled from two independent experiments. Statistical significance was determined using a Mann-Whitney *U* test. * $p<0.05$, ** $p<0.01$.

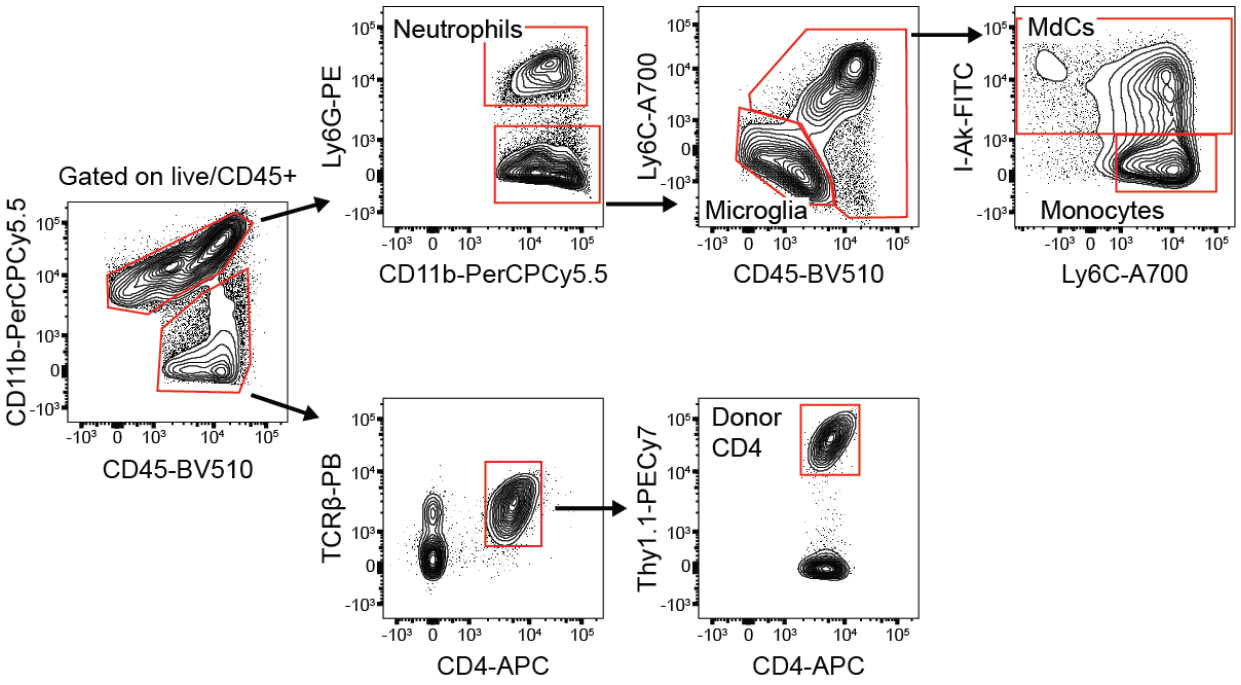

Figure 4.3. Gating strategy to identify immune cell subsets in the CNS of mice with EAE. EAE was induced by the transfer of Thy1.1$^+$ MOG-specific CD4 T cells into Thy1.2$^+$ mice that received Thy1.2$^+$ 8.8 CD8 T cells one day prior to disease induction. Mononuclear cells were isolated from the brain of a mouse with atypical EAE 7 days post-CD4 T cell transfer. Cells are initially gated on single, live, CD45$^+$ cells.

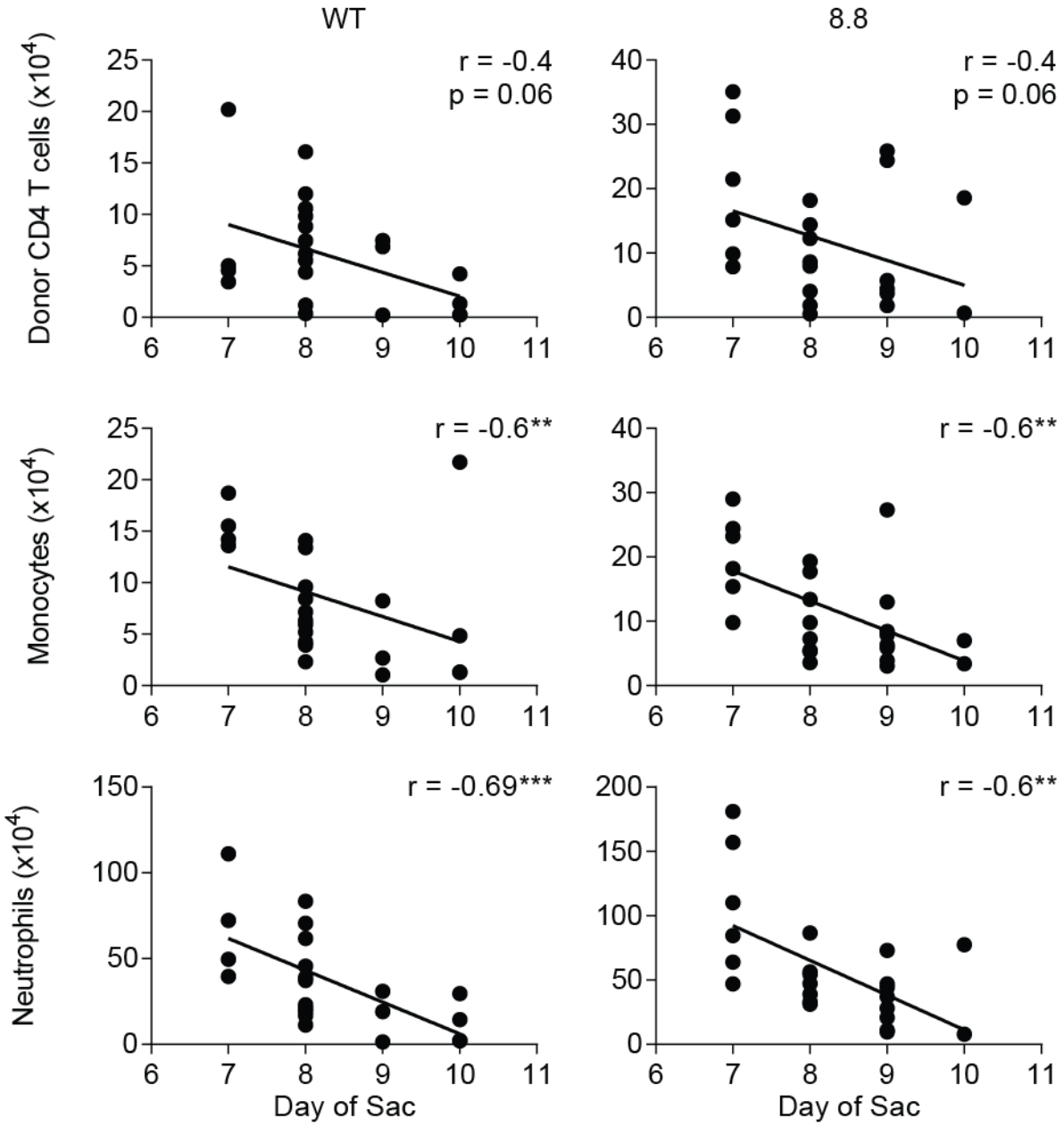

Figure 4.4. Numbers of infiltrating immune cells in the brain inversely correlate with the day of euthanasia. EAE was induced by transfer of Thy1.1$^+$ MOG-specific CD4 T cells into Thy1.2$^+$ mice that had received Thy1.2$^+$ WT or 8.8 CD8 T cells. Correlation of Thy1.1$^+$ donor CD4 T cells, CD45^{hi}CD11b$^+$Ly6C^{hi}MHCII$^-$ monocytes, and CD45^{hi}CD11b$^+$Ly6G$^+$ neutrophils isolated from the brain at peak disease with day of euthanasia. Data are compiled from 5 independent experiments (n=47; both mice that received WT and 8.8 CD8 T cells are included). Statistical significance was determined using Spearman's *r*. ** p<0.01, **** p<0.0001.

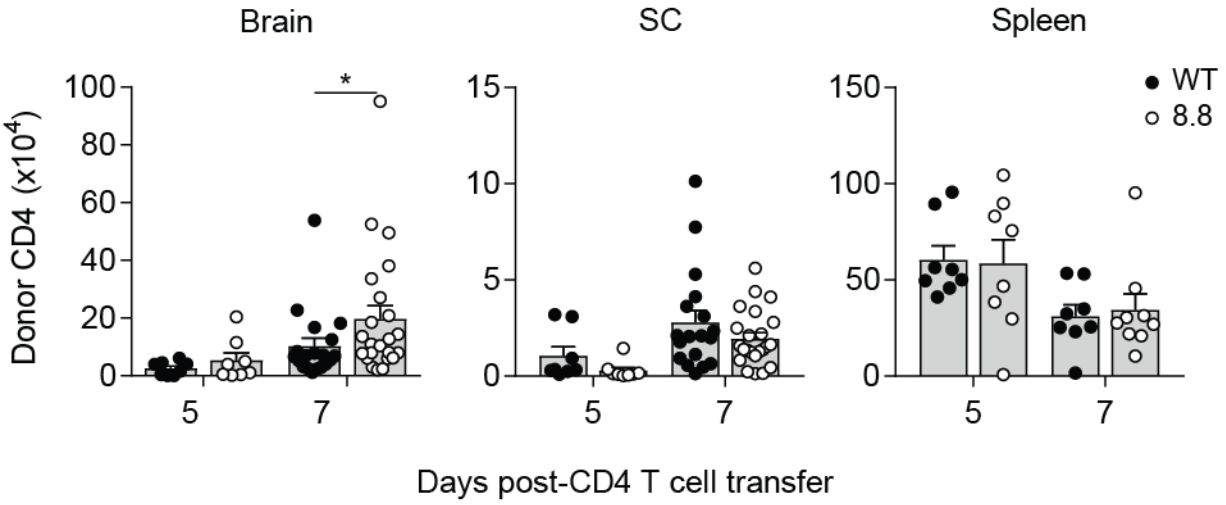

Figure 4.5. Brain-infiltrating 8.8 CD8 T cells enhance the recruitment of donor CD4 T cells. EAE was induced by transfer of Thy1.1$^+$ MOG-specific CD4 T cells into Thy1.2$^+$ mice that had received Thy1.2$^+$ WT or 8.8 CD8 T cells. The number of Thy1.1$^+$ donor CD4 T cells was determined on days 5 (n=8 per group) and 7 (WT: n=19; 8.8: n=23; Spleen: n=8 per group) post-CD4 T cell transfer for the brain, spinal cord (SC), and spleen by flow cytometry. Graphs show mean + SEM (one symbol per mouse) and are compiled from at least 2 independent experiments. Statistical significance was determined using a Mann-Whitney *U* test. * $p<0.05$.

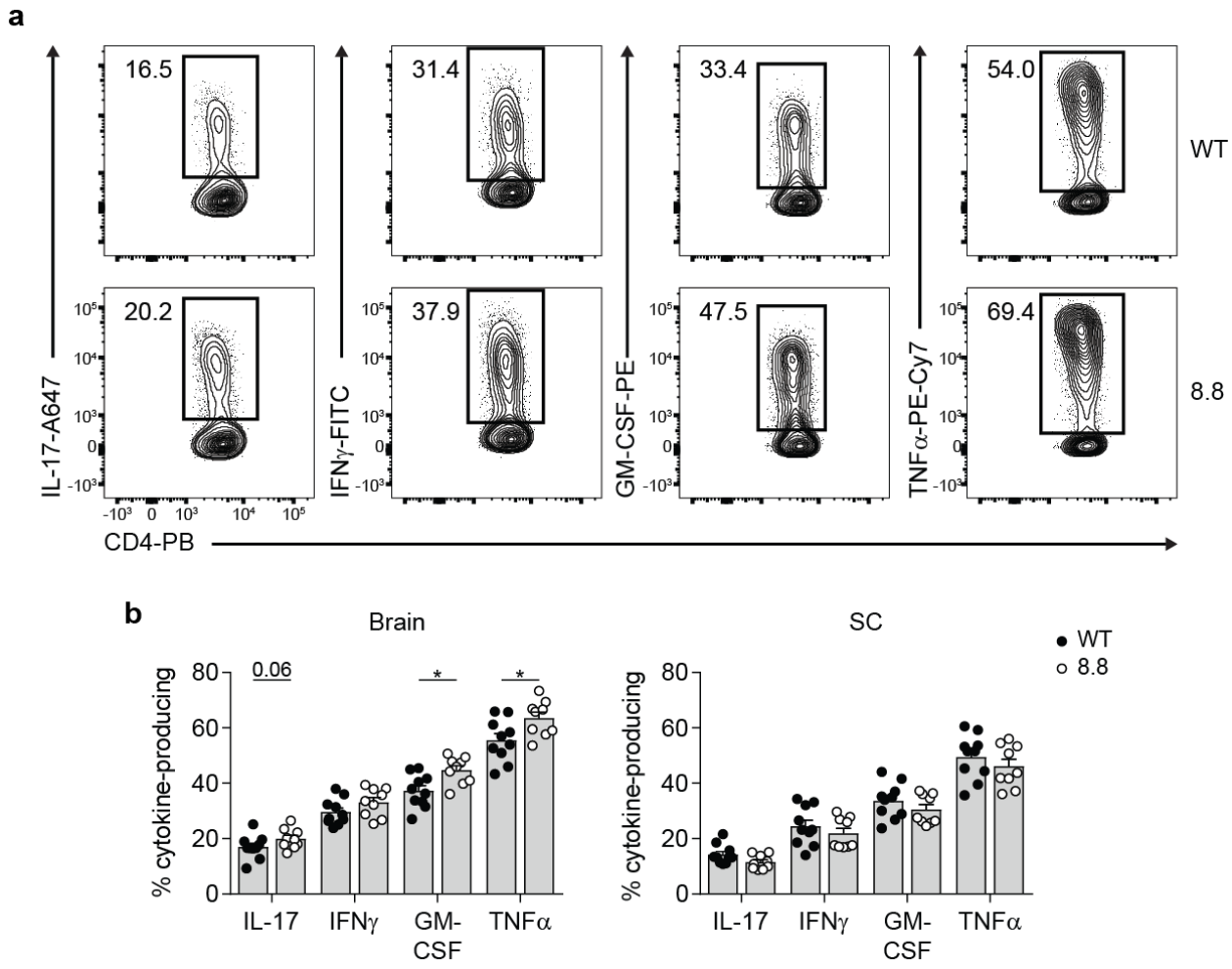

Figure 4.6. 8.8 CD8 T cells enhance the frequencies of cytokine producing donor CD4 T cells in the brain. EAE was induced by transfer of Thy1.1$^+$ MOG-specific CD4 T cells into Thy1.2$^+$ mice that had received Thy1.2$^+$ WT or 8.8 CD8 T cells. Brain and spinal cord (SC) were isolated from mice (WT: n=10; 8.8: n=9) on day 7 post-CD4 T cell transfer and mononuclear cells were stimulated with MOG_{97-114} peptide prior to intracellular cytokine staining. **(a)** Representative flow cytometry plots from the brain and **(b)** the percentages of Thy1.1$^+$ donor CD4 T cells producing the indicated cytokines were determined by flow cytometry. Graphs show mean + SEM (one symbol per mouse) and are compiled from two independent experiments. Statistical significance was determined using a Mann-Whitney *U* test. * $p<0.05$.

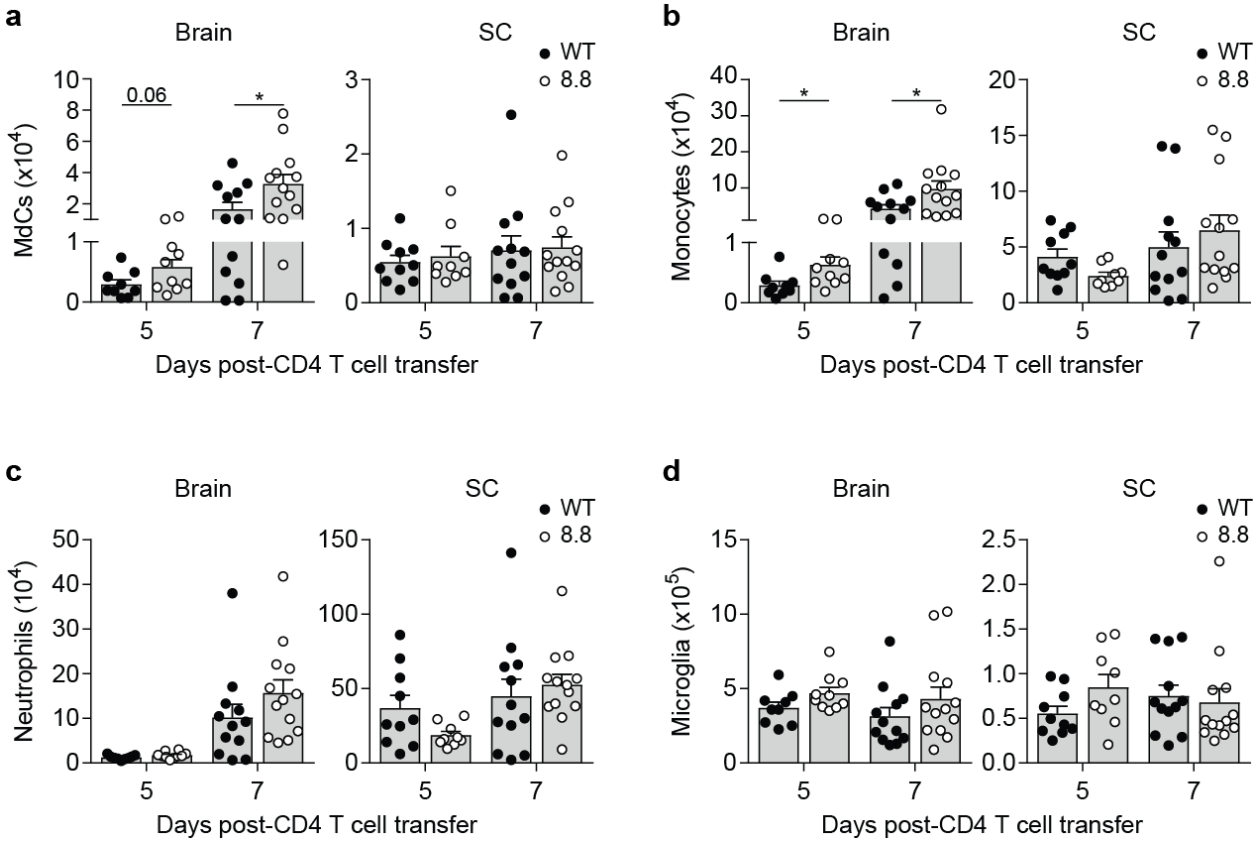

Figure 4.7. 8.8 CD8 T cells promote the recruitment and differentiation of monocytes in the brain. EAE was induced by transfer of MOG-specific CD4 T cells into WT mice that had received WT or 8.8 CD8 T cells. The numbers of **(a)** $CD45^{hi}CD11b^{+}Ly6C^{+/-}MHCII^{+}$ monocyte-derived cells (MdCs), **(b)** $CD45^{hi}CD11b^{+}Ly6C^{hi}MHCII^{-}$ monocytes, **(c)** $CD45^{hi}CD11b^{+}Ly6G^{+}$ neutrophils, and **(d)** $CD45^{lo\text{-}int}CD11b^{+}Ly6C^{-}$ microglia were determined by flow cytometric analyses from brains and spinal cords (SC) isolated on days 5 (WT: n=9; 8.8: n=10) and 7 (WT: n=12; 8.8: n=13) post-CD4 T cell transfer. Graphs show mean + SEM (one symbol per mouse) and are compiled from at least two independent experiments. Statistical significance was determined using a Mann-Whitney *U* test. * $p<0.05$.

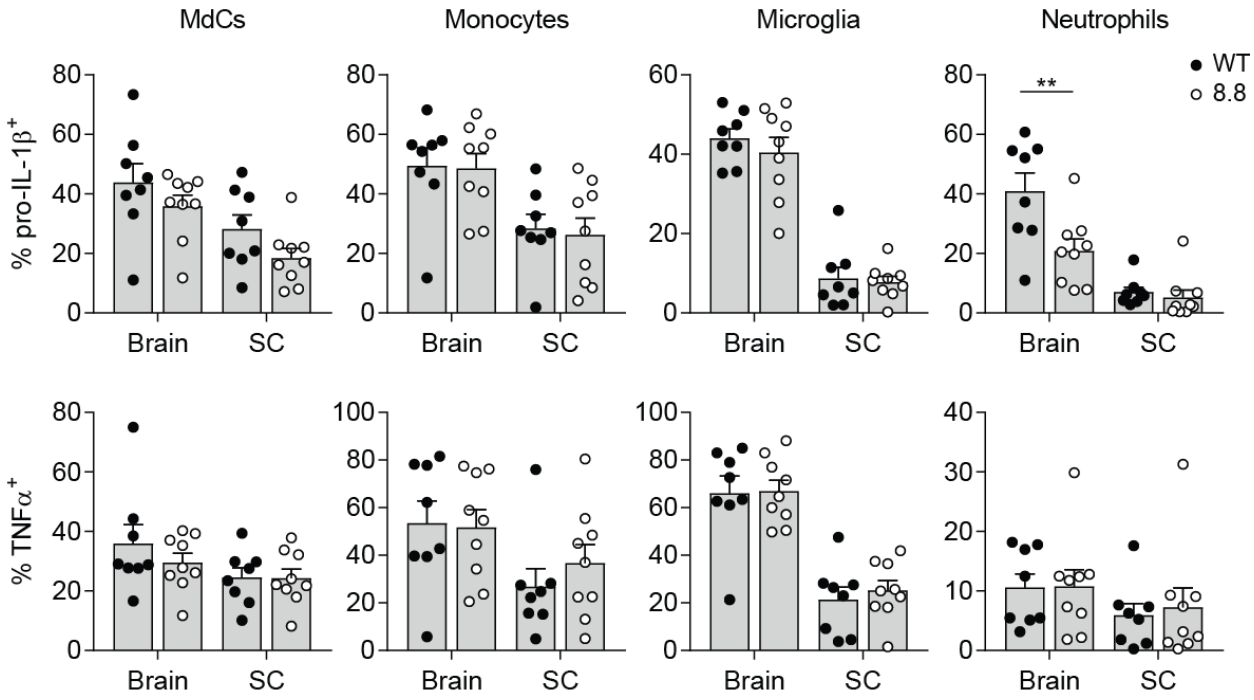

Figure 4.8. 8.8 CD8 T cells do not promote myeloid cell production of IL-1b or TNFα in the brain or spinal cord. EAE was induced by transfer of MOG-specific CD4 T cells into WT mice that had received either WT or 8.8 CD8 T cells one day earlier. Mononuclear cells were isolated from the brains and spinal cords (SC) at day 7 and cultured with GolgiPlug without stimulation prior to intracellular staining for cytokines. Cytokine-producing myeloid cells were quantified by flow cytometry (WT: n=8; 8.8: n=9). Graphs show mean + SEM (one symbol per mouse) and are compiled from two independent experiments. Statistical significance was determined using Mann-Whitney *U* test. ** $p<0.01$.

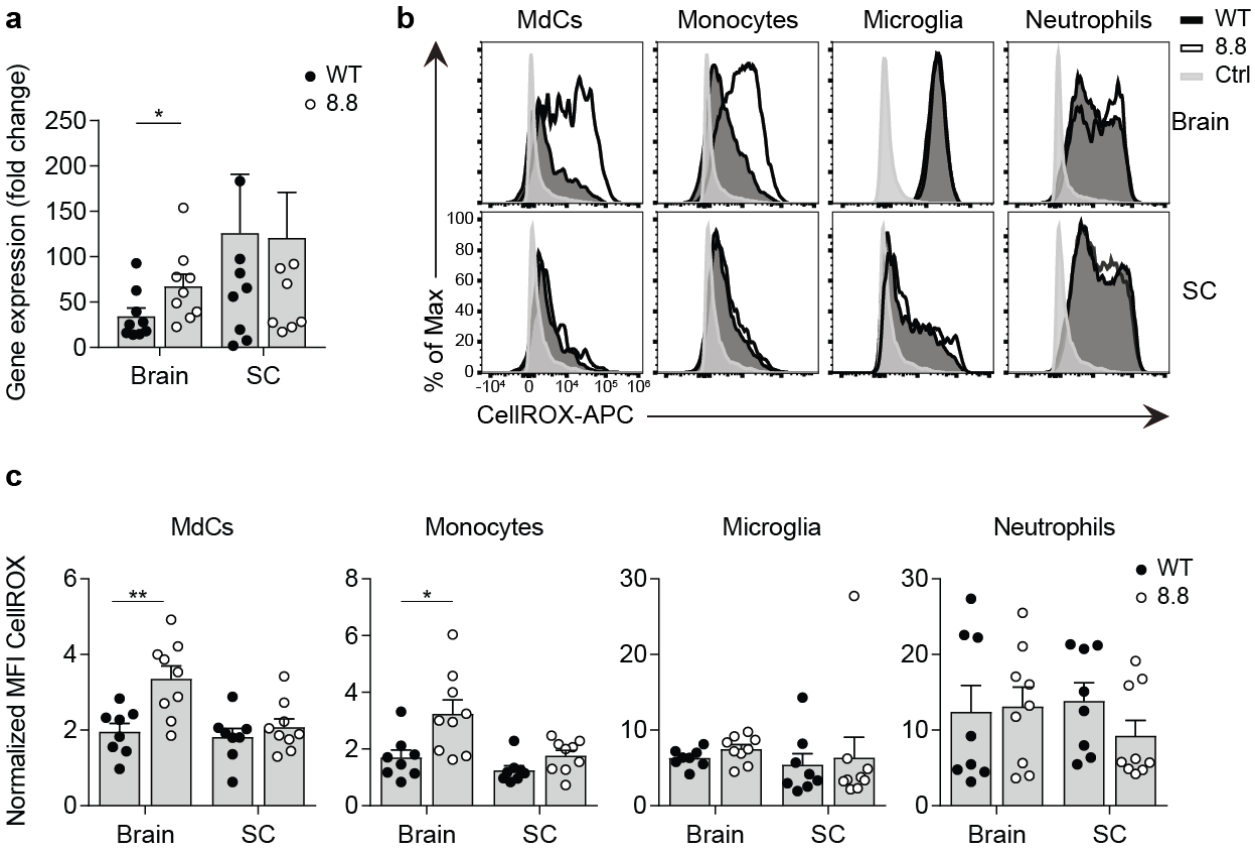

Figure 4.9. 8.8 CD8 T cells increase the production of ROS by monocytes and MdCs in the brain. EAE was induced by transfer of MOG-specific CD4 T cells into WT mice that had received either WT or 8.8 CD8 T cells one day earlier. **(a)** Brains and spinal cords (SC) were harvested 6 days post-CD4 T cell transfer and iNOS gene expression was determined by qPCR (n=9 per group). Data were normalized to GAPDH and the fold-change in expression was determined relative to irradiated control mice (n=2). **(b,c)** Mononuclear cells were isolated from the brains and spinal cords (SC) and analyzed by flow cytometry. **(b)** Representative flow cytometry and **(c)** MFIs (medians) of MdC, monocyte, microglia, and neutrophil ROS staining are shown for day 7 post-CD4 T cell transfer. Data are representative of two independent experiments (WT: n=8, 8.8: n=9). T cell CellROX expression is used as a negative control (Ctrl) to generate normalized MFI values. Graphs show mean + SEM (one symbol per mouse) and are compiled from at least two independent experiments. Statistical significance was determined using a Mann-Whitney *U* test. * $p<0.05$, ** $p<0.01$

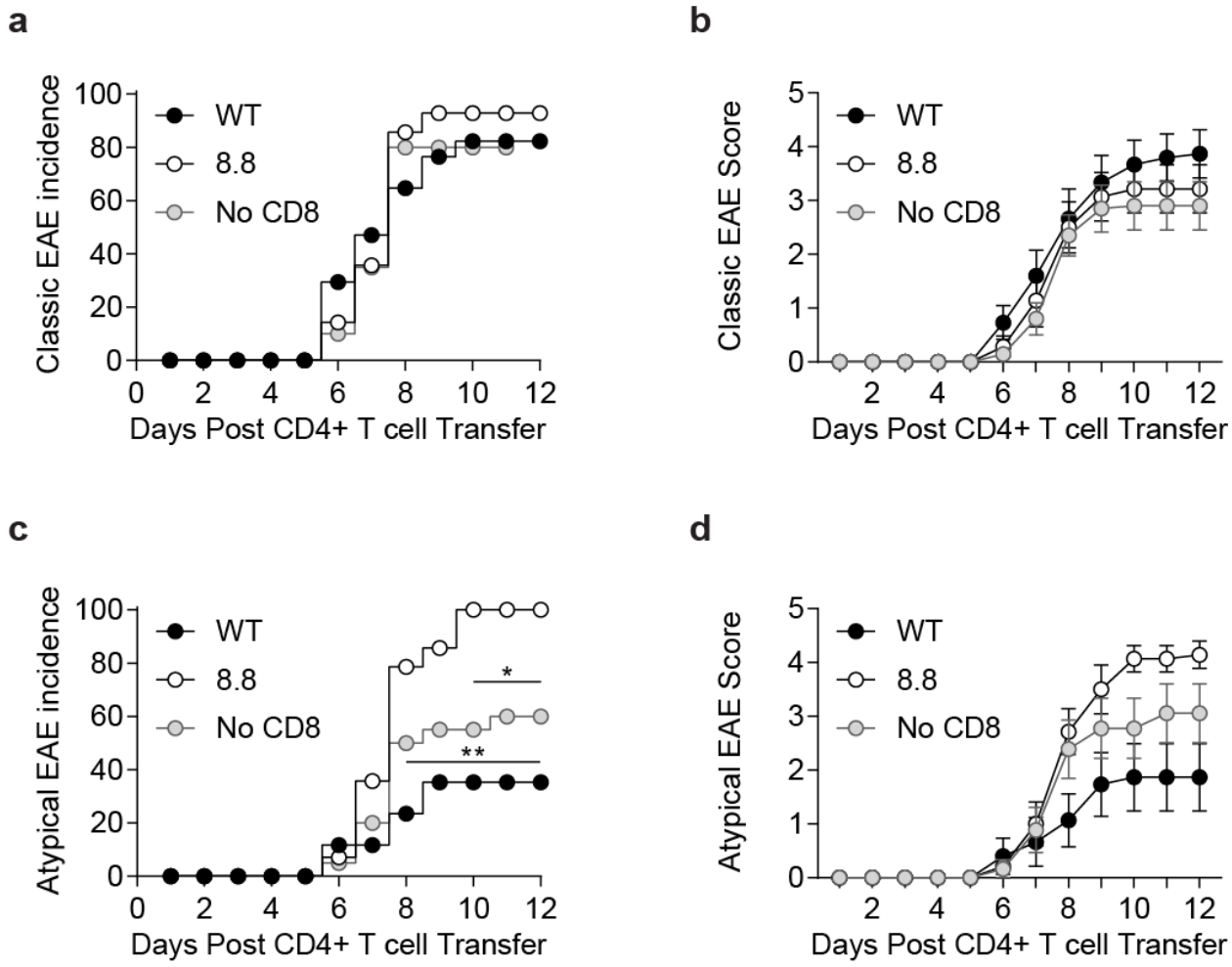

Figure 4.10. CD4-initiated/CD8$_{8.8}$ EAE mice do not exhibit enhanced incidence and severity of atypical because of a lack of regulatory CD8 T cells. EAE was induced by transfer of MOG-specific CD4 T cells into WT mice and either WT (n=17) or 8.8 (n=14) CD8 T cells or no CD8 T cells (PBS only; n=20) one day later. **(a)** Incidence of classic EAE among all mice in each indicated group. **(b)** Clinical scores of classic EAE symptoms (mean $\pm$ SEM) for mice that developed EAE. **(c)** Incidence of atypical EAE among all mice in each indicated group. **(d)** Clinical scores of atypical EAE symptoms (mean $\pm$ SEM) for mice that developed EAE. Data are compiled from 3 independent experiments. Statistical significance was determined using **(a,c)** Fisher's exact test or **(b,d)** Mann-Whitney *U* test. * $p<0.05$, ** $p<0.01$ relative to the 8.8 group.

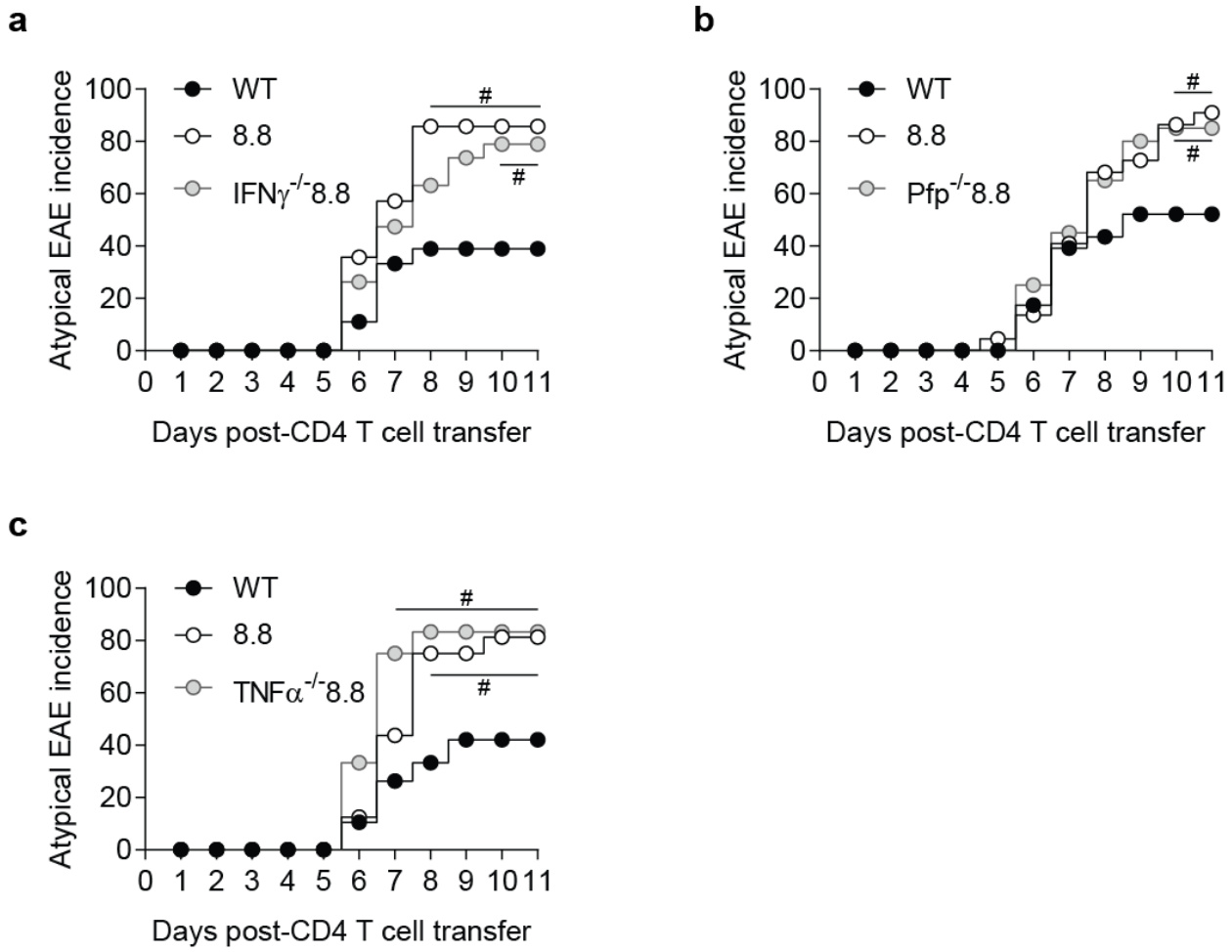

Figure 4.11. 8.8 CD8 T cells do not exacerbate atypical EAE via IFNγ-, perforin-, or TNFα-dependent mechanisms. EAE was induced by transfer of MOG-specific CD4 T cells into WT mice that had received **(a)** WT (n=18), 8.8 (n=14) or IFNγ-deficient (IFNγ $^{-/-}$) 8.8 (n=19) CD8 T cells; **(b)** WT (n=23), 8.8 (n=22) or perforin-deficient (Pfp$^{-/-}$) 8.8 (n=20) CD8 T cells; **(c)** WT (n=19), 8.8 (n=16) or TNFα –deficient (TNFα$^{-/-}$) 8.8 (n=12) CD8 T cells. The percentage of mice exhibiting atypical EAE signs is shown for each group. Data in each panel are compiled from at least 3 independent experiments. Statistical significance determined using Fisher's Exact test. $^{\#}$ indicates statistical significant difference relative to mice that received WT CD8 T cells. $^{\#}$ $p<0.05$.

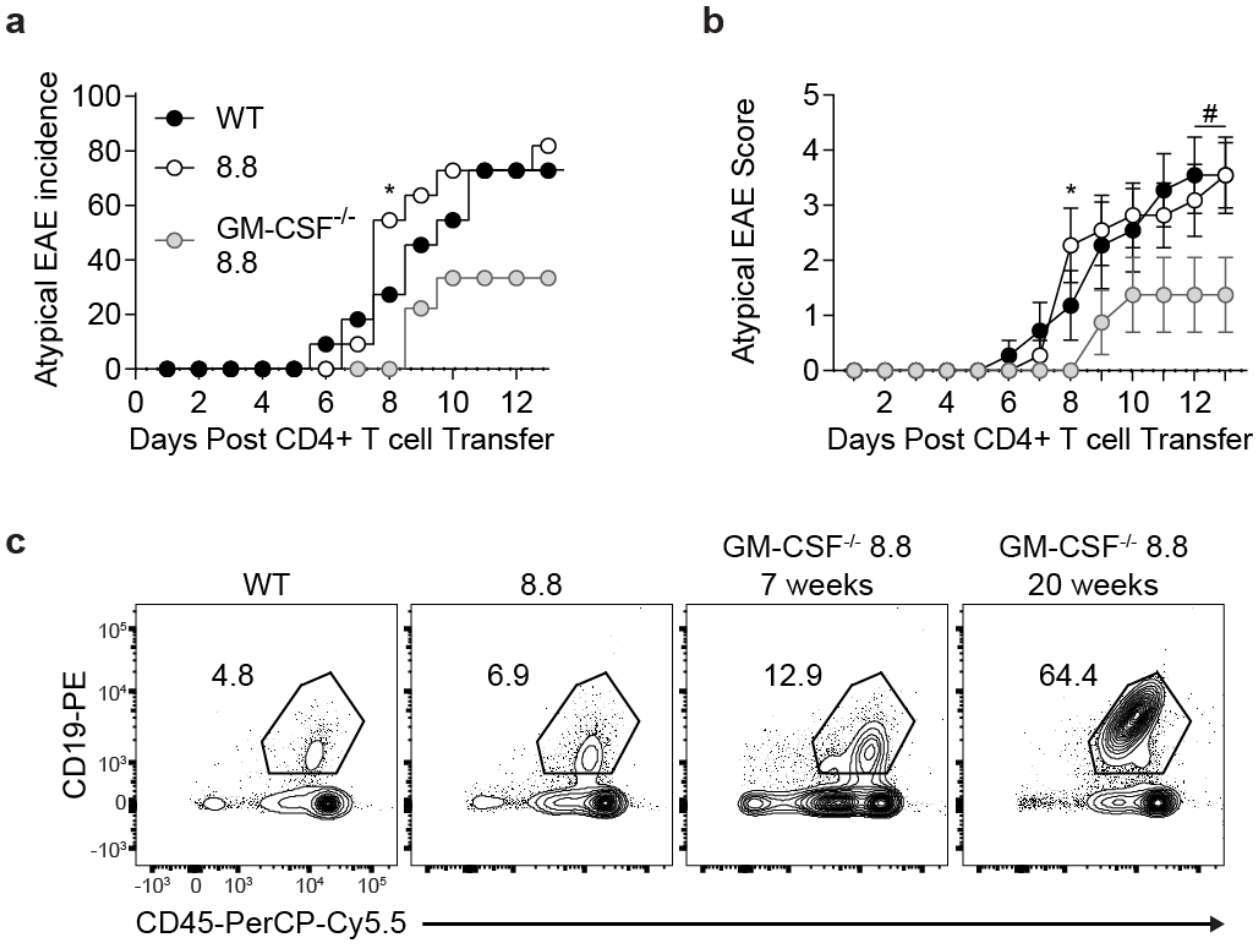

Figure 4.12. Cells from GM-CSF-/- 8.8 mice ameliorate atypical EAE. EAE was induced by transfer of MOG-specific CD4 T cells into WT mice that had received WT (n=11), 8.8 (n=11) or GM-CSF-deficient (GM-CSF $^{-/-}$) 8.8 (n=9) CD8 T cells. **(a)** Incidence of atypical EAE among all mice in each indicated group. **(b)** Clinical scores of atypical EAE symptoms (mean $\pm$ SEM) for mice that developed EAE. Data are compiled from two independent experiments. **(c)** Representative flow cytometry of CD8 enriched (as demonstrated in Methods) splenocytes from WT, 8.8, or GM-CSF-/- 8.8 mice (7 weeks and 20 weeks of age) prior to transfer. Data are representative of two independent experiments. $^{\#}$ indicates statistical significant difference of mice that received 8.8 CD8 T cells relative to mice that received GM-CSF-/- 8.8 CD8 T cells. * indicates statistical significant difference of mice that received 8.8 CD8 T cells relative to mice that received GM-CSF-/- 8.8 CD8 T cells; $^{\#}$ indicates statistical significant difference of mice that received WT CD8 T cells relative to mice that received GM-CSF-/- 8.8 CD8 T cells. Statistical significance determined using Fisher's Exact test. $^{\#}$ or * $p<0.05$.

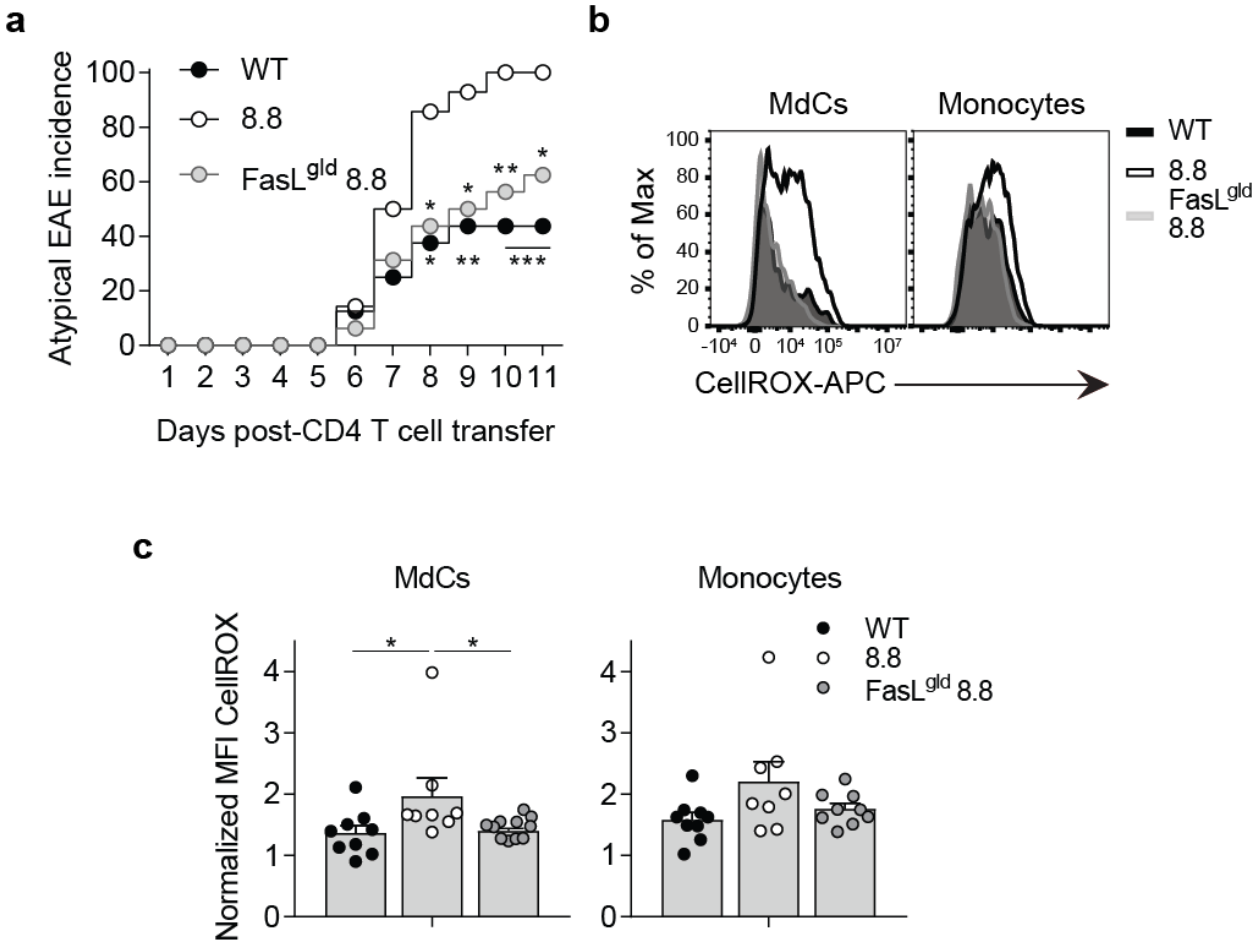

Figure 4.13. Fas-FasL signaling is required for 8.8 CD8 T cells to increase monocyte and MdC ROS production. (a) EAE was induced by transfer of MOG-specific CD4 T cells into WT mice that had received WT (n=16), 8.8 (n=14) or FasL-deficient ($FasL^{gld}$) 8.8 (n=16) CD8 T cells. The percentage of mice exhibiting atypical EAE signs is shown for each group. **(b,c)** EAE was induced by MOG-specific CD4 T cells into WT mice that had received WT (n=9), 8.8 (n=8), or $FasL^{gld}$ (n=9) CD8 T cells. **(b)** Representative flow cytometry plot and **(c)** normalized MFIs (medians) of ROS staining (measured using CellROX) gated on MdCs and monocytes within mononuclear cells isolated from the brains of mice on day 7 post-CD4 transfer. MFIs are normalized to the MFI for T cell ROS staining. **(a)** Data are compiled from 3 independent experiments. **(b,c)** Graphs show mean + SEM (one symbol per mouse) and are compiled from two independent experiments. Statistical significance determined using **(a)** Fisher's Exact test or **(c)** Mann-Whitney *U* test. * $p<0.05$, ** $p<0.01$, *** $p < 0.001$.

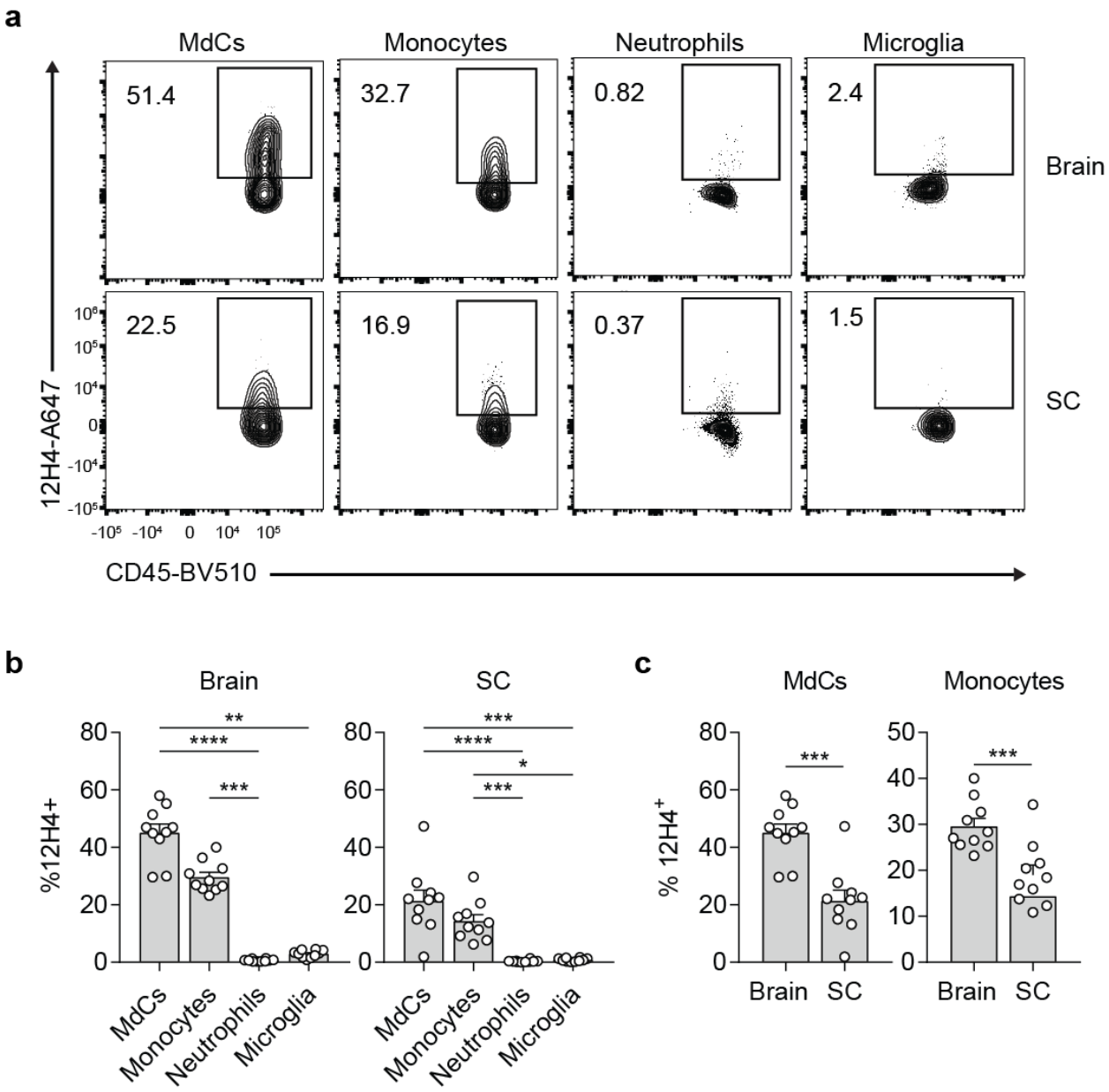

Figure 4.14. A higher frequency of MdCs and monocytes present MBP/K^k in the brain compared to the spinal cord. EAE was induced by transfer of MOG-specific CD4 T cells into WT mice (n=10). Mononuclear cells were isolated from the brains and spinal cords (SC) of mice on day 7 post-CD4 transfer. **(a)** Representative flow cytometry plots of 12H4 staining gated on MdCs, monocytes, neutrophils, and microglia. **(b)** Percentages of 12H4$^+$ MdCs, monocytes, neutrophils, and microglia is shown. **(c)** Comparison of the percentages of 12H4$^+$ MdCs and monocytes in the brain compared to the spinal cord. Data are compiled from 2 independent experiments. Graphs show mean + SEM (one symbol per mouse). Statistical significance was determined using **(b)** Kruskal-Wallis with Dunn's post-test and **(c)** Mann-Whitney *U* test. *** $p < 0.001$.

Chapter 5: Concluding remarks and outstanding questions

In this work, we used two mouse models to investigate the hypothesis that myelin antigen-specific CD8 T cells would exert distinct effector functions within the CNS depending on how and where they had been activated. Variation in the activity of antigen-specific CD8 T cells within the CNS may contribute to some of the heterogeneity seen in MS. Previous studies of EAE initiated by CD8 T cells implicated a cytotoxic function and suggested that IFNγ promotes this activity[113]. However, CD8 T cell-intrinsic effector functions required either to initiate disease or to exacerbate CD4-initiated EAE have not been identified. Here we show that MBP-specific CD8 T cells with a single specificity employ different effector mechanisms when they are triggered to initiate disease by viral infection versus when they exacerbate EAE initiated by CD4 T cells. Furthermore, we found that MBP-specific CD8 T cells affect different regions within the CNS when they initiate compared to when they exacerbate EAE.

In EAE initiated by virally activated 8.8 CD8 T cells, we found that brain lesions localized primarily in the cerebellum, as reported for other models of CD8-initiated EAE[60, 77, 80, 114]. Histological analyses revealed inflammatory cells predominantly associated with parenchymal blood vessels with minimal invasion of the surrounding tissue. Lesions with similar characteristics were also observed in the spinal cord. Notably, apoptosis was a prominent feature in CD8-initiated but not CD4-initiated lesions, consistent with tissue injury mediated by CD8 T cell cytotoxic activity. Our observations in our virally-activated CD8-initiated model are similar to the pathology seen in EAE induced by in-vitro-activated MBP-specific CD8 T cells[77] and GFAP-specific CD8 T cells activated by viral infection[80]; however, the mechanisms utilized by the CD8 T cells in these earlier models were not identified. Interestingly, we found that the cerebellum was not a major target in CD4-initiated EAE. Furthermore, although lesions were

associated with parenchymal vessels in CD4-initiated EAE as well, inflammatory cells are more often localized in the meningeal and submeningeal regions of the mid-brain, brain stem, olfactory bulb and spinal cord. Necrotic rather than apoptotic cells predominated in lesions in CD4-initiated EAE.

Using genetic models to eliminate various effector functions, we found that 8.8 CD8 T cells required both IFNγ and perforin expression to initiate EAE, while neither TNFα nor FasL expression were required. The requirement for IFNγ expression by 8.8 CD8 T cells to initiate EAE is a key difference in the pathogenic mechanisms underlying CD4- versus CD8-initiated EAE. In CD4-initiated EAE in C3Heb/Fej mice, IFNγ signaling in the brain suppressed atypical EAE by inhibiting the recruitment of neutrophils, which were required for inflammatory cells to migrate beyond the perivascular space[40]. Neutrophils were not a predominant feature in this CD8-initiated EAE model, which may account for the close localization of inflammatory cells around blood vessels. In CD8-initiated EAE, IFNγ production by 8.8 CD8 T cells likely accounts for the predominance of mononuclear cells, as IFNγ is known to recruit and activate macrophages[42, 115]. IFNγ may also be required to increase MHC class I expression on CNS-resident cells, which is limited in a naïve CNS[86, 116-118]. Increasing MHC class I expression on oligodendrocytes and axons renders them susceptible to perforin-mediated killing, consistent with our finding that perforin is also required in CD8-initiated EAE. While we have not yet determined the cell types that present MBP/K^k in CD8-initiated EAE, CD8 T cells with polarized cytotoxic granules are found in close proximity to demyelinated axons in MS brain tissues[73] and axonal damage is correlated with the presence of CD8 T cells[74].

MBP-specific CD8 T cells also exerted pathogenic activity when recruited to the CNS during CD4-initiated EAE. We found that 8.8 CD8 T cells exacerbated the incidence and

severity of atypical but not classic EAE, indicating their effects are specific to the brain. Previous studies have also shown that both MBP-specific and GFAP-specific CD8 T cells that initiate EAE preferentially target the brain, although the reasons why CNS antigen-specific CD8 T cells targeted the brain were still unknown[77, 80]. Interestingly, in this study, we found that a higher frequency of monocytes and MdCs present MBP/K^k in the brain compared to the spinal cord. Although 8.8 CD8 T cells acquired a T_{EM} phenotype and expressed effector molecules in the brain and spinal cord, a higher frequency of 8.8 CD8 T cells expressed IFNγ, TNFα, FasL, and granzyme-B in the brain compared to the spinal cord, consistent with a higher frequency of MBP/K^k-expressing cells in the brain. The enhanced severity of atypical EAE symptoms was associated with enhanced recruitment and increased pathogenicity of MOG-specific donor CD4 T cells, monocytes and MdCs in the brain but not the spinal cord of mice with CD4-initiated/$CD8_{8.8}$ compared to CD4-initiated/$CD8_{WT}$ EAE. Recruitment of 8.8 CD8 T cells also correlated with an increase in the frequency of lesions associated with parenchymal blood vessels, as well as overall tissue injury, in the brains of mice with CD4-initiated/$CD8_{8.8}$ EAE.

Although 8.8 CD8 T cells entered both the brain and spinal cord during the course of CD4-initiated/$CD8_{8.8}$ EAE, the number of 8.8 CD8 T cells increased only in the brain and not the spinal cord, even though the number of $CD45^{hi}$ inflammatory cells and MOG-specific CD4 T cells increased in both the brains and spinal cords of these mice. We found that 8.8 CD8 T cell recruitment from the periphery was important for maintaining 8.8 CD8 T cell numbers in both the brain and spinal cord. Blocking recruitment appeared to have a bigger impact on 8.8 CD8 T cell numbers in the spinal cord compared to the brain, suggesting 8.8 CD8 T cells may be maintained in the brain due to increased proliferation or survival. Consistent with previous reports, 8.8 CD8 T cell proliferation was limited in the brain and spinal cord[100-102]. Importantly,

there was a similar frequency of proliferating 8.8 CD8 T cells in the brain and spinal cord. The frequency of 8.8 CD8 T cell death was significantly higher in the spinal cord compared to the brain. However, the frequency of donor CD4 T cell and WT CD8 T cell death was also higher in the spinal cord compared to the brain, suggesting that this is a general phenomenon due to higher levels of inflammation in the spinal cord compared to the brain. Collectively, this data suggests that recruitment from the periphery, proliferation, and cell death do not account for the preferential accumulation of 8.8 CD8 T cells in the brain. We hypothesize that as brain inflammation is increased in the presence of 8.8 CD8 T cells, 8.8 CD8 T cells may be recruited from the spinal cord to the brain. Further research is needed to investigate this further.

Surprisingly, WT CD8 T cells acquired a similar activated T_{EM} phenotype and produced IFNγ, TNFα, FasL, and granzyme-B in the brain and spinal cord. This suggests that the activation and acquisition of effector molecules by 8.8 CD8 T cells is not antigen-specific and is a result of the inflammatory environment. However, we hypothesize that although WT and 8.8 CD8 T cells appear similarly activated, the execution of effector molecules is dependent on antigen-recognition as 8.8 CD8 T cells exacerbate atypical EAE compared to WT CD8 T cells. Interestingly, in contrast to 8.8 CD8 T cells, WT CD8 T cells accumulated in both the brain and spinal cord and similar frequencies expressed IFNγ, TNFα, FasL, and granzyme-B in both tissues, suggesting the preferential activation of 8.8 CD8 T cells in the brain is antigen-specific.

Using genetic models, we investigated the mechanisms by which 8.8 CD8 T cells exacerbated atypical EAE initiated by CD4 T cells. Importantly, we found that, in contrast to CD8-initiated EAE, IFNγ and perforin expression were not required by the 8.8 CD8 T cells to exacerbate atypical clinical signs in CD4-initiated EAE. Surprisingly, although 8.8 CD8 T cells produced both IFNγ and TNFα in the CNS during CD4-initiated EAE, neither cytokine was

required for the exacerbation of atypical EAE. It is possible in this model that the activity of IFNγ and TNFα may be redundant, so lack of one cytokine individually would not impact disease. We are currently in the process of creating IFNγ $^{-/-}$TNFα$^{-/-}$ 8.8 mice to address this question. However, we hypothesize that it is more likely that 8.8 CD8 T cytokine production is minimal compared to the cytokine milieu already generated by the donor CD4 T cells. Thus, these cytokines produced by the 8.8 CD8 T cells may have little impact on the severity of atypical EAE.

Importantly, we found that FasL expression by 8.8 CD8 T cells was required to exacerbate brain inflammation in CD4-initiated EAE. As engagement of Fas (the receptor for FasL) by FasL can lead to cell death via apoptosis, FasL^{+} 8.8 CD8 T cells could exacerbate brain inflammation by lysing Fas-expressing cells in the CNS. In CNS tissue from patients with MS, Fas is mainly expressed by oligodendrocytes and macrophages[119, 120]. We previously showed that oligodendrocytes present MBP/K^{k} in CD4-initiated EAE[93], and specific deletion of Fas on oligodendrocytes has been reported by others to ameliorate EAE[121]. While our histological analyses did not identify increased apoptosis upon recruitment of 8.8 CD8 T cells to the brain, this mechanism may nevertheless contribute to the pathology as the percentage of oligodendrocytes that presented MBP/K^{k} in this model was small[93] and would be difficult to detect. We also found that monocytes and MdCs present MBP/K^{k} in the brain and spinal cord, suggesting that they can interact directly with 8.8 CD8 T cells. Furthermore, we demonstrated that 8.8 CD8 T cell-mediated signaling via FasL enhanced ROS production by MdCs and possibly monocytes in the brain, supporting a nonapoptotic, proinflammatory function of Fas-FasL signaling in the brain during CD4-initiated EAE. The frequency of MBP/K^{k+} MdCs and monocytes was significantly higher in the brain compared to the spinal cord, which we believe

accounts for the increase in ROS production in the brain upon 8.8 CD8 T cell recruitment that is not observed in the spinal cord. This mechanism is consistent with reports that macrophages and dendritic cells are relatively resistant to FasL-induced apoptosis and Fas ligation instead promotes the activation of these cells[109-112]. Although we have not yet demonstrated that this is a direct interaction, we found that monocytes and MdCs present MBP/K^k suggesting that they can interact directly with 8.8 CD8 T cells.

In summary, we defined distinct effector functions that CD8 T cells employ to contribute to CNS autoimmunity. CD8 T cells activated by viral infection in the periphery or recruited as naïve cells to an inflammatory environment initiated by CD4 T cells encounter differences in the local cytokine environment, the type of cells presenting antigen, and the antigen load during priming. These differences program the CD8 T cells to exert distinct effector functions. We hypothesize that variation in interactions between genetic and environmental factors leading to CNS autoimmunity results in distinct environments for CD8 T cell priming and acquisition of different effector functions. The impact of these different pathogenic mechanisms within the target tissue may result in some of the clinical and pathological heterogeneity seen in MS. A better understanding of the different ways in which CD8 T cells contribute to CNS autoimmunity may help identify new therapeutic targets tailored to individual patients.

Chapter 6: Materials and Methods.

Mice. C3HeB/FeJ, CD45.1 (B6.SJL-*Ptprc*^{a} *Pepc*^{b}/BoyJ), *Fasl*^{gld} (C3H/HeJ-*Fasl*^{gld}/J), *PFP*$^{-/-}$ (C576L/6-*Prf1tm1*^{Sdz}/J), and Thy1.1 (B6.PL-*Thy1a*/CyJ) mice were originally purchased from The Jackson Laboratory. *Ifng*$^{-/-}$ mice were a gift from Dr. Christopher B. Wilson at the University of Washington. *Csf2*$^{-/-}$ mice[122] were obtained from Jay Heinicke at the University of Washington. TCR transgenic 8.8 mice were previously described[88]. CD45.1, Thy1.1, *Ifng*$^{-/-}$, *Csf2*$^{-/-}$, and *PFP*$^{-/-}$ mice were used after eight or more backcrosses to the C3HeB/FeJ background. *Tnf*$^{-/-}$ mice were generated by the Gene Targeting Facility of the Cancer Research Laboratory at UC Berkeley (Berkeley, CA). Two single guide RNAs (guide 1: AGAAAGCATGATCCGCGACGTGG; guide 2: TCGGGGTGATCGGTCCCCAAAGG) were injected with Cas9 mRNA into fertilized C3HeB/FeJ zygotes. Mutant mice were identified containing a 165 base pair deletion spanning the cytoplasmic and intracellular domains and a lack of both intracellular and extracellular TNFα production following T cell stimulation was confirmed by flow cytometry. These mice were bred to 8.8 mice before intercrossing to generate homozygous knockout mice. All mice were bred and maintained in a specific pathogen-free facility at the South Lake Union Campus of the University of Washington. All procedures were approved by the University of Washington Institutional Animal Care and Use Committee.

Protein and peptides. Recombinant rat myelin oligodendrocyte glycoprotein (rMOG, residues 1-125) was produced in *Escherichia coli* as previously described[123]. MOG$_{97-114}$ peptide (TCFFRDHSYQEEAAVELK) was purchased from GenScript.

CD8 T cell enrichment. Single-cell suspensions were prepared from splenocytes from naïve C3HeB/FeJ (WT) or 8.8 mice as previously described[124]. Cells were labeled with biotinylated antibodies (all from BioLegend) specific for CD4 (RM4-5), B220 (RA3-6B2), CD11b (M1/70), CD11c (N418), and TER-119 (TER-119) and then incubated with magnetic streptavidin particles (BD Biosciences; #557812) according to the manufacturer's instructions. The average frequency of CD8 T cells in the enriched populations were 53.6$\pm$1.6% or 54.9$\pm$1.1% from WT or 8.8 mice, respectively (Fig 6.1).

CD8-initiated EAE. Vac-WT and Vac-MBP were obtained and grown as previously described[81]. Female mice 6-10 weeks of age were infected intraperitoneally (i.p.) with 3-5x10^6 plaque-forming units of Vac-MBP, and 1x10^6 enriched CD8 T cells from either WT, 8.8, or IFNγ-/-, Pfp-/-, TNFα-/-, or $FasL^{gld}$ 8.8 mice were injected i.p on the same day. Mice were monitored for EAE symptoms and weighed daily. Mice were euthanized when they lost more than 20% of their original body weight or reached a clinical score of $\geq$5.

CD4-initiated EAE. EAE was induced in both male and female mice 6-12 weeks of age. Cells were isolated from the spleen and lymph nodes of mice 8 days after rMOG immunization and cultured at 9x10^6 cells/mL for 3 days with MOG_{97-114} (10uM). All cells were skewed toward a Th17 phenotype via addition of IL-23 (R&D Systems; 1ng/mL), unless otherwise stated. For cells that were skewed toward a Th1 phenotype, IL-12 (R&D Systems; 10ng/mL) was included. Following isolation of viable cells via a Lympholyte gradient (Cedarlane Laboratories), donor

CD4 T cell cytokine production was analyzed following incubation with GolgiPlug (BD Biosciences) and MOG_{97-114} peptide (1uM) for 4 hours at 37°C. Unless otherwise stated, $2.x10^5$ CD4 T cell blasts ($CD4^+FSC^{hi}/SSC^{hi}$) were transferred into WT and 8.8 mice that were sublethally irradiated (250 rad) on day -1. To induce CD4-initiated/$CD8_{8.8}$ and CD4-initiated/$CD8_{WT}$ EAE, mice were sublethally irradiated on day -2, $2x10^6$ enriched WT or 8.8 CD8 T cells were transferred i.p on day -1 and CD4 T cells blasts as described above were transferred i.p on day 0. Mice were age- and sex-matched between groups and scored for EAE symptoms daily in a blinded manner. Mice were euthanized at a clinical score of $\geq$5.

Clinical scoring scale. Classic EAE clinical signs were scored as: grade 1, paralyzed tail; grade 2, hindlimb weakness; grade 3, one paralyzed hindlimb; grade 4, two paralyzed hindlimbs; grade 5, forelimb weakness; grade 6, moribund. Atypical EAE clinical signs were scored as: grade 1, ataxia; grade 2, head tilt; grade 3, mild body lean; grade 4, moderate body lean; grade 5, severe body lean; grade 6, rolling.

Flow cytometry. Single-cell suspensions from the spleen, brain, and spinal cord of perfused mice were prepared as previously described[41]. To discriminate live and dead cells, cells were incubated with an amine reactive dye (Succinimidyl Ester Pacific Orange; Molecular Probes, Invitrogen) for 20 minutes at 4°C. After washing, cells were incubated with Fc block (2.4G2; eBioscience) in 5% mouse serum (MP Biomedicals) for 15 minutes at 4°C, washed, and stained with antibodies for 30 min at 4°C. CD4 T cell cytokine production was analyzed after incubation of cells with GolgiPlug (BD Biosciences) and MOG_{97-114} peptide (1uM) for 4 hours at 37°C.

Alternatively, CD8 T cell cytokine production in intact TCR transgenic 8.8 mice was analyzed directly ex vivo by incubating freshly isolated cells with GolgiPlug alone or with the addition of PMA (50ng/mL) and ionomycin (500ng/mL) for 4 hours at 37°C. Intracellular cytokine staining was performed using the Cytofix/Cytoperm Kit (BD Biosciences) according to the manufacturer's instructions. Data were acquired with FACSCanto (BD Biosciences) or Aurora (Cytek Biosciences) cytometers and analyzed using FlowJo software (Tree Star).

Antibodies. Antibodies specific for CD4 (RM4-5 and GK1.5), CD45 (30-F11), I-A^k (11-5.2), IFNγ (XMG1.2), IL-17 (TC11-18H10), Ly6C (AL-21), Ly6G (1A8), Thy1.1 (OX-7), CD62L (MEL-14), KLRG1 (2F1), CD69 (H1.2F3), CD103 (M290) and the isotype controls for IFNγ (rat IgG1, k) and IL-17 (rat IgG1, k) were from BD Biosciences. Antibodies specific for CD8 (53-6.7), CD25 (PC61), CD45.1 (A20), CD45.2 (104), TCRβ (H57-597), Thy1.2 (30-H12, TNFα (MP6-XT22), and the isotype control for TNFα (rat IgG1, k) were from BioLegend. Antibodies specific for CD8 (53-67), CD11b (M1/70), CD44 (IM7), GM-CSF (MP1-22E9), granzyme-B (NGZB), IL-1b (NJTEN3), FasL (MFL3) and the isotype for GM-CSF (rat IgG2a, k) were from eBiosciences. Ki67 (SolA15) was from Invitrogen. 12H4 antibody specific for MBP/K^k was generated and validated as previously described[93]. For ROS staining, CellROX Deep Red reagent (Life Technologies) was used according to the manufacturer's instructions. BrdU staining kits were purchased from BD Biosciences and used according to the manufacturer's instructions.

FTY720 injection. CD4-initiated EAE was induced as described above following transfer of 8.8 CD8 T cells. On day 6, 3 mg/kg FTY720 (Sigma-Aldrich) or vehicle (5% DMSO) was injected

intraperitoneally. CNS and spleen mononuclear cells were isolated on day 7 for flow cytometry analysis.

Quantitative RT-PCR. Brains and spinal cords of perfused mice with EAE (day 6 post-CD4 T cell transfer) or sublethally-irradiated healthy control mice were flash-frozen in liquid nitrogen. Tissues were homogenized in QIAzol Lysis Reagent (Qiagen) and total RNA extracted using the RNeasy Lipid Tissue Mini kit (Qiagen). cDNA was synthesized using the SuperScript III first-strand synthesis system (Invitrogen). RT-qPCR was performed using SYBR Green master mix on a ViiA7 Real-Time PCR system (Applied Biosystems). Data were normalized to *GAPDH* and analyzed using the comparative Ct method. Fold induction of gene expression in EAE mice was calculated relative to expression in sublethally irradiated healthy control mice. Primer sequences are listed in Table 6.1.

Histology. Brain and spinal cord from mice with CD4-initiated EAE or CD8-initiated EAE (day 7 or 8 post-CD4 T cell transfer) were fixed in 10% neutral-buffered formalin, sectioned, embedded in paraffin, and stained with H&E. Tissue injury was assessed histologically using a semi-quantitative grading system. Approximately eight evenly distributed cross-sectional areas of each brain were taken from the rostral olfactory region to the caudal portion of the cerebellar cortex. The spinal cord of each mouse was examined using 1.5-2 cm long segments of the cervical, thoracic and lumbar regions. Three hematoxylin and eosin-stained histologic step sections of each brain area and one sagittal section of each spinal cord area were then examined by a board-certified veterinary pathologist (Dr. Denny Liggitt) who was blinded to group

assignments. Lesions were graded for degree of inflammatory cell involvement on an all-inclusive severity scale of 0 (normal) to 4+ (severe). An aggregate histology score for the brain and spinal cord tissue of each mouse was generated by assigning severity grades for each section that reflects the lesion severity as well as whether the lesions involved the meninges only, meninges and submeningeal regions, and parenchyma surrounding blood vessels (including the perivascular space), and then averaging these scores. Included in the assessment of inflammation was evaluation for changes consistent with necrosis and apoptosis.

Statistics. EAE incidence and frequencies of parenchymal inflammation were compared using a Fisher's Exact Test. For all other analyses with two groups, comparisons were made using a two-tailed Mann-Whitney *U* test. For multiple comparisons, Kruskal-Wallis with Dunn's post-test was used. Data are presented as one symbol per mouse with mean + SEM or mean +/- SEM unless otherwise stated in figure legends. GraphPad Prism 7 was used for all analyses and *P* values of less than 0.05 were considered statistically significant.

Table 6.1. Primers used for qRT-PCR.

Gene	Forward primer (5'-3')	Reverse primer (5'-3')
CCL2	TGG GCC TGC TGT TCA CAG TT	TGG GGC GTT AAC TGC ATC TGG
CCL3	ACC AAG TCT TCT CAG CGC CA	GTC AGG AAA ATG ACA CCT GGC TG
CCL4	AGC CAG CTG TGG TAT TCC TGA C	TCT CCT GAA GTG GCT CCT CCT
CCL5	TCA CCA TAT GGC TCG GAC ACC	CAC ACT TGG CGG TTC CTT CG
CCL6	CCG GGC ATC ATC TTT ATC AGC A	TGA CAA TGC CTG CCC TCC TT
CCL9	CAG CTG GGT CTG CCC ACT AA	CTC TGT TGC ATG TGT GAT CTG GG
CCL11	TCC ATC TGT CTC CCT CCA CCA	AAG TTG GGA TGG AGC CTG GGT
CCL17	ATG TAG GCC GAG AGT GCT GC	TGC ACA GAT GAG CTT GCC CT
CCL20	AGG CAG AAG CAA GCA ACT ACG A	GCT TCA TCG GCC ATC TGT CTT G
CCL22	CAA AAT CCT GCC GCA AGC CT	GCC TGG GAT CGG CAC AGA TA
CCL24	CCA AGG CAG GGG TCA TCT TCA TC	TTG GCC CCT TTA GAA GGC TGG
CXCL2	ACT GAA CAA AGG CAA GGC TAA CTG	AGA CAG CGA GGC ACA TCA GG
CXCL9	TGC CAT GAA GTC CGC TGT TCT	AGG GTT CCT CGA ACT CCA CAC T
CXCL10	CCA CGT GTT GAG ATC ATT GCC A	TGC GTG GCT TCA CTC CAG TT
IL-17A	TGG ACT CTC CAC CGC AAT GA	TCC AGC TTT CCC TCC GCA TT
IFNγ	GTT TGA GGT CAA CAA CCC ACA GG	GCG ACT CCT TTT CCG CTT CC
TNFα	CAG GCG GTG CCT ATG TCT CA	GCC ATT TGG GAA CTT CTC ATC CC
GM-CSF	AAC TCC GGA AAC GGA CTG TGA	CTG GCC TGG GCT TCC TCA TT
IL-1β	CCC CAA AAG ATG AAG GGC TGC	TGC CTG CCT GAA GCT CTT GT
IL-6	ATT CTG CTC TGG AGC CCA CC	GCA ACT GGA TGG AAG TCT CTT GC
IL-10	GCG CTG TCA TCG ATT TCT CCC	TGG CCT TGT AGA CAC CTT GGT C
IL-12 p35	TGA CAT GGT GAA GAC GGC CA	ATG TGC TGG TTT GGT CCC GT
IL-23 p19	TGT GCC CCG TAT CCA GTG TG	TCC TTT GCA AGC AGA ACT GGC
IFNb	TCA ACC TCA CCT ACA GGG CG	CAT TCC ACC CAG TGC TGG AGA
TGFb	ACT CCC GTG GCT TCT AGT GC	ACA GGA TCT GGC CAC GGA TG
iNOS	ATG AGA GCG GCA GCT ACT GG	GGG TGG GAG GGG TCG TAA TG
GAPDH	TCG GTG TGA ACG GAT TTG GC	TGA AGG GGT CGT TGA TGG CAA

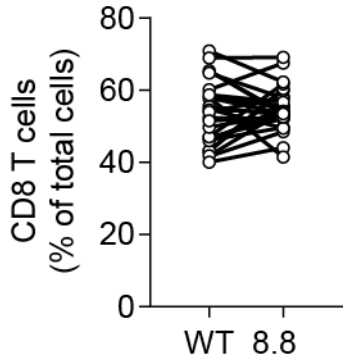

Figure 6.1. Similar frequencies of CD8 T cells in enriched populations from WT or 8.8 mice. Splenocytes were isolated from naïve WT or 8.8 mice and CD8 T cells were enriched by negative selection as described in Methods. Percentages of CD8 T cells in the total cell population is shown. Symbols represent enriched populations from one experiment with linked points representing values from the same experiment (n = 28). Statistical significance was determined using Wilcoxon signed-rank test. No significant difference was observed ($p = 0.4$).

References

1. Aktas, O., Kieseier, B. & Hartung, H.P. Neuroprotection, regeneration and immunomodulation: broadening the therapeutic repertoire in multiple sclerosis. *Trends Neurosci* **33**, 140-152 (2010).
2. Dendrou, C.A., Fugger, L. & Friese, M.A. Immunopathology of multiple sclerosis. *Nat Rev Immunol* **15**, 545-558 (2015).
3. Wagner, C.A. & Goverman, J.M. Novel Insights and Therapeutics in Multiple Sclerosis. *F1000Research* **4**, 517 (2015).
4. Hafler, D.A. *et al.* Risk alleles for multiple sclerosis identified by a genomewide study. *N Engl J Med* **357**, 851-862 (2007).
5. Goverman, J. Autoimmune T cell responses in the central nervous system. *Nat Rev Immunol* **9**, 393-407 (2009).
6. van Oosten, B.W. *et al.* Treatment of multiple sclerosis with the monoclonal anti-CD4 antibody cM-T412: results of a randomized, double-blind, placebo-controlled, MR-monitored phase II trial. *Neurology* **49**, 351-357 (1997).
7. Simmons, S.B., Pierson, E.R., Lee, S.Y. & Goverman, J.M. Modeling the heterogeneity of multiple sclerosis in animals. *Trends Immunol* **34**, 410-422 (2013).
8. Reich, D.S., Lucchinetti, C.F. & Calabresi, P.A. Multiple Sclerosis. *N Engl J Med* **378**, 169-180 (2018).
9. Filippi, M. *et al.* Multiple sclerosis. *Nature reviews. Disease primers* **4**, 43 (2018).
10. Lublin, F.D. & Reingold, S.C. Defining the clinical course of multiple sclerosis: results of an international survey. National Multiple Sclerosis Society (USA) Advisory Committee on Clinical Trials of New Agents in Multiple Sclerosis. *Neurology* **46**, 907-911 (1996).
11. Filippi, M. *et al.* Serial contrast-enhanced MR in patients with multiple sclerosis and varying levels of disability. *AJNR. American journal of neuroradiology* **18**, 1549-1556 (1997).
12. Trapp, B.D. & Nave, K.A. Multiple sclerosis: an immune or neurodegenerative disorder? *Annual review of neuroscience* **31**, 247-269 (2008).
13. Frischer, J.M. *et al.* The relation between inflammation and neurodegeneration in multiple sclerosis brains. *Brain* **132**, 1175-1189 (2009).
14. Hochmeister, S. *et al.* Dysferlin is a new marker for leaky brain blood vessels in multiple sclerosis. *J Neuropathol Exp Neurol* **65**, 855-865 (2006).
15. Nociti, V. *et al.* Clinical characteristics, course and prognosis of spinal multiple sclerosis. *Spinal Cord* **43**, 731-734 (2005).
16. Thorpe, J.W. *et al.* Spinal MRI in patients with suspected multiple sclerosis and negative brain MRI. *Brain* **119 (Pt 3)**, 709-714 (1996).
17. Lucchinetti, C. *et al.* Heterogeneity of multiple sclerosis lesions: implications for the pathogenesis of demyelination. *Ann.Neurol.* **47**, 707-717 (2000).
18. Metz, I. *et al.* Pathologic heterogeneity persists in early active multiple sclerosis lesions. *Ann Neurol* **75**, 728-738 (2014).
19. King, I.L., Dickendesher, T.L. & Segal, B.M. Circulating Ly-6C+ myeloid precursors migrate to the CNS and play a pathogenic role during autoimmune demyelinating disease. *Blood* **113**, 3190-3197 (2009).

20. Selmaj, K.W. & Raine, C.S. Tumor necrosis factor mediates myelin and oligodendrocyte damage in vitro. *Ann.Neurol.* **23**, 339-346 (1988).
21. Akassoglou, K. *et al.* Oligodendrocyte apoptosis and primary demyelination induced by local TNF/p55TNF receptor signaling in the central nervous system of transgenic mice: models for multiple sclerosis with primary oligodendrogliopathy. *Am J Pathol* **153**, 801-813 (1998).
22. Cross, A.H. *et al.* Inducible nitric oxide synthase gene expression and enzyme activity correlate with disease activity in murine experimental autoimmune encephalomyelitis. *J Neuroimmunol* **71**, 145-153 (1996).
23. Nikic, I. *et al.* A reversible form of axon damage in experimental autoimmune encephalomyelitis and multiple sclerosis. *Nat Med* **17**, 495-499 (2011).
24. Miller, S.D., McMahon, E.J., Schreiner, B. & Bailey, S.L. Antigen presentation in the CNS by myeloid dendritic cells drives progression of relapsing experimental autoimmune encephalomyelitis. *Ann N Y Acad Sci* **1103**, 179-191 (2007).
25. Kroenke, M.A., Carlson, T.J., Andjelkovic, A.V. & Segal, B.M. IL-12- and IL-23-modulated T cells induce distinct types of EAE based on histology, CNS chemokine profile, and response to cytokine inhibition. *J Exp Med* **205**, 1535-1541 (2008).
26. Baron, J.L., Madri, J.A., Ruddle, N.H., Hashim, G. & Janeway, C.A., Jr. Surface expression of alpha 4 integrin by CD4 T cells is required for their entry into brain parenchyma. *Journal of Experimental Medicine* **177**, 57-68 (1993).
27. Segal, B.M. & Shevach, E.M. IL-12 unmasks latent autoimmune disease in resistant mice. *J Exp Med* **184**, 771-775 (1996).
28. Panitch, H.S., Hirsch, R.L., Schindler, J. & Johnson, K.P. Treatment of multiple sclerosis with gamma interferon: exacerbations associated with activation of the immune system. *Neurology* **37**, 1097-1102 (1987).
29. Steinman, L. A brief history of T(H)17, the first major revision in the T(H)1/T(H)2 hypothesis of T cell-mediated tissue damage. *Nat Med* **13**, 139-145 (2007).
30. Cua, D.J. *et al.* Interleukin-23 rather than interleukin-12 is the critical cytokine for autoimmune inflammation of the brain. *Nature* **421**, 744-748 (2003).
31. Lock, C. *et al.* Gene-microarray analysis of multiple sclerosis lesions yields new targets validated in autoimmune encephalomyelitis. *Nature Medicine* **8**, 500-508 (2002).
32. Haak, S. *et al.* IL-17A and IL-17F do not contribute vitally to autoimmune neuro-inflammation in mice. *J Clin Invest* **119**, 61-69 (2009).
33. Codarri, L. *et al.* RORgammat drives production of the cytokine GM-CSF in helper T cells, which is essential for the effector phase of autoimmune neuroinflammation. *Nat Immunol* **12**, 560-567 (2011).
34. El-Behi, M. *et al.* The encephalitogenicity of T(H)17 cells is dependent on IL-1- and IL-23-induced production of the cytokine GM-CSF. *Nat Immunol* **12**, 568-575 (2011).
35. Ponomarev, E.D. *et al.* GM-CSF production by autoreactive T cells is required for the activation of microglial cells and the onset of experimental autoimmune encephalomyelitis. *J Immunol* **178**, 39-48 (2007).
36. Sheng, W. *et al.* STAT5 programs a distinct subset of GM-CSF-producing T helper cells that is essential for autoimmune neuroinflammation. *Cell research* **24**, 1387-1402 (2014).
37. Noster, R. *et al.* IL-17 and GM-CSF expression are antagonistically regulated by human T helper cells. *Science translational medicine* **6**, 241ra280 (2014).

38. Muller, D.M., Pender, M.P. & Greer, J.M. A neuropathological analysis of experimental autoimmune encephalomyelitis with predominant brain stem and cerebellar involvement and differences between active and passive induction. *Acta Neuropathol (Berl)* **100**, 174-182 (2000).
39. Stromnes, I.M., Cerretti, L.M., Liggitt, D., Harris, R.A. & Goverman, J.M. Differential regulation of central nervous system autoimmunity by T(H)1 and T(H)17 cells. *Nat Med* **14**, 337-342 (2008).
40. Simmons, S.B., Liggitt, D. & Goverman, J.M. Cytokine-Regulated Neutrophil Recruitment Is Required for Brain but Not Spinal Cord Inflammation during Experimental Autoimmune Encephalomyelitis. *J Immunol* **193**, 555-563 (2014).
41. Pierson, E.R. & Goverman, J.M. GM-CSF is not essential for experimental autoimmune encephalomyelitis but promotes brain-targeted disease. *JCI insight* **2**, e92362 (2017).
42. Miller, N.M., Wang, J., Tan, Y. & Dittel, B.N. Anti-inflammatory mechanisms of IFN-gamma studied in experimental autoimmune encephalomyelitis reveal neutrophils as a potential target in multiple sclerosis. *Frontiers in neuroscience* **9**, 287 (2015).
43. Mueller, S.N., Gebhardt, T., Carbone, F.R. & Heath, W.R. Memory T cell subsets, migration patterns, and tissue residence. *Annu Rev Immunol* **31**, 137-161 (2013).
44. Kaech, S.M. & Cui, W. Transcriptional control of effector and memory CD8+ T cell differentiation. *Nat Rev Immunol* **12**, 749-761 (2012).
45. Joshi, N.S. *et al.* Inflammation directs memory precursor and short-lived effector CD8(+) T cell fates via the graded expression of T-bet transcription factor. *Immunity* **27**, 281-295 (2007).
46. Obar, J.J. *et al.* Pathogen-induced inflammatory environment controls effector and memory CD8+ T cell differentiation. *J Immunol* **187**, 4967-4978 (2011).
47. Pearce, E.L. & Shen, H. Generation of CD8 T cell memory is regulated by IL-12. *J Immunol* **179**, 2074-2081 (2007).
48. Takemoto, N., Intlekofer, A.M., Northrup, J.T., Wherry, E.J. & Reiner, S.L. Cutting Edge: IL-12 inversely regulates T-bet and eomesodermin expression during pathogen-induced CD8+ T cell differentiation. *J Immunol* **177**, 7515-7519 (2006).
49. Hauser, S.L. *et al.* Immunohistochemical analysis of the cellular infiltrate in multiple sclerosis lesions. *Ann Neurol* **19**, 578-587 (1986).
50. Booss, J., Esiri, M.M., Tourtellotte, W.W. & Mason, D.Y. Immunohistological analysis of T lymphocyte subsets in the central nervous system in chronic progressive multiple sclerosis. *J.Neurol.Sci.* **62**, 219-232 (1983).
51. Babbe, H. *et al.* Clonal expansions of CD8(+) T cells dominate the T cell infiltrate in active multiple sclerosis lesions as shown by micromanipulation and single cell polymerase chain reaction. *Journal of Experimental Medicine* **192**, 393-404 (2000).
52. Jacobsen, M. *et al.* Oligoclonal expansion of memory CD8+ T cells in cerebrospinal fluid from multiple sclerosis patients. *Brain* **125**, 538-550 (2002).
53. Skulina, C. *et al.* Multiple sclerosis: brain-infiltrating CD8+ T cells persist as clonal expansions in the cerebrospinal fluid and blood. *Proceedings of the National Academy of Sciences of the United States of America* **101**, 2428-2433 (2004).
54. Junker, A. *et al.* Multiple sclerosis: T-cell receptor expression in distinct brain regions. *Brain* **130**, 2789-2799 (2007).
55. Tsuchida, T. *et al.* Autoreactive CD8+ T-cell responses to human myelin protein- derived peptides. *Proc.Natl.Acad.Sci.U.S.A.* **91**, 10859-10863 (1994).

56. Dressel, A. *et al.* Autoantigen recognition by human CD8 T cell clones: enhanced agonist response induced by altered peptide ligands. *Journal of Immunology* **159**, 4943-4951 (1997).
57. Elong Ngono, A. *et al.* Frequency of circulating autoreactive T cells committed to myelin determinants in relapsing-remitting multiple sclerosis patients. *Clin Immunol* **144**, 117-126 (2012).
58. Crawford, M.P. *et al.* High prevalence of autoreactive, neuroantigen-specific CD8+ T cells in multiple sclerosis revealed by novel flow cytometric assay. *Blood* **103**, 4222-4231 (2004).
59. Mars, L.T., Saikali, P., Liblau, R.S. & Arbour, N. Contribution of CD8 T lymphocytes to the immuno-pathogenesis of multiple sclerosis and its animal models. *Biochim Biophys Acta* **1812**, 151-161 (2011).
60. Friese, M.A. *et al.* Opposing effects of HLA class I molecules in tuning autoreactive CD8+ T cells in multiple sclerosis. *Nat Med* **14**, 1227-1235 (2008).
61. Antel, J.P., Bania, M.B., Reder, A. & Cashman, N. Activated suppressor cell dysfunction in progressive multiple sclerosis. *J Immunol* **137**, 137-141 (1986).
62. Correale, J. & Villa, A. Isolation and characterization of CD8+ regulatory T cells in multiple sclerosis. *J Neuroimmunol* **195**, 121-134 (2008).
63. Jiang, H., Braunstein, N.S., Yu, B., Winchester, R. & Chess, L. CD8+ T cells control the TH phenotype of MBP-reactive CD4+ T cells in EAE mice. *Proceedings of the National Academy of Sciences of the United States of America* **98**, 6301-6306 (2001).
64. Tang, X. *et al.* Regulation of immunity by a novel population of Qa-1-restricted CD8alphaalpha+TCRalphabeta+ T cells. *J Immunol* **177**, 7645-7655 (2006).
65. Ayers, C.L. *et al.* Modulation of immune function occurs within hours of therapy initiation for multiple sclerosis. *Clin Immunol* **147**, 105-119 (2013).
66. Tyler, A.F., Mendoza, J.P., Firan, M. & Karandikar, N.J. CD8(+) T Cells Are Required For Glatiramer Acetate Therapy in Autoimmune Demyelinating Disease. *PLoS One* **8**, e66772 (2013).
67. Cunnusamy, K. *et al.* Disease exacerbation of multiple sclerosis is characterized by loss of terminally differentiated autoregulatory CD8+ T cells. *Clin Immunol* **152**, 115-126 (2014).
68. Baughman, E.J. *et al.* Neuroantigen-specific CD8+ regulatory T-cell function is deficient during acute exacerbation of multiple sclerosis. *J Autoimmun* **36**, 115-124 (2011).
69. York, N.R. *et al.* Immune regulatory CNS-reactive CD8+T cells in experimental autoimmune encephalomyelitis. *J Autoimmun* **35**, 33-44 (2010).
70. Itani, F.R. *et al.* Suppression of autoimmune demyelinating disease by preferential stimulation of CNS-specific CD8 T cells using Listeria-encoded neuroantigen. *Scientific reports* **7**, 1519 (2017).
71. Ortega, S.B. *et al.* The disease-ameliorating function of autoregulatory CD8 T cells is mediated by targeting of encephalitogenic CD4 T cells in experimental autoimmune encephalomyelitis. *J Immunol* **191**, 117-126 (2013).
72. Kashi, V.P., Ortega, S.B. & Karandikar, N.J. Neuroantigen-specific autoregulatory CD8+ T cells inhibit autoimmune demyelination through modulation of dendritic cell function. *PLoS One* **9**, e105763 (2014).
73. Neumann, H., Medana, I.M., Bauer, J. & Lassmann, H. Cytotoxic T lymphocytes in autoimmune and degenerative CNS diseases. *Trends Neurosci* **25**, 313-319 (2002).

74. Bitsch, A., Schuchardt, J., Bunkowski, S., Kuhlmann, T. & Bruck, W. Acute axonal injury in multiple sclerosis. Correlation with demyelination and inflammation. *Brain* **123 (Pt 6)**, 1174-1183 (2000).
75. Jurewicz, A., Biddison, W.E. & Antel, J.P. MHC class I-restricted lysis of human oligodendrocytes by myelin basic protein peptide-specific CD8 T lymphocytes. *Journal of Immunology* **160**, 3056-3059 (1998).
76. Zang, Y.C. *et al.* Increased CD8+ cytotoxic T cell responses to myelin basic protein in multiple sclerosis. *Journal of Immunology* **172**, 5120-5127 (2004).
77. Huseby, E.S. *et al.* A pathogenic role for myelin-specific CD8(+) T cells in a model for multiple sclerosis. *Journal of Experimental Medicine* **194**, 669-676 (2001).
78. Sun, D. *et al.* Myelin antigen-specific CD8+ T cells are encephalitogenic and produce severe disease in C57BL/6 mice. *Journal of Immunology* **166**, 7579-7587 (2001).
79. Ford, M.L. & Evavold, B.D. Specificity, magnitude, and kinetics of MOG-specific CD8+ T cell responses during experimental autoimmune encephalomyelitis. *European Journal of Immunology* **35**, 76-85 (2005).
80. Sasaki, K. *et al.* Relapsing-remitting central nervous system autoimmunity mediated by GFAP-specific CD8 T cells. *J Immunol* **192**, 3029-3042 (2014).
81. Ji, Q., Perchellet, A. & Goverman, J.M. Viral infection triggers central nervous system autoimmunity via activation of CD8+ T cells expressing dual TCRs. *Nat Immunol* **11**, 628-634 (2010).
82. Anderson, A.C. *et al.* A Transgenic Model of Central Nervous System Autoimmunity Mediated by CD4+ and CD8+ T and B Cells. *J Immunol* **188**, 2084-2092 (2012).
83. Sinha, S., Boyden, A.W., Itani, F.R., Crawford, M.P. & Karandikar, N.J. CD8(+) T-Cells as Immune Regulators of Multiple Sclerosis. *Frontiers in immunology* **6**, 619 (2015).
84. Saxena, A. *et al.* Cutting edge: Multiple sclerosis-like lesions induced by effector CD8 T cells recognizing a sequestered antigen on oligodendrocytes. *J Immunol* **181**, 1617-1621 (2008).
85. Gobel, K. *et al.* Collateral neuronal apoptosis in CNS gray matter during an oligodendrocyte-directed CD8(+) T cell attack. *Glia* **58**, 469-480 (2010).
86. Mars, L.T. *et al.* CD8 T cell responses to myelin oligodendrocyte glycoprotein-derived peptides in humanized HLA-A*0201-transgenic mice. *J Immunol* **179**, 5090-5098 (2007).
87. Huseby, E.S., Ohlen, C. & Goverman, J. Cutting edge: myelin basic protein-specific cytotoxic T cell tolerance is maintained in vivo by a single dominant epitope in H-2k mice. *Journal of Immunology* **163**, 1115-1118 (1999).
88. Perchellet, A., Stromnes, I., Pang, J.M. & Goverman, J. CD8+ T cells maintain tolerance to myelin basic protein by 'epitope theft'. *Nature Immunology* **5**, 606-614 (2004).
89. Guyenet, S.J. *et al.* A simple composite phenotype scoring system for evaluating mouse models of cerebellar ataxia. *Journal of visualized experiments : JoVE* (2010).
90. Sabelko, K.A., Kelly, K.A., Nahm, M.H., Cross, A.H. & Russell, J.H. Fas and Fas ligand enhance the pathogenesis of experimental allergic encephalomyelitis, but are not essential for immune privilege in the central nervous system. *Journal of Immunology* **159**, 3096-3099 (1997).
91. Suvannavejh, G.C., Dal Canto, M.C., Matis, L.A. & Miller, S.D. Fas-mediated apoptosis in clinical remissions of relapsing experimental autoimmune encephalomyelitis. *J Clin Invest* **105**, 223-231 (2000).

92. Su, M.W., Walden, P.R., Golan, D.B. & Eisen, H.N. Cognate peptide-induced destruction of CD8+ cytotoxic T lymphocytes is due to fratricide. *J Immunol* **151**, 658-667 (1993).
93. Ji, Q., Castelli, L. & Goverman, J.M. MHC class I-restricted myelin epitopes are cross-presented by Tip-DCs that promote determinant spreading to CD8(+) T cells. *Nat Immunol* (2013).
94. Lefrancois, L. Development, trafficking, and function of memory T-cell subsets. *Immunol Rev* **211**, 93-103 (2006).
95. Ifergan, I. *et al.* Central nervous system recruitment of effector memory CD8+ T lymphocytes during neuroinflammation is dependent on alpha4 integrin. *Brain* **134**, 3560-3577 (2011).
96. Krakowski, M.L. & Owens, T. Naive T lymphocytes traffic to inflamed central nervous system, but require antigen recognition for activation. *Eur J Immunol* **30**, 1002-1009 (2000).
97. Steinert, E.M. *et al.* Quantifying Memory CD8 T Cells Reveals Regionalization of Immunosurveillance. *Cell* **161**, 737-749 (2015).
98. Bartholomaus, I. *et al.* Effector T cell interactions with meningeal vascular structures in nascent autoimmune CNS lesions. *Nature* **462**, 94-98 (2009).
99. Webb, M. *et al.* Sphingosine 1-phosphate receptor agonists attenuate relapsing-remitting experimental autoimmune encephalitis in SJL mice. *J Neuroimmunol* **153**, 108-121 (2004).
100. Bauer, J. *et al.* T-cell apoptosis in inflammatory brain lesions: destruction of T cells does not depend on antigen recognition. *Am J Pathol* **153**, 715-724 (1998).
101. Ohmori, K., Hong, Y., Fujiwara, M. & Matsumoto, Y. In situ demonstration of proliferating cells in the rat central nervous system during experimental autoimmune encephalomyelitis. Evidence suggesting that most infiltrating T cells do not proliferate in the target organ. *Lab.Invest.* **66**, 54-62 (1992).
102. Juedes, A.E. & Ruddle, N.H. Resident and infiltrating central nervous system APCs regulate the emergence and resolution of experimental autoimmune encephalomyelitis. *J Immunol* **166**, 5168-5175 (2001).
103. Haider, L. *et al.* Oxidative damage in multiple sclerosis lesions. *Brain* **134**, 1914-1924 (2011).
104. Fischer, M.T. *et al.* NADPH oxidase expression in active multiple sclerosis lesions in relation to oxidative tissue damage and mitochondrial injury. *Brain* **135**, 886-899 (2012).
105. van Horssen, J., Witte, M.E., Schreibelt, G. & de Vries, H.E. Radical changes in multiple sclerosis pathogenesis. *Biochim Biophys Acta* **1812**, 141-150 (2011).
106. Montecino-Rodriguez, E., Leathers, H. & Dorshkind, K. Identification of a B-1 B cell-specified progenitor. *Nat Immunol* **7**, 293-301 (2006).
107. Peterson, L.K., Tsunoda, I. & Fujinami, R.S. Role of CD5+ B-1 cells in EAE pathogenesis. *Autoimmunity* **41**, 353-362 (2008).
108. Rothstein, T.L., Herzenberg, L.A., Holodick, N.E. & Ghosn, E. B-1 Cell Development and Function. *Ann N Y Acad Sci* **1362**, v-vi (2015).
109. Yi, F., Frazzette, N., Cruz, A.C., Klebanoff, C.A. & Siegel, R.M. Beyond Cell Death: New Functions for TNF Family Cytokines in Autoimmunity and Tumor Immunotherapy. *Trends in molecular medicine* **24**, 642-653 (2018).
110. Chakour, R. *et al.* A new function of the Fas-FasL pathway in macrophage activation. *J Leukoc Biol* **86**, 81-90 (2009).

111. Park, D.R. *et al.* Fas (CD95) induces proinflammatory cytokine responses by human monocytes and monocyte-derived macrophages. *J Immunol* **170**, 6209-6216 (2003).
112. Ma, Y. *et al.* Fas ligation on macrophages enhances IL-1R1-Toll-like receptor 4 signaling and promotes chronic inflammation. *Nat Immunol* **5**, 380-387 (2004).
113. Salou, M., Nicol, B., Garcia, A. & Laplaud, D.A. Involvement of CD8(+) T Cells in Multiple Sclerosis. *Frontiers in immunology* **6**, 604 (2015).
114. Na, S.Y. *et al.* Naive CD8 T-cells initiate spontaneous autoimmunity to a sequestered model antigen of the central nervous system. *Brain* **131**, 2353-2365 (2008).
115. Ottum, P.A., Arellano, G., Reyes, L.I., Iruretagoyena, M. & Naves, R. Opposing Roles of Interferon-Gamma on Cells of the Central Nervous System in Autoimmune Neuroinflammation. *Frontiers in immunology* **6**, 539 (2015).
116. Hoftberger, R. *et al.* Expression of major histocompatibility complex class I molecules on the different cell types in multiple sclerosis lesions. *Brain Pathology* **14**, 43-50 (2004).
117. Neumann, H., Schmidt, H., Cavalie, A., Jenne, D. & Wekerle, H. Major histocompatibility complex (MHC) class I gene expression in single neurons of the central nervous system: differential regulation by interferon (IFN)-gamma and tumor necrosis factor (TNF)-alpha. *J Exp Med* **185**, 305-316 (1997).
118. Massa, P.T., Ozato, K. & McFarlin, D.E. Cell type-specific regulation of major histocompatibility complex (MHC) class I gene expression in astrocytes, oligodendrocytes, and neurons. *Glia* **8**, 201-207 (1993).
119. Dowling, P. *et al.* Involvement of the CD95 (APO-1/Fas) receptor/ligand system in multiple sclerosis brain. *J Exp Med* **184**, 1513-1518 (1996).
120. D'Souza, S.D. *et al.* Multiple sclerosis: Fas signaling in oligodendrocyte cell death. *J Exp Med* **184**, 2361-2370 (1996).
121. Hovelmeyer, N. *et al.* Apoptosis of oligodendrocytes via Fas and TNF-R1 is a key event in the induction of experimental autoimmune encephalomyelitis. *J Immunol* **175**, 5875-5884 (2005).
122. Dranoff, G. & Mulligan, R.C. Activities of granulocyte-macrophage colony-stimulating factor revealed by gene transfer and gene knockout studies. *Stem Cells* **12 Suppl 1**, 173-182; discussion 182-174 (1994).
123. Abdul-Majid, K.B. *et al.* Screening of several H-2 congenic mouse strains identified H-2(q) mice as highly susceptible to MOG-induced EAE with minimal adjuvant requirement. *J Neuroimmunol* **111**, 23-33 (2000).
124. Stromnes, I.M. & Goverman, J.M. Passive induction of experimental allergic encephalomyelitis. *Nature Protocols* **1**, 1952-1960 (2006).